國 立 交 通 大 學
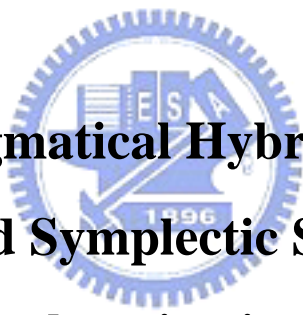
機械工程學系

碩士論文

測速器的渾沌現象, 實用混合投影廣義及交織同步, 應用GYC部分區域穩定理論之廣義同步與控制和鳥群行為渾沌控制

Chaos, Pragmatical Hybrid Projective Generalized and Symplectic Synchronization, Generalized Synchronization and Control by GYC Partial Region Stability Theory and Boids Control of Chaos for a Tachometer System

研 究 生: 江峻宇

指 導 教 授: 戈正銘 教授

中華民國九十七年六月

測速器的渾沌現象,實用混合投影廣義及交織同步,應用GYC

部分區域穩定理論之廣義同步與控制和鳥群行為渾沌控制

Chaos, Pragmatical Hybrid Projective Generalized and

Symplectic Synchronization, Generalized Synchronization

and Control by GYC Partial Region Stability Theory and

Boids Control of Chaos for a Tachometer System

研 究 生：江峻宇　　　　　　　　　　　Student：Chun-Yu Chian

指導教授：戈正銘　　　　　　　　　　　Advisor：Zheng-Ming Ge

國 立 交 通 大 學

機 械 工 程 研 究 所

碩 士 論 文

A Thesis
Submitted to Department of Mechanical Engineering
College of Engineering
National Chiao Tung University
in Partial Fulfillment of the Requirement
for the Degree of Master of Science
in
Mechanical Engineering
June 2008
Hsinchu, Taiwan, Republic of China

中華民國九十七年六月

國立交通大學

論文口試委員會審定書

本校___機 械 工 程___學系碩士班___江峻宇_____君

所提論文(中文) 測速器的渾沌現象,實用混合投影廣義及交織同步,應用
GYC 部分區域穩定理論之廣義同步與控制和鳥群行為渾
沌控制

(英文)Chaos, Pragmatical Hybrid Projective Generalized and
Symplectic Synchronization, Generalized Synchronization and
Control by GYC Partial Region Stability Theory and Boids
Control of Chaos for a Tachometer System

合於碩士資格水準、業經本委員會評審認可。

口試委員：_____   _____

古富能   林宗南

陳恒輝   _____

指導教授：_____   _____

戈正銘

系 主 任：_____   教授

中 華 民 國   97   年   6   月   12   日

測速器的渾沌現象,實用混合投影廣義及交織同步,應用 GYC部分區域穩定理論之廣義同步與控制和鳥群行為渾沌控制

學　　生：江峻宇　　　　　　　　　指導教授：戈正銘

摘要

　　測速器動態系統的渾沌行為藉由相圖,龐卡萊圖,分岔圖,功率譜,和李亞普諾夫指數圖來表示.藉由逆步和適應控制的實用混合投影廣義同步與兩個測速器動態系統與不同階數的渾沌系統之GYC實用混合投影交織同步,並由數值模擬來驗證其有效性.除此之外,利用GYC部分區域穩定理論來模擬測速器動態系統之廣義超渾沌的同步與控制.更進一步, 測速器動態系統之鳥群行為的渾沌控制與延遲同步也可以達成.最後藉由數值模擬來顯示驗證的結果.

Chaos, Pragmatical Hybrid Projective Generalized and Symplectic Synchronization, Generalized Synchronization and Control by GYC Partial Region Stability Theory and Boids Control of Chaos for a Tachometer System

Student：Chun-Yu Chiang   Advisor：Zheng-Ming Ge

ABSTRACT

The hyperchaotic dynamics of a tachometer system is studied by means of phase portraits, Poincare maps, bifurcation diagram, power spectra and Lyapunov exponents. Pragmatical hybrid projective hyperchaotic generalized synchronization and GYC pragmatical hybrid projective hyperchaotic symplectic synchronization (PHPHSS) of two hyperchaotic tachometer system with different order system as a constituent by adaptive backstepping control are obtained and verified by numerical simulation. Besides, hyperchaotic generalized synchronization and chaos control of tachometer system by GYC partial region stability are proposed. Furthermore, boids control and lag synchronization of tachometer system can be successfully obtained. Finally, numerical simulations are shown they are work.

誌 謝

　　此篇論文及碩士學業之完成，首先感謝指導教授 戈正銘老師的耐心指導及諄諄教誨。老師在讀書、人生、真理方面的經驗是令學生敬佩的。無論是兩個金字塔、特定人誕生之機率、剃刀原則等等皆讓我受益無窮；而老師的博學也令學生見識到大師的風采，特別是詩詞方面令學生體會到傳統中國文化之美。

　　兩年攻讀碩士光陰中，在此要感謝博士班學長張晉銘、楊振雄和李仕宇，還有已畢業碩士班學長李乾豪、吳宗訓、李式中和翁郁婷在課業上的幫忙；也感謝同學李彥賢、許凱銘及何俊諺陪伴我度過二年快樂的求學生涯。感謝我的家人，在我求學期間能使我無後顧之憂完成我的學業；謝謝你們！

CONTENTS

LIST OF FIGURES

Chapter 1

Introduction

Chaos is defined as the phenomenon of occurence of bounded nonperiodic evolution in completely deterministic nonlinear dynamical system with high sensitive dependence on initial conditional [1]. Phase portraits, Poincare maps, bifurcation diagram, power spectrum and two positive Lyapunov exponents diagram are used to present a hyperchaotic tachometer system which will be studied in this proposal.

Synchronization in chaotic dynamical systems has been a theme in nonlinear sciences and received considerable attention. Since the pioneering work by Pecora and Carroll [2], much attention has been devoted to research on synchronization of chaos. In recent years, synchronization in chaotic dynamical systems has widely studied in the past decade [3-13], and has many possible applications especially in secret communication, chemical reaction, and biological systems [14].An interesting synchronization, termed as projective synchronization, has been reported by Mainieri and Rehack [15] that the drive and response vectors synchronize up to a scaling factor. Backstepping has become one of the most popular design methods for adaptive nonlinear control and synchronization [16-19]. Most of the control methods are based on the exact knowledge of the system structure and fully known parameters. But some of the system parameters are uncertain. Many researchers have dedicated to solve this problem by adaptive synchronization [20-24]. In current researches [25-29], by Lyapunov asymptotical stability theorem and Babalat lemma, the error vector can be proved to tend to zero. But the question that why the estimated parameters also approach uncertain values remain no answer. In this thesis, the question is answered strictly by pragmatical asymptotical stability theorem.

In Chapter 2, chaos of tachometer system is studied by Lyapunov exponents, bifurcation diagram, phase portraits, time histories of state variables and power spectra.

In Chapter 3, generalized synchronization is investigated [30-35]. This means that we give a function relationship between the states of the master and slave is $y = G(x)$. A specific case, hybrid projective chaotic generalized synchronization

$$y = G(x) = px(t)z(t)^3 \tag{1-1}$$

is studied, where x, y are the state vectors of master and slave, z is state vector of a functional chaotic system, p is a constant vector with positive and negative entries to form hybrid projective synchronization. Numerical simulations are presented.

In Chapter 4, we give a functional relationship between the states of the "master"-"slave"and "slave". This means that the final desired state y of the "slave"system not only depends upon the "master"system state x but also depends upon the state y itself. Namely, the "slave"system plays a rule to determine the final desired state y itself and is not a pure slave [36]. This kind of synchronization, is called"symplectic synchronization"*, and the "master"system is called partner A, the "slave"system is called partner B. The GYC pragmatical hybrid projective hyperchaotic generalized symplectic synchronization

$$y = H(x, y, z, t) = px(t)z(t)y(t) \tag{1-2}$$

is studied, where x, y are the state vectors of partner A and partner B, z is state vector of a different order chaotic system, p is a constant vector with positive and negative entries. When the"slave"state y is removed from the function $H(x, y, z, t)$, this traditional generalized synchronizations is obtained, which is the special cases of the symplectic synchronization. Namely:

$$y = H(x, z, t) = px(t)z(t) \tag{1-3}$$

Numerical simulations show that it can be achieved.

The term **"symplectic"** comes from the Greek for ''interwined''. H. Weyl first introduced the term in 1939 in his book "The Classical Groups"(P. 165 in both the first edition, 1939, and second edition, 1946, Princeton University Press).

In Chapter 5, a new generalized synchronization by GYC partial region stability is proposed [37, 38]. The Lyapunov function is a simple linear function and the controllers are simpler by using the GYC partial region stability theory. The simulation results are more precise because the controllers are in lower degree than that of traditional controllers. Numerical simulations can show that it can be achieved. In Chapter 6, chaos control by GYC partial region stability [37, 38] is also proposed.

In Chapter 7, boids (short for "Birdoid") control [39] is proposed as an artificial life program, simulating animal motion such as flocking behavior of birds, herding behavior of land animals and schooling behavior of fish [40]. Flocks and related synchronized group behaviors such as schools of fish or herds of land animals are both beautiful to watch and intriguing to contemplate. As with most artificial life simulations, boids exhibit complex flocking behavior, which arises from the interaction of simple local rules. Yet all evidence indicate that flock motion must be merely the aggregate result of the actions of individual animals, each acting solely on the basis of its own local perception of the world. The boids framework is often used in computer graphics, providing a realistic scene with a flock of birds, schools of fish or herds of animals. This approach assumes a flock is simply the result of the interaction between the behaviors of individual birds. The synchronization behavior of boids is also similar to chaotic synchronization, since flocks behave in a chaotic fashion and synchronize their speed with nearby flockmates. To simulate a flock we simulate the behavior of an individual bird, we also simulate portions of the bird's perceptual mechanisms and aspects of the physics of aerodynamics flight. We investigate the complex flocking behavior and the emergent behavior by using computer simulations.

In Chapter 8, lag synchronization for tachometer system is studied. Backstepping control is used to achieve the lag synchronization of two tachometer system. Controllers are obtained by backstepping design method that recursively interlace the choice of a

Lyapunov function with the design of feedback control. The simulations for the tachometer system show that the control technique is successful.

This paper is organized as follows. In Chapter 2, chaos of tachometer system is presented. In Chapter 3, pragmatical hybrid projective hyperchaotic generalized synchronization (PHPHGS) of hyperchaotic tachometer system by adaptive backstepping control is introduced. In Chapter 4, pragmatical hybrid projective hyperchaotic symplectic synchronization of hyperchaotic tachometer systems with different order system by adaptive backstepping control is presented. In Chapter 5, hyperchaotic generalized synchronization of tachometer system by GYC partial region stability theory is shown. In Chapter 6, chaos control of tachometer system is studied by GYC partial region stability theory. In Chapter 7, boids control of chaos for tachometer system is introduced. In Chapter 8, lag synchronization for tachometer system is presented. Numerical simulations are shown in the end of this proposal. Finally, conclusions are drawn in Chapter 9.
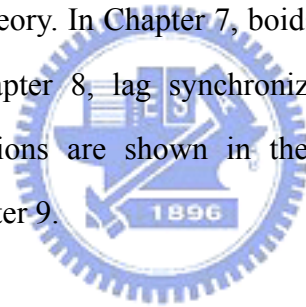
Chapter 2

Chaos of Tachometer System

The tachometer system considered is shown in Fig. 1 [41]. The masses of the rods and vertical axis O_1O_2 are neglected, and ball A and B are assumed as particles with equal mass m_1. The vertical axis rotates with constant speed η and is subjected to a vertical vibration $A\sin x_3$ where x_3 is a state variable, A is the amplitude of vibration. m_2 is the mass of the sleeve C, l is the length of rod BC, $2l$ is the length of AB. ϕ is the angle between rod AB and vertical axis O_1O_2, k_1 is the spring constant of a restoring spiral spring which is used to restrain the angle ϕ caused by centrifugal forces of A and B, k_2 is the viscous damping coefficient caused by friction in the bearings. Let $x_1 = \phi$, $x_2 = \dot{\phi}$, $x_4 = \dot{x}_3$.
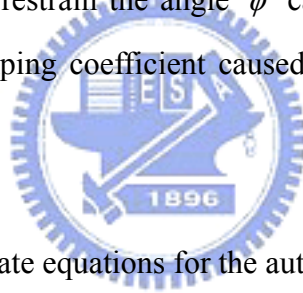
By Lagrange equation, the state equations for the autonomous tachometer system are

$$
\begin{cases}
\dfrac{d}{dt}x_1 = x_2 \\[2mm]
\dfrac{d}{dt}x_2 = \dfrac{1}{2m_1 + 4m_2 \sin^2 x_1}\left(\dfrac{-2m_2 g \sin x_1}{l} + \dfrac{2m_2 A \sin x_3 \sin x_1}{l}\right. \\[2mm]
\qquad\qquad \left. - 4m_2 x_2^2 \sin x_1 \cos x_1 + 2m_1 \sin x_1 \cos x_1 \eta^2 - \dfrac{k_1 x_1}{l^2} - \dfrac{k_2 x_2}{l^2}\right) \\[2mm]
\dfrac{d}{dt}x_3 = x_4 \\[2mm]
\dfrac{d}{dt}x_4 = -A\sin x_3
\end{cases}
\qquad (2\text{-}1)
$$

The third and fourth equations of system (2-1) give a simple harmonic vibration system. When A=0, at steady state, a given constant η corresponds to a definite ϕ, therefore this system can be used as a tachometer.

Choose m_1=3, m_2=3, g=9.8, l=1.5, A=5, k_1=4, k_2=1. η is used as a variable parameter. η=1 gives period 1 motion, η=1.5 gives period 3 motion, η=4 gives chaotic motion. Taking η as abscissa, the Lyapunov exponents diagram is shown as Fig. 2. Hyperchaos [42] with two positive LE is found. Bifurcation diagram, phase portraits and Poincare maps, time histories, and power spectra are presented in Figs 3~6.
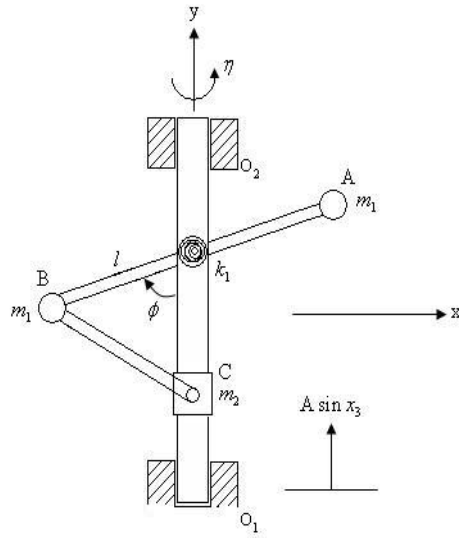
Fig. 1   Sketch of a tachometer with vibrating base.
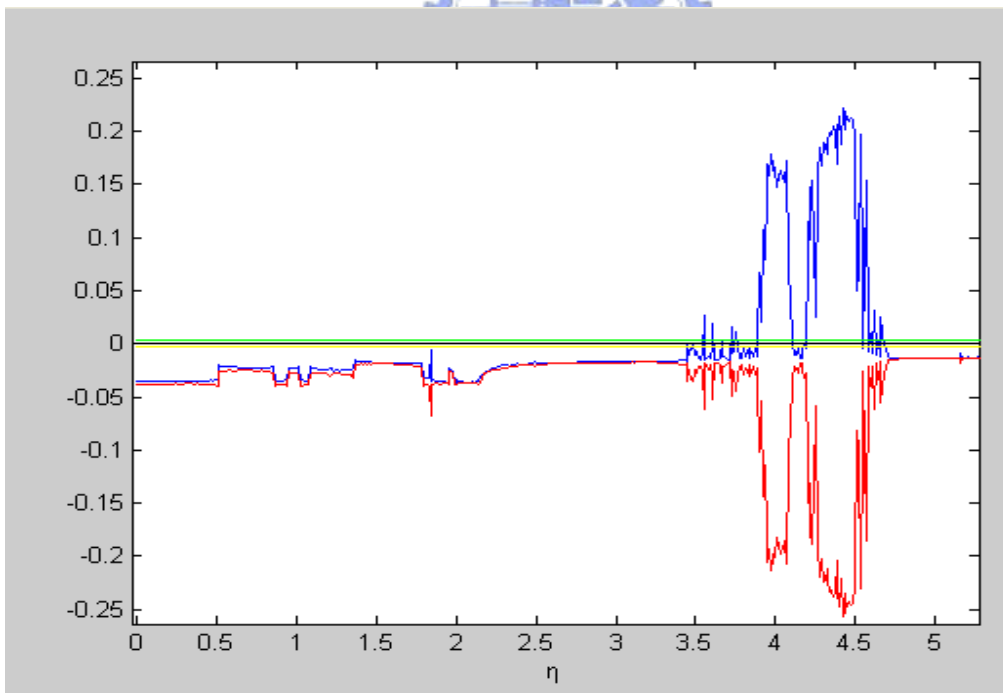
Fig. 2   Lyapunov exponents for tachometer system.
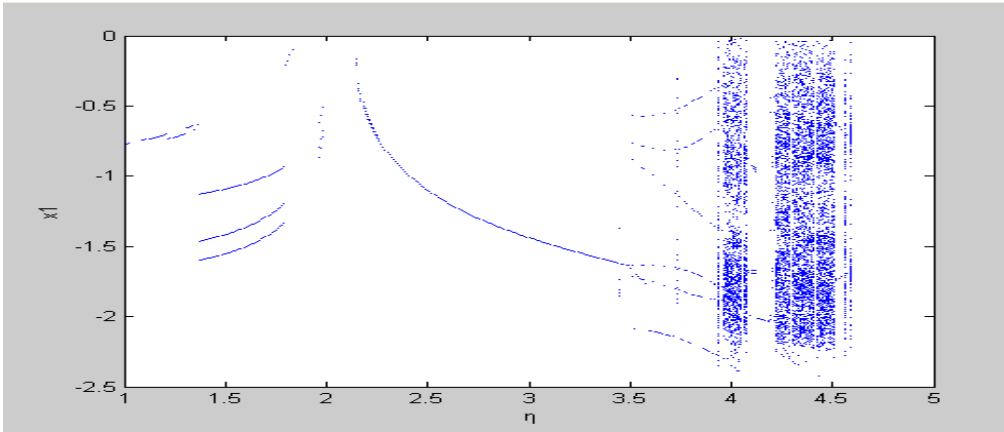
Fig. 3   Bifurcation diagram.
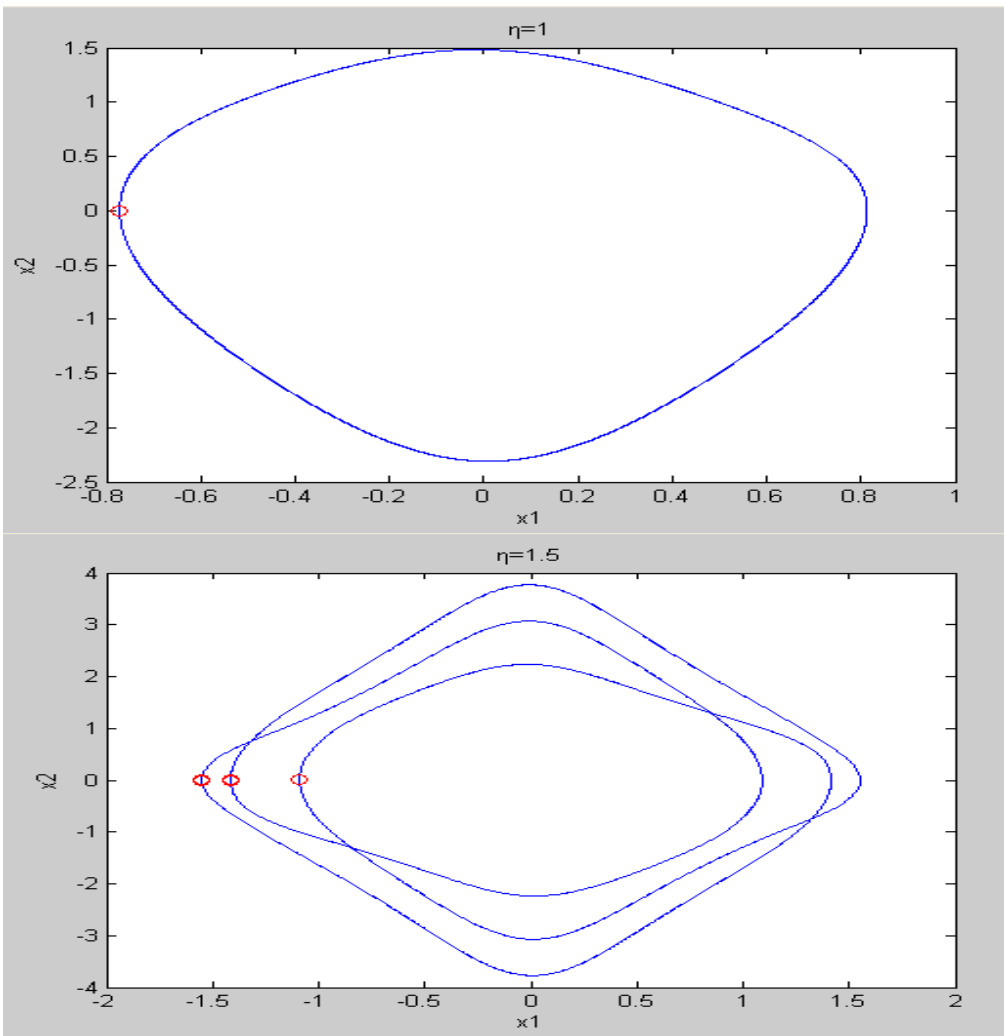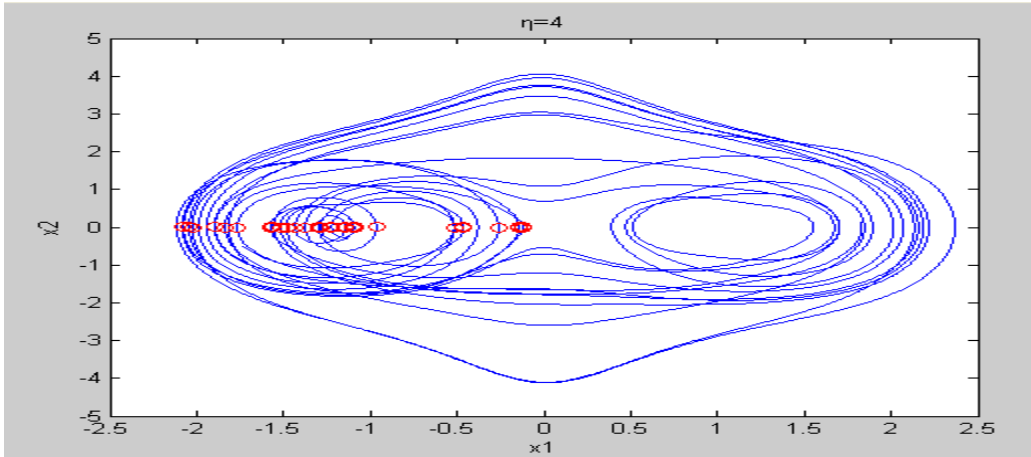
Fig. 4   Phase portraits of η=1, η=1.5, η=4, respectively.
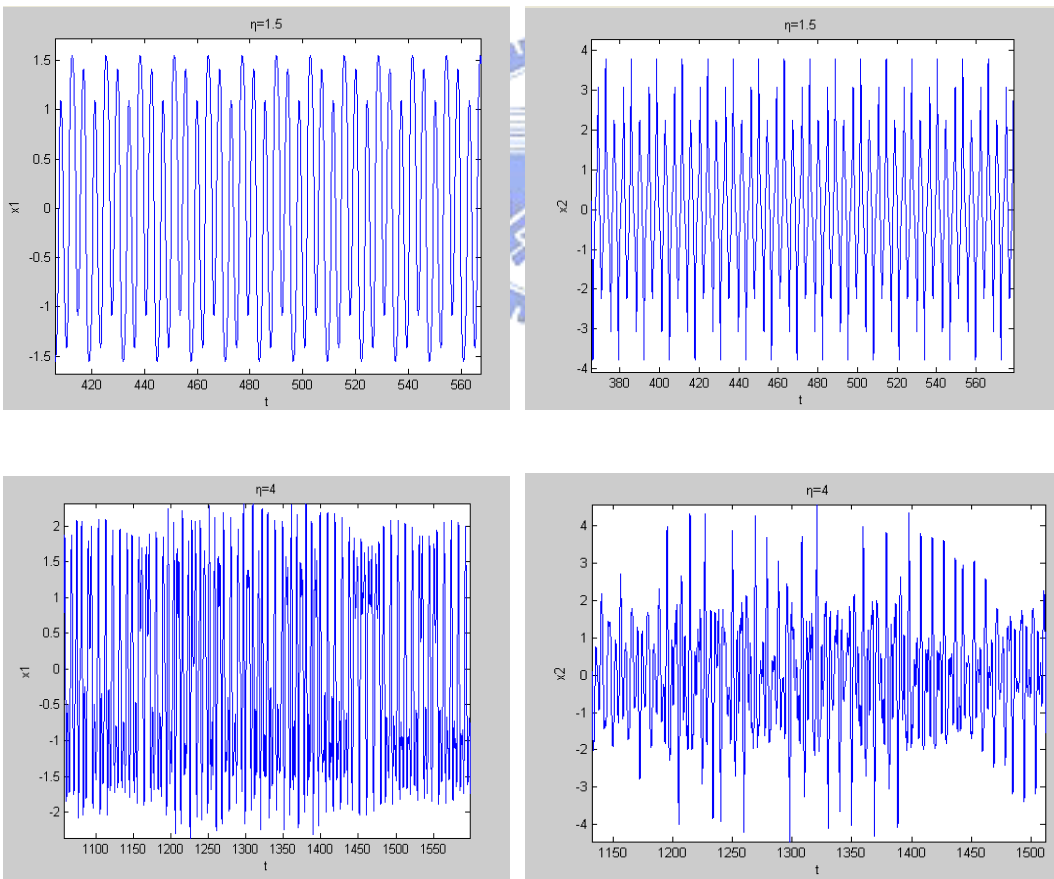
Fig. 5   Time histories of state variables for η=1.5, η=4, respectively.
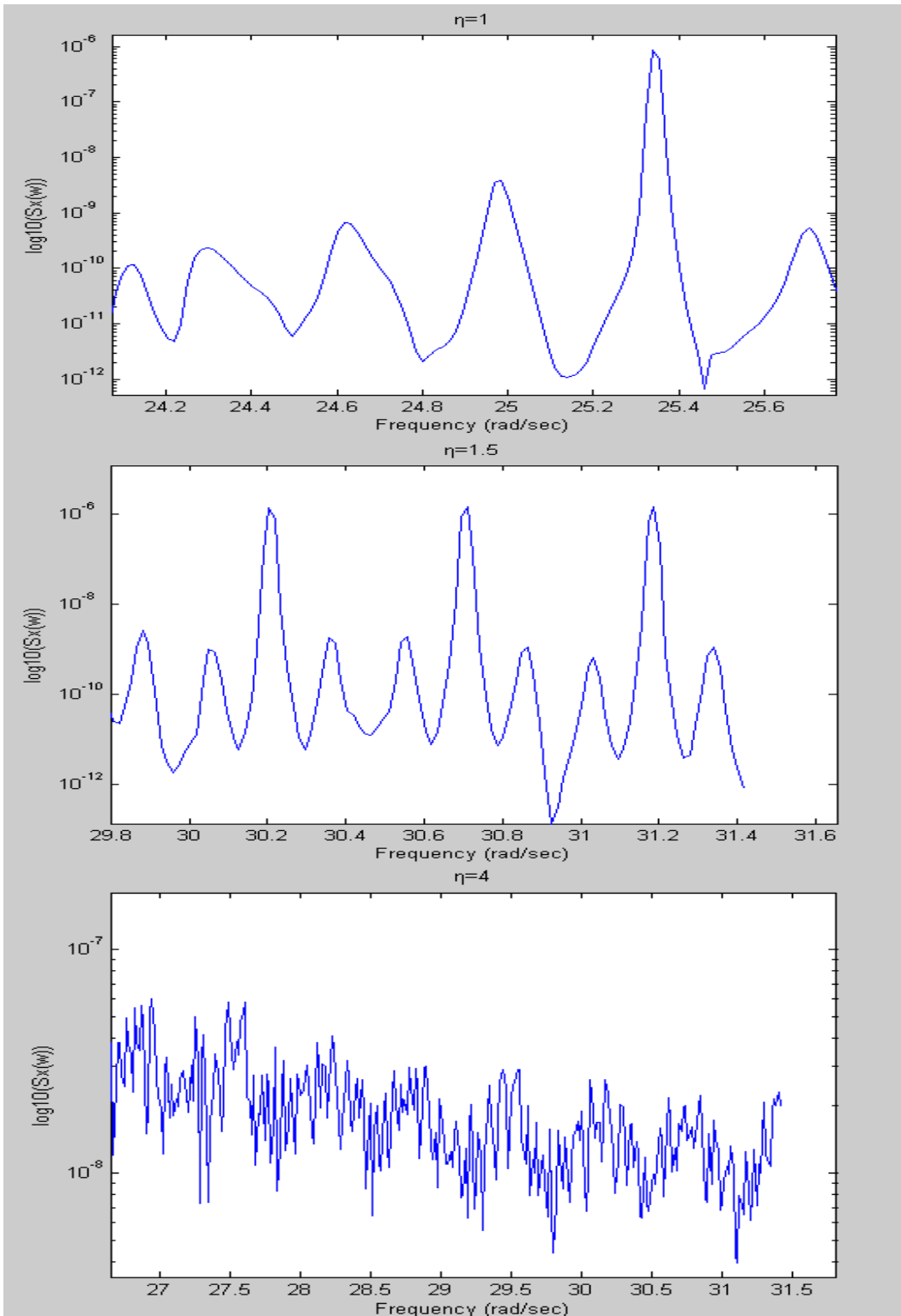
Fig. 6   Power spectra for η=1, η=1.5, η=4.

Chapter 3

Pragmatical Hybrid Projective Hyperchaotic Generalized Synchronization (PHPHGS) of Hyperchaotic Tachometer System by Adaptive Backstepping control

In this chapter, pragmatical hybrid projective hyperchaotic generalized synchronization of two hyperchaotic tachometer system by adaptive backstepping control is obtained. The state vectors of Mathieu-Duffing system with hyperchaotic Lyapunov exponents are constituent of the functional relation between master system and slave system. Pragmatical hybrid projective hyperchaotic generalized synchronization is obtained and verified by numerical simulation.

3.1   Pragmatical hybrid projective generalized synchronization scheme

The drive system is described by

$$\dot{x} = f(x) \tag{3-1}$$

where $x = [x_1, x_2, \cdots, x_n]^T \in \Re^n$ is the state vector, some parameters of Eq (3-1) are uncertain. The slave system is

$$\dot{y} = f(y) + u \tag{3-2}$$

where $y = [y_1, y_2, \cdots, y_n]^T \in \Re^n$ is the state vector, and u is a controlled vector, some parameters of Eq (3-2) are estimated. The functional chaotic system is

$$\dot{z} = f(z) \tag{3-3}$$

where $z = [z_1, z_2, \cdots, z_n]^T \in \Re^n$ is a hyperchaotic state vector and all parameters of Eq (3-3) are known.

The control target is forcing the slave system to track an n-dimensional desired vector

$$h(t) = [h_1(t), h_2(t), \cdots, h_n(t)] = \left[p_1 x_1(t) z^3{}_1(t), p_2 x_2(t) z_2^3(t), \cdots p_n x_n(t) z_n^3(t) \right]$$

where $p_1, p_2, \cdots, p_n$ are constant vector whose entries are either positive or negative to form hybrid projective synchronization. Define the error vector as

$$e(t) = y(t) - h(t) = y - pxz^3, \tag{3-4}$$
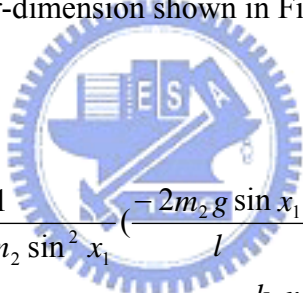
where $e(t) = [e_1, e_2, \cdots, e_n]^T \in \Re^n$.

The controlling goal is that the error dynamical vector

$$\lim_{t \to \infty} e = 0 \tag{3-5}$$

3.2 Hyperchaotic tachometer system and Mathieu-Duffing system with two positive Lyapunov exponents

The tachometer system of four-dimension shown in Fig. 1 is given by:

$$
\begin{cases}
\dfrac{d}{dt} x_1 = x_2 \\[2mm]
\dfrac{d}{dt} x_2 = \dfrac{-k_1 x_1}{2m_1 l^2} + \cdots + \dfrac{1}{2m_1 + 4m_2 \sin^2 x_1} \left(\dfrac{-2m_2 g \sin x_1}{l} + \dfrac{2m_2 A \sin x_3 \sin x_1}{l} \right. \\[3mm]
\qquad \left. - 4m_2 x_2^2 \sin x_1 \cos x_1 + 2m_1 \sin x_1 \cos x_1 \eta^2 - \dfrac{k_2 x_2}{l^2} \right) \\[3mm]
\dfrac{d}{dt} x_3 = x_4 \\[2mm]
\dfrac{d}{dt} x_4 = -A \sin x_3
\end{cases}
\tag{3-6}
$$

where x_1, x_2, x_3, x_4 are state variables and k_1, k_2, A, l, g, m_1, m_2 are constants, when $k_1 = 4$, $k_2 = 1$, $m_2 = 3$, $m_1 = 3$, A=5, $\eta = 4.55$, g=9.8, l=1.5, the system exhibits chaotic behavior with hyperchaotic Lyapunov exponents as shown in Fig. 2.

The Mathieu-Duffing system of four-dimension is given by:

$$
\begin{cases}
\dfrac{d}{dt}z_1 = z_2 \\[2mm]
\dfrac{d}{dt}z_2 = -az_1 - bz_3 z_1 - az_1^3 - bz_3 z_1^3 - cz_2 + dz_3 \\[2mm]
\dfrac{d}{dt}z_3 = z_4 \\[2mm]
\dfrac{d}{dt}z_4 = -z_3 - z_3^3 - tz_4 + fz_1
\end{cases}
\tag{3-7}
$$

where a=20.30, b=0.5970, c=0.005, d=-24.4400478, e=0.002, f=14.63, the system exhibits chaotic behavior with hyperchaotic Lyapunov exponents as shown in Fig. 7.

3.3 Numerical simulations for pragmatical hybrid projective hyperchaotic generalized synchronization (PHPHGS) of hyperchaotic tachometer system by adaptive backstepping control

The tachometer system is the master system:

$$
\begin{cases}
\dfrac{d}{dt}x_1 = x_2 \\[2mm]
\dfrac{d}{dt}x_2 = \dfrac{-k_1 x_1}{2m_1 l^2} + \cdots + \dfrac{1}{2m_1 + 4m_2 \sin^2 x_1}\left(\dfrac{-2m_2 g \sin x_1}{l} + \dfrac{2m_2 A \sin x_3 \sin x_1}{l}\right. \\[2mm]
\qquad \left. - 4m_2 x_2^2 \sin x_1 \cos x_1 + 2m_1 \sin x_1 \cos x_1 \eta^2 - \dfrac{k_2 x_2}{l^2}\right) \\[2mm]
\dfrac{d}{dt}x_3 = x_4 \\[2mm]
\dfrac{d}{dt}x_4 = -A \sin x_3
\end{cases}
\tag{3-8}
$$
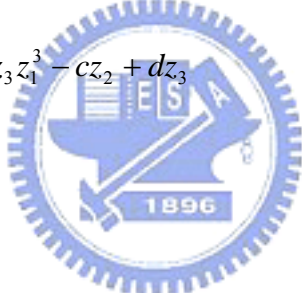
where k_1, A are uncertain parameters.

The slave system is as follow:

$$\begin{cases} \dfrac{d}{dt}y_1 = y_2 \\[2mm] \dfrac{d}{dt}y_2 = \dfrac{-\hat{k}_1 y_1}{2m_1 l^2} + \cdots + \dfrac{1}{2m_1 + 4m_2 \sin^2 y_1}\left(\dfrac{-2m_2 g \sin y_1}{l} + \dfrac{2m_2 A \sin y_3 \sin y_1}{l} \right. \\[2mm] \qquad\qquad \left. - 4m_2 y_2^2 \sin y_1 \cos y_1 + 2m_1 \sin y_1 \cos y_1 \eta^2 - \dfrac{k_2 y_2}{l^2}\right) \\[2mm] \dfrac{d}{dt}y_3 = y_4 \\[2mm] \dfrac{d}{dt}y_4 = -\hat{A}\sin y_3 \end{cases} \qquad (3\text{-}9)$$

where $\hat{k}_1$, $\hat{A}$ are estimated parameters.

Mathieu-Duffing system is the hyperchaotic functional system:

$$\begin{cases} \dfrac{d}{dt}z_1 = z_2 \\[2mm] \dfrac{d}{dt}z_2 = -az_1 - bz_3 z_1 - az_1^3 - bz_3 z_1^3 - cz_2 + dz_3 \\[2mm] \dfrac{d}{dt}z_3 = z_4 \\[2mm] \dfrac{d}{dt}z_4 = -z_3 - z_3^3 - tz_4 + fz_1 \end{cases} \qquad (3\text{-}10)$$

where a=20.3, b==0.597, c=0.005, d=-24.4399, t=0.002,f=14.63.

In order to lead (y_1, y_2, y_3, y_4) to ($p_1 x_1 z_1^3$, $p_2 x_2 z_2^3$, $p_3 x_3 z_3^3$, $p_4 x_4 z_4^3$) , choose u_1, u_2, u_3, u_4 as controller adding to Eq (3-9), namely:

$$\begin{cases} \dfrac{d}{dt}y_1 = y_2 + u_1 \\[2mm] \dfrac{d}{dt}y_2 = \dfrac{-\hat{k}_1 y_1}{2m_1 l^2} + \cdots + \dfrac{1}{2m_1 + 4m_2 \sin^2 y_1}\left(\dfrac{-2m_2 g \sin y_1}{l} + \dfrac{2m_2 A \sin y_3 \sin y_1}{l} \right. \\[2mm] \qquad\qquad \left. - 4m_2 y_2^2 \sin y_1 \cos y_1 + 2m_1 \sin y_1 \cos y_1 \eta^2 - \dfrac{k_2 y_2}{l^2}\right) + u_2 \\[2mm] \dfrac{d}{dt}y_3 = y_4 + u_3 \\[2mm] \dfrac{d}{dt}y_4 = -\hat{A}\sin y_3 + u_4 \end{cases} \qquad (3\text{-}11)$$

Define error states as follows:

$$\begin{cases} e_1 = y_1 - p_1 x_1 z_1^3 \\ e_2 = y_2 - p_2 x_2 z_2^3 \\ e_3 = y_3 - p_3 x_3 z_3^3 \\ e_4 = y_4 - p_4 x_4 z_4^3 \end{cases} \tag{3-12}$$

where x_1, x_2, x_3, x_4, z_1, z_2, z_3, z_4, y_1, y_2, y_3, y_4 are states, p_1, p_2, p_3, p_4 are given parameters and we choose p_1=3, p_2=-4, p_3=6, p_4=-2 to give hybrid projective synchronization.

Differentiating Eq (3-12) with respect to time, we obtain the error dynamics:

$$\dot{e}_1 = e_2 + p_2 x_2 z_2^3 - p_1 x_2 z_1^3 - 3 p_1 x_1 z_1^2 z_2 + u_1$$

$$\begin{aligned} \dot{e}_2 = &-\frac{\hat{k}_1 e_1}{2m_1 l^2} - \frac{\hat{k}_1 p_1 x_1 z_1^3}{2m_1 l^2} - \frac{p_2 k_1 x_1 z_2^3}{2m_1 l^2} + \cdots + 3a p_2 x_2 z_1 z_2^2 + 3b p_2 x_2 z_1 z_2^2 z_3 \\ &+ 3a p_2 x_2 z_1^3 z_2^2 + 3b p_2 x_2 z_1^3 z_2^2 z_3 + 3c p_2 x_2 z_2^3 - 3d p_2 x_2 z_2^2 z_3 \\ &+ \frac{1}{2m_1 + 4m_2 \sin^2 y_1}(-\frac{2m_2 g \sin y_1}{l} + \frac{2m_2 A \sin y_3 \sin y_1}{l} - 4m_2 y_2^2 \sin y_1 \cos y_1 \\ &+ 2m_1 \sin y_1 \cos y_1 \eta^2 - \frac{k_2 y_2}{l^2}) \\ &- \frac{p_2 z_2^3}{2m_1 + 4m_2 \sin^2 x_1}(-\frac{2m_2 g \sin x_1}{l} + \frac{2m_2 A \sin x_3 \sin x_1}{l} - 4m_2 x_2^2 \sin x_1 \cos x_1 \\ &+ 2m_1 \sin x_1 \cos x_1 \eta^2 - \frac{k_2 x_2}{l^2}) + u_2 \end{aligned}$$

$$\dot{e}_3 = e_4 + p_4 x_4 z_4^3 - p_3 x_4 z_3^3 - 3 p_3 x_3 z_3^2 z_4 + u_3$$

$$\dot{e}_4 = -\hat{A} \sin y_3 + p_4 A \sin x_3 z_4^3 + 3 p_4 x_4 z_3 z_4^2 + 3 p_4 x_4 z_3^3 z_4^2 + 3t p_4 x_4 z_4^3 - 3f p_4 x_4 z_1 z_4^2 + u_4 \tag{3-13}$$

Choose a positive definite control Lyapunov function:

$$V_1 = \frac{1}{2} e_1^2 \tag{3-14}$$

Then by first equation of error dynamics, it is obtained that

$$\dot{V}_1 = e_1(e_2 + p_2 x_2 z_2^3 - p_1 x_2 z_1^3 - 3 p_1 x_1 z_1^2 z_2 + u_1) \tag{3-15}$$

Choose $u_1 = -p_2 x_2 z_2^3 + p_1 x_2 z_1^3 + 3 p_1 x_1 z_1^2 z_2$, $e_2 = \alpha_1(e_1) = -e_1$, Eq (3-15) can be written as

$$\dot{V}_1 = -e_1^2 < 0 \tag{3-16}$$

then $e_1 = 0$ is asymptotically stable. When e_2 is considered as a controller, $\alpha_1(e_1)$ is an estimative function.

Define $W_2 = e_2 - \alpha_1(e_1) = e_2 + e_1$ and

$$\dot{W}_2 = \dot{e}_2 + \dot{e}_1 . \tag{3-17}$$

Choose a positive definite control Lyapunov function:

$$V_2 = V_1 + \frac{1}{2}W_2^2 + \frac{1}{2}\tilde{k}_1^2 \tag{3-18}$$

where $\tilde{k}_1 = k_1 - \hat{k}_1$, $\hat{k}_1$ is estimated value of the unknown parameter k_1.

Differentiating Eq (3-18), we obtain

$$\dot{V}_2 = \dot{V}_1 + W_2\dot{W}_2 + \tilde{k}_1\dot{\tilde{k}}_1 \tag{3-19}$$

$$
\begin{aligned}
\dot{V}_2 = &-e_1^2 + W_2\{W_2 - e_1 - \frac{\hat{k}_1 e_1}{2m_1 l^2} - \frac{\hat{k}_1 p_1 x_1 z_1^3}{2m_1 l^2} + \frac{p_2 k_1 x_1 z_2^3}{2m_1 l^2} + \cdots \\
&+ 3ap_2 x_2 z_1 z_2^2 + 3bp_2 x_2 z_1 z_2^2 z_3 + 3ap_2 x_2 z_1^3 z_2^2 + 3bp_2 x_2 z_1^3 z_2^2 z_3 \\
&+ 3cp_2 x_2 z_2^3 - 3dp_2 x_2 z_2^3 z_3 \\
&- \frac{p_2 z_2^3}{2m_1 + 4m_2 \sin^2 x_1}\left(-\frac{2m_2 g \sin x_1}{l} + \frac{2m_2 A \sin x_3 \sin x_1}{l} - 4m_2 x_2^2 \sin x_1 \cos x_1\right. \\
&\left.+ 2m_1 \sin x_1 \cos x_1 \eta^2 - \frac{k_2 x_2}{l^2}\right) \\
&+ \frac{1}{2m_1 + 4m_2 \sin^2 y_1}\left(-\frac{2m_2 g \sin y_1}{l} + \frac{2m_2 A \sin y_3 \sin y_1}{l} - 4m_2 y_2^2 \sin y_1 \cos y_1\right. \\
&\left.+ 2m_1 \sin y_1 \cos y_1 \eta^2 - \frac{k_2 y_2}{l^2}\right) \\
&+ u_2\} + (k_1 - \hat{k}_1)\dot{\tilde{k}}_1
\end{aligned}
\tag{3-20}
$$

Choose

$$\dot{\tilde{k}}_1 = -\dot{\hat{k}}_1 = -\frac{p_2 x_1 z_2^3 W_2}{2m_1 l^2} \tag{3-21}$$

$$u_2 = -2W_2 + e_1 + \frac{\hat{k}_1 e_1}{2m_1 l^2} + \frac{\hat{k}_1 p_1 x_1 z_1^3}{2m_1 l^2} - \frac{\hat{k}_1 p_2 x_1 z_2^3}{2m_1 l^2}$$

$$-3ap_2 x_2 z_1 z_2^2 - 3bp_2 x_2 z_1 z_2^2 z_3 - 3ap_2 x_2 z_1^3 z_2^2 - 3bp_2 x_2 z_1^3 z_2^2 z_3$$

$$-3cp_2 x_2 z_2^3 + 3dp_2 x_2 z_2^2 z_3$$

$$+ \frac{p_2 z_2^3}{2m_1 + 4m_2 \sin^2 x_1}(-\frac{2m_2 g \sin x_1}{l} + \frac{2m_2 A \sin x_3 \sin x_1}{l} - 4m_2 x_2^2 \sin x_1 \cos x_1 \quad (3\text{-}22)$$

$$+ 2m_1 \sin x_1 \cos x_1 \eta^2 - \frac{k_2 x_2}{l^2})$$

$$- \frac{1}{2m_1 + 4m_2 \sin^2 y_1}(-\frac{2m_2 g \sin y_1}{l} + \frac{2m_2 A \sin y_3 \sin y_1}{l} - 4m2 y_2^2 \sin y_1 \cos y_1$$

$$+ 2m_1 \sin y_1 \cos y_1 \eta^2 - \frac{k_2 y_2}{l^2})$$

Eq (3-20) becomes:

$$\dot{V}_2 = -e_1^2 - W_2^2 < 0 \tag{3-23}$$

then $e_2 = 0$ is asymptotically stable.

Choose a positive definite control Lyapunov function:

$$V_3 = V_1 + V_2 + \frac{1}{2} e_3^2 \tag{3-24}$$

Differentiating Eq (3-24), it is obtained that:

$$\dot{V}_3 = \dot{V}_1 + \dot{V}_2 + e_3 \dot{e}_3$$
$$= -e_1^2 - W_2^2 + e_3(e_4 + p_4 x_4 z_4^3 - p_3 x_4 z_3^3 - 3p_3 x_3 z_3^2 z_4 + u_3) \tag{3-25}$$

Choose $u_3 = -p_4 x_4 z_4^3 + p_3 x_4 z_3^3 + 3p_3 x_3 z_3^2 z_4$, and $e_4 = \alpha_1(e_3) = -e_3$, Eq (3-25)

becomes:

$$\dot{V}_3 = -e_1^2 - W_2^2 - e_3^2 < 0 \tag{3-26}$$

then $e_3 = 0$ is asymptotically stable.

When e_4 is considered as a controller, $\alpha_1(e_3)$ is a estimative function. Define

$$W_4 = e_4 - \alpha_1(e_3) = e_4 + e_3, \text{ then}$$

$$\dot{W}_4 = \dot{e}_4 + \dot{e}_3 \tag{3-27}$$

Choose a positive definite control Lyapunov function:

17

$$V_4 = V_1 + V_2 + V_3 + \frac{1}{2}W_4^2 + \frac{1}{2}\widetilde{A}^2 \tag{3-28}$$

where $\widetilde{A} = A - \hat{A}$.

Differentiating Eq (3-28), it is obtained that

$$
\begin{aligned}
\dot{V}_4 &= \dot{V}_1 + \dot{V}_2 + \dot{V}_3 + W_4\dot{W}_4 + \widetilde{A}\dot{\widetilde{A}} \\
&= -e_1^2 - W_2^2 - e_3^2 + W_4(W_4 - e_3 - \hat{A}\sin y_3 + p_4 A z_4^3 \sin x_3 + 3p_4 x_4 z_3 z_4^2 \\
&\quad + 3p_4 x_4 z_3^3 z_4^2 + 3t p_4 x_4 z_4^3 - 3f p_4 x_4 z_1 z_4^2 + u_4) + (A - \hat{A})\dot{\hat{A}}
\end{aligned}
\tag{3-29}
$$

Choose

$$\dot{\widetilde{A}} = -\dot{\hat{A}} = -p_4 z_4^3 \sin x_3 W_4 \tag{3-30}$$

$$
\begin{aligned}
u_4 &= -2W_4 + e_3 + \hat{A}\sin Y_3 - p_4\hat{A}z_4^3\sin x_3 - 3p_4 x_4 z_3 z_4^2 \\
&\quad - 3p_4 x_4 z_3^3 z_4^2 - 3t p_4 x_4 z_4^3 + 3f p_4 x_4 z_1 z_4^2
\end{aligned}
\tag{3-31}
$$

Eq (3-29) becomes:

$$\dot{V}_4 = -e_1^2 - W_2^2 - e_3^2 - W_4^2 < 0 \tag{3-32}$$

then $e_4 = 0$ is asymptotically stable. The backstepping design is accomplished. Numerical simulations show that the result is satisfactory as shown in Figs 8, 9, 10, 11, 12, 13.

The Lyapunov function $\dot{V}_4$

$$\dot{V}_4 = -e_1^2 - (e_1 + e_2)^2 - e_3^2 - (e_3 + e_4)^2 < 0 \tag{3-33}$$

is a negative semi-definite function of e_1, e_2, e_3, e_4, $\widetilde{k}_1$, $\widetilde{A}$, while from Eqs (3-14), (3-18), (3-24), (3-28)

$$V = V_4 = \frac{1}{2}e_1^2 + \frac{1}{2}(e_1 + e_2)^2 + \frac{1}{2}e_3^2 + \frac{1}{2}(e_3 + e_4)^2 + \frac{1}{2}\widetilde{k}_1^2 + \frac{1}{2}\widetilde{A}^2 \tag{3-34}$$

is a positive definite function of $e_1, e_2, e_3, e_4, \widetilde{k}_1, \widetilde{A}$.

The Lyapunov asymptotical stability theory can not be satisfied in this case. The common origin of error dynamics and parameter update dynamics cannot be determined to be asymptotically stable. By pragmatical asymptotical stability theory (see Appendix-A), D is a 6 -manifold, n = 6 and the number of error state variables p = 4. When $e_1 = e_2 = e_3 = e_4 = 0$ and $\hat{k}_1$, $\hat{A}$ take arbitrary values, $\dot{V} = 0$, so X is a 2D

manifold, m = n – p = 6 – 4 = 2. m + 1≤ n are satisfied. By the pragmatical asymptotical stability theorem, not only the error vector e tends to zero but also all estimated parameters approach their uncertain parameters. PHPHGS of chaotic systems by adaptive backstepping control is accomplished. The equilibrium point $e_1 = e_2 = e_3 = e_4 = \widetilde{k}_1 = \widetilde{A} = 0$ is pragmatically asymptotically stable. The numerical results are shown in Figs 8~13, the generalized synchronization is accomplished after 800s with hybrid projective constants $p_1=1$, $p_2=-1$, $p_3=1$, $p_4=-1$ with $e_1(0)$ is 600, $e_2(0)$ is 1012, $e_3(0)$ is 400, and $e_4(0)$ is 532. The estimated parameters approach the uncertain parameters of the chaotic system with two positive Lyapunov exponents as shown in Figs 12-13. The initial values of estimated parameters are $\widetilde{k}_1(0)=\widetilde{A}(0)=0$.
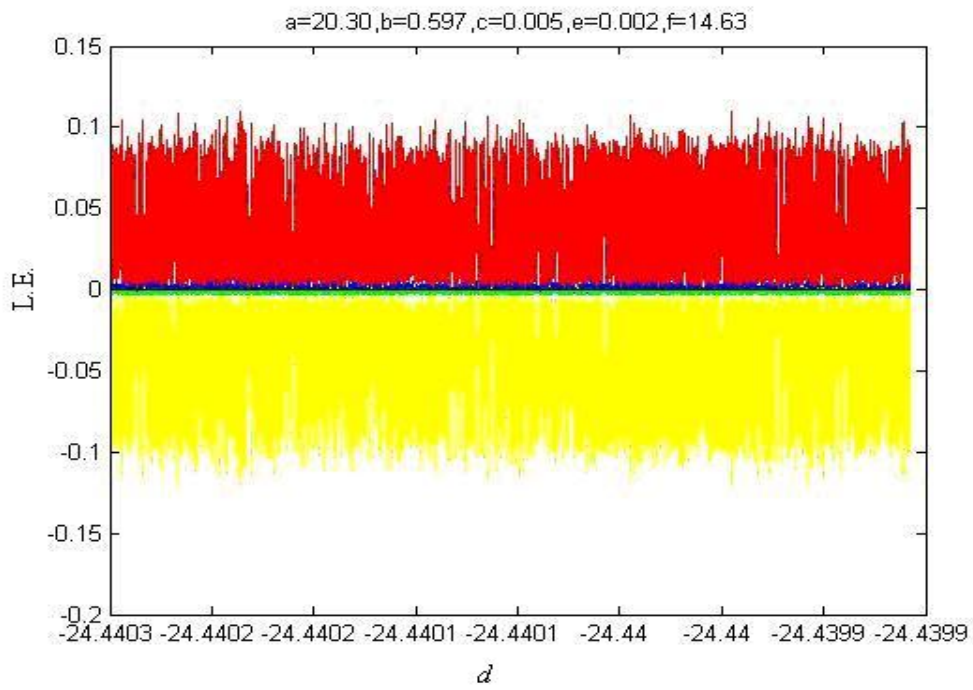
Fig. 7 The Mathieu-Duffing system with two positive Lyapunov exponents.
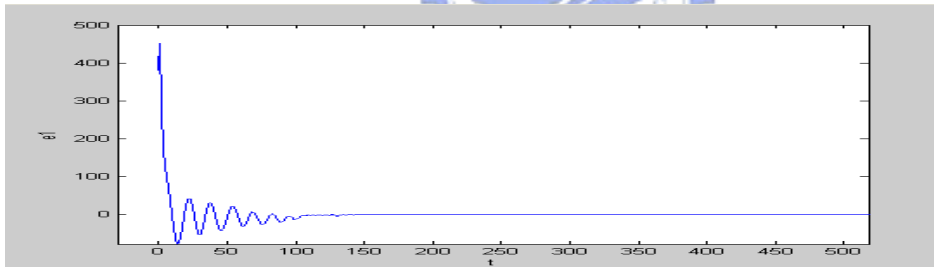
Fig. 8 Time history of e_1 when e_{10} is 381.3.
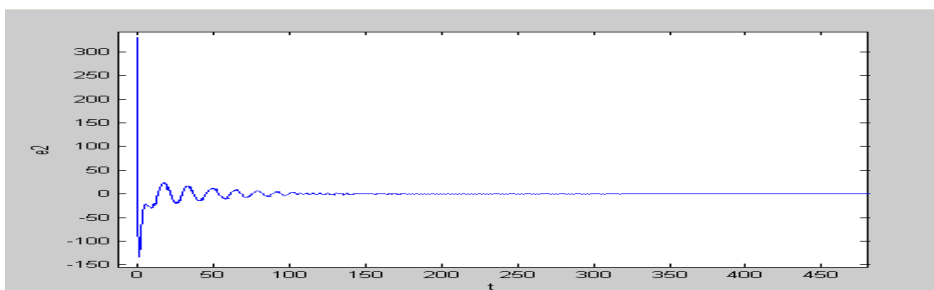
Fig. 9 Time history of e_2 when e_{20} is 330.

20
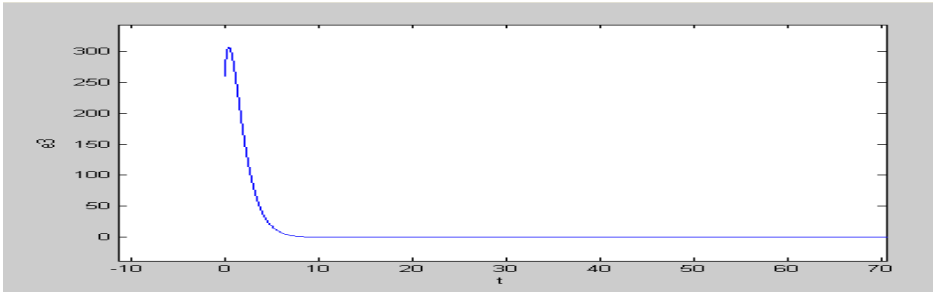
Fig. 10   Time history of e_3 when e_{30} is 260.
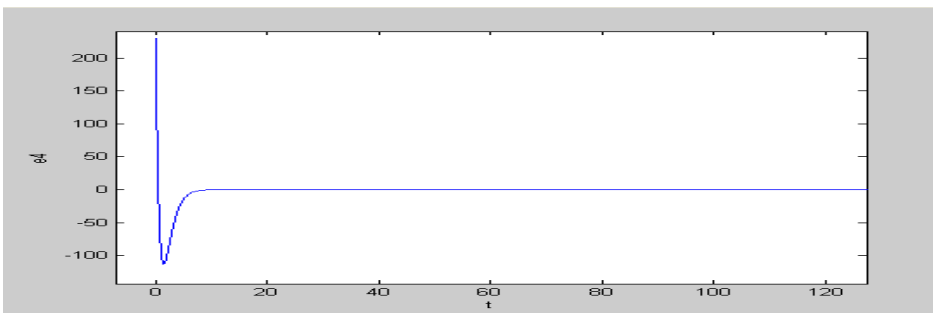
Fig. 11   Time history of e_4 when e_{40} is 230.
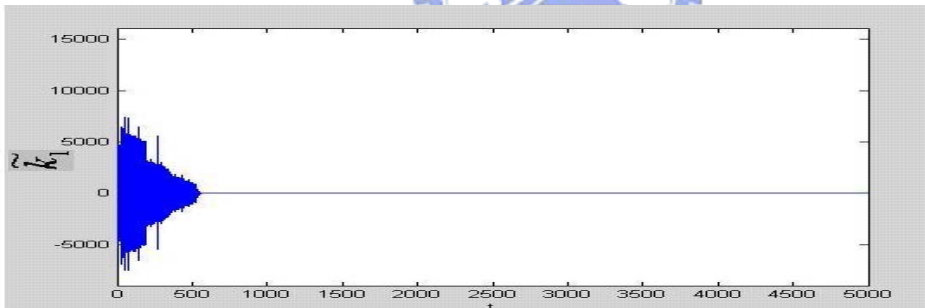
Fig. 12   Time history of $\tilde{k}_1 = k_1 - \hat{k}_1$.
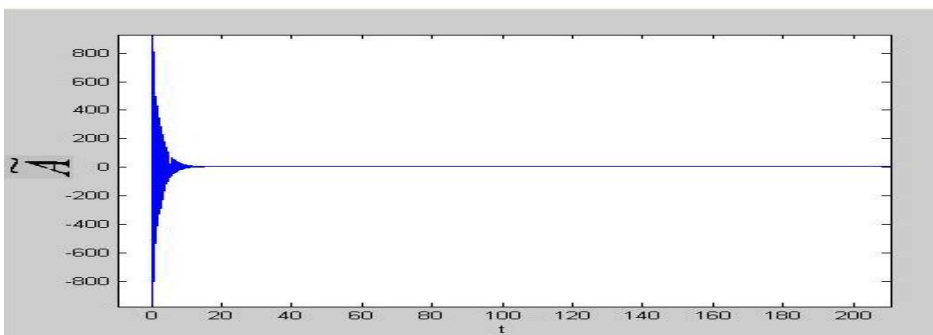
Fig. 13   Time history of $\tilde{A} = A - \hat{A}$.

Chapter 4

Pragmatical Hybrid Projective Hyperchaotic Symplectic Synchronization of Hyperchaotic Tachometer Systems with Different Order System by Adaptive Backstepping Control

In this chapter, GYC pragmatical hybrid projective hyperchaotic symplectic synchronization (PHPHSS) of two hyperchaotic tachometer system with different order system as a constituent by adaptive backstepping control is obtained. The state vector of extended Lorenz system is the constituent of the functional relation between "master"-"slave" and "slave". Traditional generalized synchronizations are special cases of the symplectic synchronization. GYC pragmatical asymptotical stability theorem is used. Both projective synchronization and projective antisynchronization are obtained. Pragmatical hybrid projective hyperchaotic symplectic synchronization is obtained and verified by numerical simulation.

4.1 Synchronization scheme

The partner A is described by

$$\dot{x} = f(x) \tag{4-1}$$

where $x = [x_1, x_2, \cdots, x_n]^T \in \Re^n$ is the state vector function, the parameters of Eq (4-1) are uncertain. The partner B is described by

$$\dot{y} = f(y) + u \tag{4-2}$$

where $y = [y_1, y_2, \cdots, y_n]^T \in \Re^n$ is the state vector, and u is a controlled vector, the parameters of Eq (4-2) are estimated. The functional different order chaotic system is

$$\dot{z} = f(z) \tag{4-3}$$

where $z = [z_1, z_2, \cdots, z_n]^T \in \Re^n$ is a chaotic state vector function and all parameters of

Eq (4-3) are known.

The control target is forcing the state vector y of partner B to track an n-dimensional desired vector

$$h(t) = \left[h_1(t), h_2(t), \cdots, h_n(t)\right] = \left[p_1 x_1(t) y_1(t) z_1(t), p_2 x_2(t) y_2(t) z_2(t), \cdots p_n x_n(t) y_n(t) z_n(t)\right]$$

where $p_1, p_2, \cdots, p_n$ are constant vector with positive and negative entries.

Define the tracking error as

$$e_i(t) = y_i(t) - h_i(t) = y_i - p_i x_i y_i z_i, \text{ (i =1, 2,…,n)} \tag{4-4}$$

where $e(t) = \left[e_1, e_2, \cdots, e_n\right]^T \in \Re^n$ denotes an error vector.

The controlling goal is that the error vector

$$\lim_{t \to \infty} e = 0 \tag{4-5}$$

4.2 Hyperchaotic tachometer system and Lorenz system

The tachometer system of four-dimension shown in Fig. 1 is given by:

$$\begin{cases} \dfrac{d}{dt} x_1 = x_2 \\[2mm] \dfrac{d}{dt} x_2 = \dfrac{-k_1 x_1}{2m_1 l^2} + \cdots + \dfrac{1}{2m_1 + 4m_2 \sin^2 x_1} \left(\dfrac{-2m_2 g \sin x_1}{l} + \dfrac{2m_2 A \sin x_3 \sin x_1}{l} \right. \\[3mm] \qquad \left. - 4m_2 x_2^2 \sin x_1 \cos x_1 + 2m_1 \sin x_1 \cos x_1 \eta^2 - \dfrac{k_2 x_2}{l^2} \right) \\[3mm] \dfrac{d}{dt} x_3 = x_4 \\[2mm] \dfrac{d}{dt} x_4 = -A \sin x_3 \end{cases} \tag{4-6}$$

where x_1, x_2, x_3, x_4 are state variables and k_1, k_2, A, l, g, m_1, m_2 are constants, when $k_1 = 4$, $k_2 = 1$, $m_2 = 3$, m_1=3, A=5, η=4.55, g=9.8, l=1.5, the system exhibits chaotic behavior with hyperchaotic Lyapunov exponents as shown in Fig. 2 .

The Lorenz system of three-dimension is given by:

$$\begin{cases} \dfrac{d}{dt} z_1 = c_1 (z_2 - z_1) \\[2mm] \dfrac{d}{dt} z_2 = c_2 z_1 - z_2 - z_1 z_3 \\[2mm] \dfrac{d}{dt} z_3 = -c_3 z_3 + z_1 z_2 \end{cases} \tag{4-7}$$

where $c_1=10$, $c_2=28$, $c_3=8/3$, the system exhibits chaotic behavior as shown in Fig.

14. Choose Lorenz system as the different order system.

The fourth equation can be chosen as $z_4 = z_1^2$. The equation (4-7) can be extended to

four-state system:

$$\begin{cases} \dfrac{d}{dt} z_1 = c_1 (z_2 - z_1) \\[2mm] \dfrac{d}{dt} z_2 = c_2 z_1 - z_2 - z_1 z_3 \\[2mm] \dfrac{d}{dt} z_3 = -c_3 z_3 + z_1 z_2 \\[2mm] \dfrac{d}{dt} z_4 = 2 c_1 z_1 (z_2 - z_1) \end{cases} \tag{4-8}$$

4.3 Numerical simulations for pragmatical hybrid projective hyperchaotic symplectic synchronization of hyperchaotic tachometer systems with different order system by adaptive backstepping control

The partner A of the tachometer system is:

$$\begin{cases} \dfrac{d}{dt} x_1 = x_2 \\[2mm] \dfrac{d}{dt} x_2 = \dfrac{-k_1 x_1}{2 m_1 l^2} + \cdots + \dfrac{1}{2 m_1 + 4 m_2 \sin^2 x_1} \left(\dfrac{-2 m_2 g \sin x_1}{l} + \dfrac{2 m_2 A \sin x_3 \sin x_1}{l} \right. \\[2mm] \left. \qquad - 4 m_2 x_2^2 \sin x_1 \cos x_1 + 2 m_1 \sin x_1 \cos x_1 \eta^2 - \dfrac{k_2 x_2}{l^2} \right) \\[2mm] \dfrac{d}{dt} x_3 = x_4 \\[2mm] \dfrac{d}{dt} x_4 = -A \sin x_3 \end{cases} \tag{4-9}$$

where k_1, A are uncertain parameters.

The partner B of the tachometer system is:

$$
\begin{cases}
\dfrac{d}{dt} y_1 = y_2 \\[2mm]
\dfrac{d}{dt} y_2 = \dfrac{-\hat{k}_1 y_1}{2 m_1 l^2} + \cdots + \dfrac{1}{2 m_1 + 4 m_2 \sin^2 y_1}\left(\dfrac{-2 m_2 g \sin y_1}{l} + \dfrac{2 m_2 A \sin y_3 \sin y_1}{l} \right. \\[3mm]
\qquad\quad \left. - 4 m_2 y_2^2 \sin y_1 \cos y_1 + 2 m_1 \sin y_1 \cos y_1 \eta^2 - \dfrac{k_2 y_2}{l^2} \right) \\[3mm]
\dfrac{d}{dt} y_3 = y_4 \\[2mm]
\dfrac{d}{dt} y_4 = -\hat{A} \sin y_3
\end{cases}
\tag{4-10}
$$

where $\hat{k}_1$, $\hat{A}$ are estimated parameters.

Choose chaotic extended Lorenz system as a different order system:

$$
\begin{cases}
\dfrac{d}{dt} z_1 = c_1 (z_2 - z_1) \\[2mm]
\dfrac{d}{dt} z_2 = c_2 z_1 - z_2 - z_1 z_3 \\[2mm]
\dfrac{d}{dt} z_3 = -c_3 z_3 + z_1 z_2 \\[2mm]
\dfrac{d}{dt} z_4 = 2 c_1 z_1 (z_2 - z_1)
\end{cases}
\tag{4-11}
$$

where $c_1 = 10$, $c_2 = 28$, $c_3 = 8/3$.

In order to lead (y_1, y_2, y_3, y_4) to ($p_1 x_1 y_1 z_1$, $p_2 x_2 y_2 z_2$, $p_3 x_3 y_3 z_3$, $p_4 x_4 y_4 z_4$) , add u_1, u_2, u_3, u_4 as controllers to Eq (4-10):

$$\begin{cases} \dfrac{d}{dt}y_1 = y_2 + u_1 \\[2mm] \dfrac{d}{dt}y_2 = \dfrac{-\hat{k}_1 y_1}{2m_1 l^2} + \cdots + \dfrac{1}{2m_1 + 4m_2 \sin^2 y_1}\left(\dfrac{-2m_2 g \sin y_1}{l} + \dfrac{2m_2 A \sin y_3 \sin y_1}{l}\right. \\[3mm] \qquad\qquad \left. - 4m_2 y_2^2 \sin y_1 \cos y_1 + 2m_1 \sin y_1 \cos y_1 \eta^2 - \dfrac{k_2 y_2}{l^2}\right) + u_2 \\[3mm] \dfrac{d}{dt}y_3 = y_4 + u_3 \\[2mm] \dfrac{d}{dt}y_4 = -\hat{A}\sin y_3 + u_4 \end{cases} \qquad (4\text{-}12)$$

Define error states as follows:

$$\begin{cases} e_1 = y_1 - p_1 x_1 y_1 z_1 \\ e_2 = y_2 - p_2 x_2 y_2 z_2 \\ e_3 = y_3 - p_3 x_3 y_3 z_3 \\ e_4 = y_4 - p_4 x_4 y_4 z_4 \end{cases} \qquad (4\text{-}13)$$

where x_1, x_2, x_3, x_4, z_1, z_2, z_3, z_4, y_1, y_2, y_3, y_4 are states, p_1, p_2, p_3, p_4 are constants, both positive and negative. We choose p_1=0.0003, p_2=-0.0004, p_3=0.0006, p_4=-0.0002 to give hybrid projective synchronization.

Differentiating Eq (4-13) with respect to time, we obtain the error dynamics:

$$\dot{e}_1 = e_2 + p_2 x_2 y_3 z_2 - p_1 x_2 y_1 z_1 - p_1 c_1 x_1 y_1 z_2 + p_1 c_1 x_1 y_1 z_1 - p_1 x_1 y_2 z_1 + u_1$$

$$\begin{aligned} \dot{e}_2 =\ & -\dfrac{\hat{k}_1 e_1}{2m_1 l^2} - \dfrac{\hat{k}_1 p_1 x_1 y_1 z_1}{2m_1 l^2} + \dfrac{p_2 \hat{k}_1 x_2 y_1 z_2}{2m_1 l^2} + \dfrac{p_2 k_1 x_1 y_2 z_2}{2m_1 l^2} \\ & - p_2 c_2 x_2 y_2 z_1 + p_2 x_2 y_2 z_2 + p_2 x_2 y_2 z_1 z_3 + \cdots \\ & + \dfrac{1}{2m_1 + 4m_2 \sin^2 y_1}\left(-\dfrac{2m_2 g \sin y_1}{l} + \dfrac{2m_2 A \sin y_3 \sin y_1}{l} - 4m_2 y_2^2 \sin y_1 \cos y_1\right. \\ & \left. + 2m_1 \sin y_1 \cos y_1 \eta^2 - \dfrac{k_2 y_2}{l^2}\right) \\ & - \dfrac{p_2 y_2 z_2}{2m_1 + 4m_2 \sin^2 x_1}\left(-\dfrac{2m_2 g \sin x_1}{l} + \dfrac{2m_2 A \sin x_3 \sin x_1}{l} - 4m_2 x_2^2 \sin x_1 \cos x_1\right. \\ & \left. + 2m_1 \sin x_1 \cos x_1 \eta^2 - \dfrac{k_2 x_2}{l^2}\right) \\ & - \dfrac{p_2 x_2 z_2}{2m_1 + 4m_2 \sin^2 y_1}\left(\dfrac{-2m_2 g \sin y_1}{l} + \dfrac{2m_2 A \sin y_3 \sin y_1}{l} - 4m_2 y_2^2 \sin y_1 \cos y_1\right. \\ & \left. + 2m_1 \sin y_1 \cos y_1 \eta^2 - \dfrac{k_2 y_2}{l^2}\right) + u_2 \end{aligned} \qquad (4\text{-}14)$$

$$\dot{e}_3 = e_4 + p_4 x_4 y_4 z_4 - p_3 x_4 y_3 z_3 + p_3 c_3 x_3 y_3 z_3 - p_3 x_3 y_3 z_1 z_2 - p_3 x_3 z_3 y_4 + u_3$$

$$\dot{e}_4 = -\hat{A}\sin y_3 + p_4 A y_4 z_4 \sin x_3 - 2 p_4 c_1 x_4 y_4 z_1 z_2 + 2 p_4 c_1 x_4 y_4 z_1^2 + p_4 \hat{A} x_4 z_4 \sin y_3 + u_4$$

Choose a positive definite Lyapunov function:

$$V_1 = \frac{1}{2} s_1 e_1^2 \qquad\qquad (4\text{-}15)$$

where s_1 is a positive constant. Then by first equation of error dynamics (4-14), it is obtained that

$$\dot{V}_1 = s_1 e_1 (e_2 + p_2 x_2 y_3 z_2 - p_1 x_2 y_1 z_1 - p_1 c_1 x_1 y_1 z_2 + p_1 c_1 x_1 y_1 z_1 - p_1 x_1 y_2 z_1 + u_1) \qquad (4\text{-}16)$$

Choose $u_1 = -p_2 x_2 y_3 z_2 + p_1 x_2 y_1 z_1 + p_1 c_1 x_1 y_1 z_2 - p_1 c_1 x_1 y_1 z_1 + p_1 x_1 y_2 z_1$, $e_2 = \alpha_1(e_1) = -e_1$,

Eq (4-16) could be written as

$$\dot{V}_1 = -s_1 e_1^2 < 0 \qquad\qquad (4\text{-}17)$$

$e_1 = 0$ is asymptotically stable. When e_2 is considered as a controller, $\alpha_1(e_1)$ is an estimative function. Define $W_2 = e_2 - \alpha_1(e_1) = e_2 + e_1$ and

$$\dot{W}_2 = \dot{e}_2 + \dot{e}_1 \qquad\qquad (4\text{-}18)$$

Choose a positive definite Lyapunov function:

$$V_2 = V_1 + \frac{1}{2} s_2 W_2^2 + \frac{1}{2} \tilde{k}_1^2 \qquad\qquad (4\text{-}19)$$

where $\tilde{k}_1 = k_1 - \hat{k}_1$, $\hat{k}_1$ is estimated value of the unknown parameter k_1, s_2 is a positive constant. Differentiating Eq (4-19), we obtain

$$\dot{V}_2 = \dot{V}_1 + s_2 W_2 \dot{W}_2 + \tilde{k}_1 \dot{\tilde{k}}_1$$

$$
\begin{aligned}
\dot{V}_2 = &-e_1^2 + s_2 W_2 \Big\{ W_2 - e_1 - \frac{\hat{k}_1 e_1}{2m_1 l^2} - \frac{\hat{k}_1 p_1 x_1 y_1 z_1}{2m_1 l^2} + \frac{p_2 \hat{k}_1 x_2 y_1 z_2}{2m_1 l^2} + \frac{p_2 k_1 x_1 y_2 z_2}{2m_1 l^2} \\
&- p_2 c_2 x_2 y_2 z_1 + p_2 x_2 y_2 z_2 + p_2 x_2 y_2 z_1 z_3 + \cdots \\
&+ \frac{1}{2m_1 + 4m_2 \sin^2 y_1}\Big(-\frac{2m_2 g \sin y_1}{l} + \frac{2m_2 A \sin y_3 \sin y_1}{l} - 4m_2 y_2^2 \sin y_1 \cos y_1 \\
&+ 2m_1 \sin y_1 \cos y_1 \eta^2 - \frac{k_2 y_2}{l^2}\Big) \\
&- \frac{p_2 y_2 z_2}{2m_1 + 4m_2 \sin^2 x_1}\Big(-\frac{2m_2 g \sin x_1}{l} + \frac{2m_2 A \sin x_3 \sin x_1}{l} - 4m_2 x_2^2 \sin x_1 \cos x_1 \\
&+ 2m_1 \sin x_1 \cos x_1 \eta^2 - \frac{k_2 x_2}{l^2}\Big) \\
&- \frac{p_2 x_2 z_2}{2m_1 + 4m_2 \sin^2 y_1}\Big(\frac{-2m_2 g \sin y_1}{l} + \frac{2m_2 A \sin y_3 \sin y_1}{l} - 4m_2 y_2^2 \sin y_1 \cos y_1 \\
&+ 2m_1 \sin y_1 \cos y_1 \eta^2 - \frac{k_2 y_2}{l^2}\Big) \\
&+ u_2 \Big\} + (k_1 - \hat{k}_1)\dot{\tilde{k}}_1
\end{aligned}
$$

$(4\text{-}20)$ $(4\text{-}21)$

Choose

$$\dot{\hat{k}}_1 = -\dot{\tilde{k}}_1 = -\frac{p_2 x_1 y_2 z_2 W_2 s_2}{2m_1 l^2} \tag{4-22}$$

$$u_2 = -2W_2 + e_1 + \frac{\hat{k}_1 e_1}{2m_1 l^2} + \frac{\hat{k}_1 p_1 x_1 y_1 z_1}{2m_1 l^2} - \frac{p_2 \hat{k}_1 x_2 y_1 z_2}{2m_1 l^2} - \frac{p_2 \hat{k}_1 x_1 y_2 z_2}{2m_1 l^2}$$

$$+ p_2 c_2 x_2 y_2 z_1 - p_2 x_2 y_2 z_2 - p_2 x_2 y_2 z_1 z_3 + \cdots$$

$$- \frac{1}{2m_1 + 4m_2 \sin^2 y_1} \left(-\frac{2m_2 g \sin y_1}{l} + \frac{2m_2 A \sin y_3 \sin y_1}{l} - 4m_2 y_2^2 \sin y_1 \cos y_1 \right.$$

$$+ 2m_1 \sin y_1 \cos y_1 \eta^2 - \frac{k_2 y_2}{l^2} \right)$$

$$+ \frac{p_2 y_2 z_2}{2m_1 + 4m_2 \sin^2 x_1} \left(-\frac{2m_2 g \sin x_1}{l} + \frac{2m_2 A \sin x_3 \sin x_1}{l} - 4m_2 x_2^2 \sin x_1 \cos x_1 \right.$$

$$+ 2m_1 \sin x_1 \cos x_1 \eta^2 - \frac{k_2 x_2}{l^2} \right)$$

$$+ \frac{p_2 x_2 z_2}{2m_1 + 4m_2 \sin^2 y_1} \left(\frac{-2m_2 g \sin y_1}{l} + \frac{2m_2 A \sin y_3 \sin y_1}{l} - 4m_2 y_2^2 \sin y_1 \cos y_1 \right.$$

$$+ 2m_1 \sin y_1 \cos y_1 \eta^2 - \frac{k_2 y_2}{l^2} \right) \tag{4-23}$$

Take the initial value of uncertain parameter as $\hat{k}_1(0) = 3.998440$. Eq (4-21) becomes:

$$\dot{V}_2 = -s_1 e_1^2 - s_2 W_2^2 < 0 \tag{4-24}$$

$e_2 = 0$ is asymptotically stable.

Choose a positive definite Lyapunov function:

$$V_3 = V_1 + V_2 + \frac{1}{2} s_3 e_3^2 \tag{4-25}$$

where s_3 is a positive constant. Differentiating Eq (4-25), it is obtained that:

$$\dot{V}_3 = \dot{V}_1 + \dot{V}_2 + s_3 e_3 \dot{e}_3$$

$$= -e_1^2 - W_2^2 + s_3 e_3 (e_4 + p_4 x_4 y_4 z_4 - p_3 x_4 y_3 z_3 + p_3 c_3 x_3 y_3 z_3$$

$$- p_3 x_3 y_3 z_1 z_2 - p_3 x_3 z_3 y_4 + u_3) \tag{4-26}$$

Choose

$$u_3 = -p_4 x_4 y_4 z_4 + p_3 x_4 y_3 z_3 - p_3 c_3 x_3 y_3 z_3 + p_3 x_3 y_3 z_1 z_2 + p_3 x_3 z_3 y_4 + u_3$$

$$e_4 = \alpha_1(e_3) = -e_3$$

Eq (4-26) becomes:

$$\dot{V}_3 = -s_1 e_1^2 - s_2 W_2^2 - s_3 e_3^2 < 0 \tag{4-27}$$

$e_3 = 0$ is asymptotically stable.

When e_4 is considered as a controller, $\alpha_1(e_3)$ is a estimative function. Define $W_4 = e_4 - \alpha_1(e_3) = e_4 + e_3$, then

$$\dot{W}_4 = \dot{e}_4 + \dot{e}_3 \tag{4-28}$$

Choose a positive definite Lyapunov function:

$$V_4 = V_1 + V_2 + V_3 + \frac{1}{2}s_4 W_4^2 + \frac{1}{2}\tilde{A}^2 \tag{4-29}$$

where $\tilde{A} = A - \hat{A}$, s_4 is a positive constant.

Differentiating Eq (4-29), it is obtained that

$$\begin{aligned} \dot{V}_4 &= \dot{V}_1 + \dot{V}_2 + \dot{V}_3 + s_4 W_4 \dot{W}_4 + \tilde{A}\dot{\tilde{A}} \\ &= -s_1 e_1^2 - s_2 W_2^2 - s_3 e_3^2 + s_4 W_4(e_4 - \hat{A}\sin y_3 + p_4 A y_4 z_4 \sin x_3 \\ &\quad - 2p_4 c_1 x_4 y_4 z_1 z_2 + 2p_4 c_1 x_4 y_4 z_1^2 + p_4 \hat{A} x_4 z_4 \sin y_3 + u_4) + (A - \hat{A})\dot{\tilde{A}} \end{aligned} \tag{4-30}$$

Choose

$$\dot{\tilde{A}} = -\dot{\hat{A}} = -p_4 y_4 z_4 \sin x_3 W_4 \tag{4-31}$$

$$\begin{aligned} u_4 &= -2W_4 + e_3 + \hat{A}\sin y_3 - p_4 \hat{A} y_4 z_4 \sin x_3 + 2p_4 c_1 x_4 y_4 z_1 z_2 \\ &\quad - 2p_4 c_1 x_4 y_4 z_1^2 - p_4 \hat{A} x_4 z_4 \sin y_3 \end{aligned} \tag{4-32}$$

Take the initial value of uncertain parameter as $\hat{A}(0) = 4.99379$. Eq (4-30) becomes:

$$\dot{V}_4 = -s_1 e_1^2 - s_2 W_2^2 - s_3 e_3^2 - s_4 W_4^2 < 0 \tag{4-33}$$

$e_4 = 0$ is asymptotically stable. The backstepping design is accomplished. Numerical simulations show that the result is satisfactory as shown in Figs 15~20.

The Lyapunov function $\dot{V}_4$

$$\dot{V}_4 = -s_1 e_1^2 - s_2(e_1 + e_2)^2 - s_3 e_3^2 - s_4(e_3 + e_4)^2 < 0 \tag{4-34}$$

is a negative semi-definite function of e_1, e_2, e_3, e_4, $\tilde{k}_1$, $\tilde{A}$, while from Eqs (4-15), (4-19), (4-25), (4-29)

$$V = V_4 = \frac{1}{2}s_1 e_1^2 + \frac{1}{2}s_2(e_1 + e_2)^2 + \frac{1}{2}s_3 e_3^2 + \frac{1}{2}s_4(e_3 + e_4)^2 + \frac{1}{2}\tilde{k}_1^2 + \frac{1}{2}\tilde{A}^2 \tag{4-35}$$

is a positive definite function of $e_1, e_2, e_3, e_4, \tilde{k}_1, \tilde{A}$.

The Lyapunov asymptotical stability theory can not be satisfied in this case. The common origin of error dynamics and parameter update dynamics cannot be determined

to be asymptotically stable. By GYC pragmatical asymptotical stability theorem (see Appendix-A) D is a 6 -manifold, n = 6 and the number of error state variables p = 4. When $e_1 = e_2 = e_3 = e_4 = 0$ and $\hat{k}_1$, $\hat{A}$ take arbitrary values , $\dot{V} = 0$, so X is a 2D manifold, m = n – p = 6 – 4 = 2. m + 1≤ n are satisfied. By GYC the pragmatical asymptotical stability theorem, not only the error vector e tends to zero but also all estimated parameters approach their uncertain parameters. PHPHSS of chaotic systems by adaptive backstepping control is accomplished. The equilibrium point $e_1 = e_2 = e_3 = e_4 = \widetilde{k}_1 = \widetilde{A} = 0$ is pragmatically asymptotically stable. The numerical results are shown in Figs 15~20, the generalized synchronization is accomplished after 20s with $s_1 = s_2 = s_3 = s_4 = 0.0001$ and hybrid projective constants p_1 =0.0003, p_2 =-0.0004, p_3 =0.0006, p_4 =-0.0002, $e_1(0)$ =697.9, $e_2(0)$ =654.16, $e_3(0)$ = 478.402, and $e_4(0) =$ 464.3712. The estimated parameters approach the uncertain parameters of the hyperchaotic system as shown in Figs 19-20. The initial values of estimated parameters are $\widetilde{k}_1(0) = \widetilde{A}(0) = 0$.

30
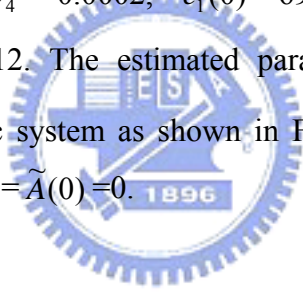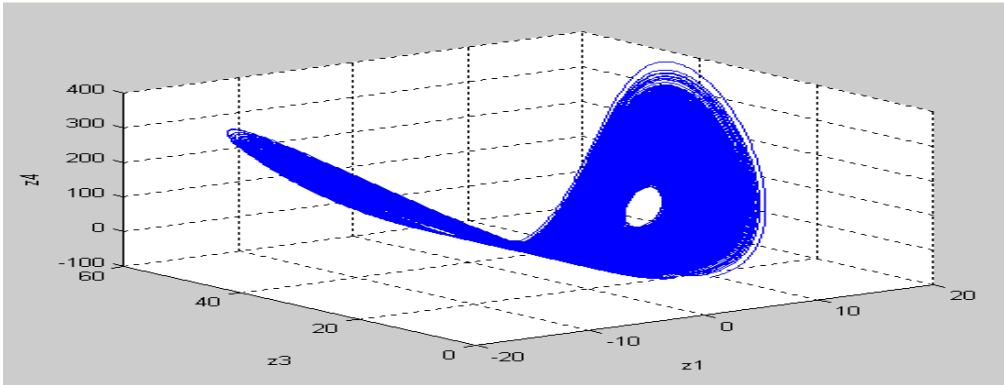
Fig. 14   Phase portrait of chaotic for Lorenz system.
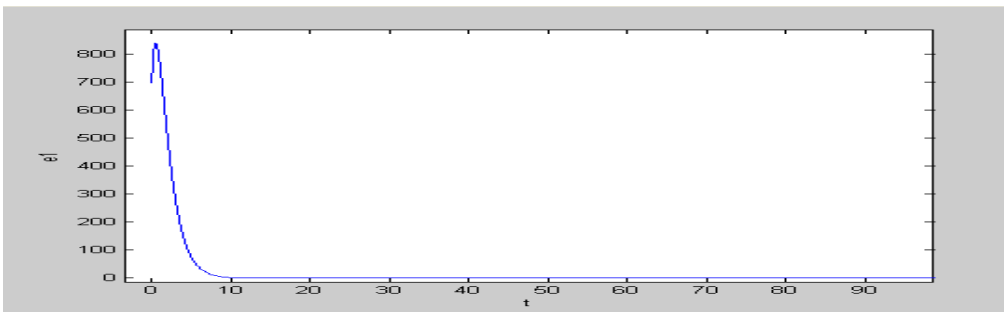

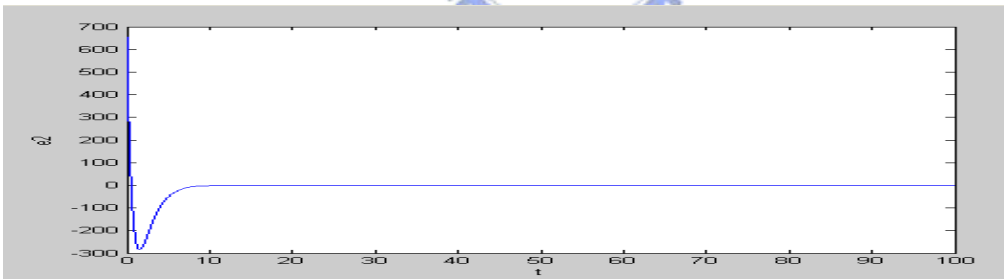Fig. 15   Time history of e_1 when e_{10} is 697.9.

Fig. 16   Time history of e_2 when e_{20} is 654.16.
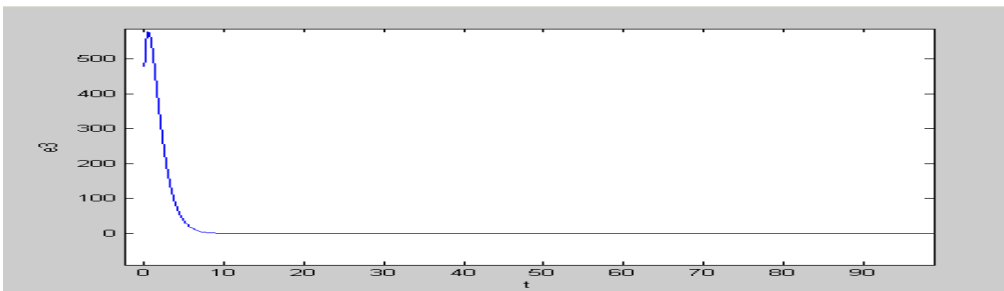
Fig. 17   Time history of e_3 when e_{30} is 478.402.
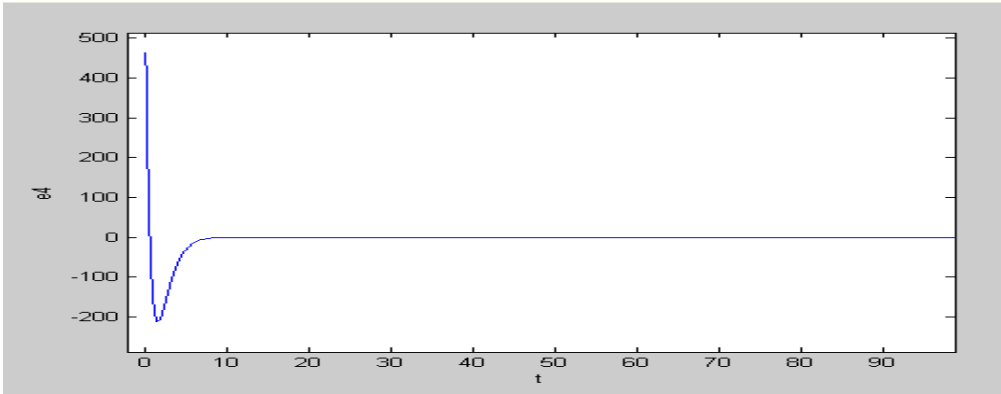
Fig. 18　　Time history of e_4　when e_{40}　is　464.3712.
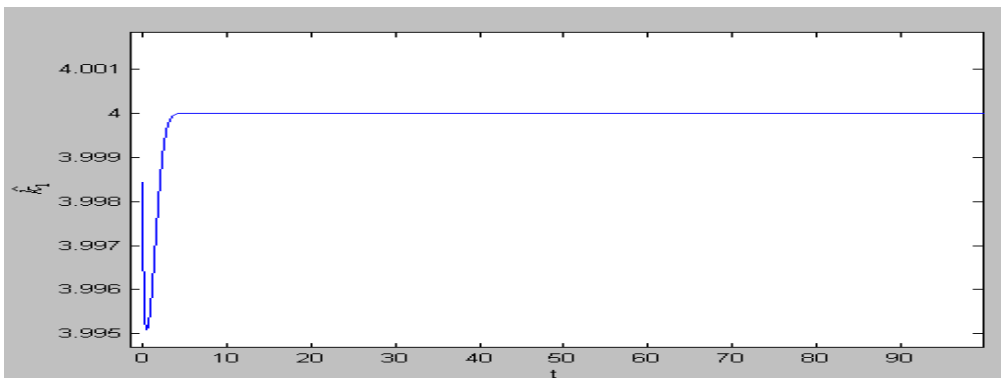
Fig. 19　　Time history of $\hat{k}_1$.
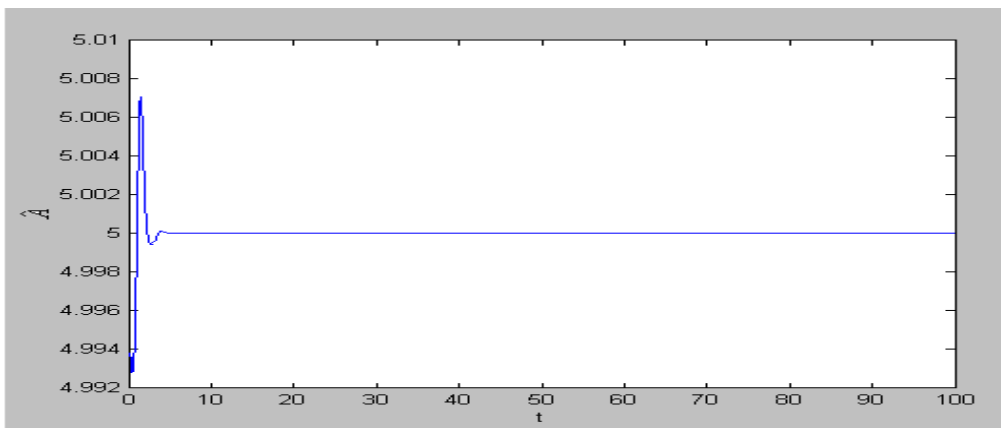
Fig. 20　　Time history of $\hat{A}$.

Chapter 5

Hyperchaotic Generalized Synchronization of Tachometer Systems by GYC Partial Region Stability Theory

In this chapter, hyperchaotic generalized synchronization of tachometer systems by GYC partial region stability theory is proposed. The Lyapunov function is a simple linear function and the controllers are simpler by using the GYC partial region stability theory. The simulation results are more precise because the controllers are in lower degree than that of traditional controllers. Hyperchaotic generalized synchronization of tachometer system by GYC partial region stability is obtained and verified by numerical simulation.

5.1 Chaos generalized synchronization strategy by GYC partial region stability theory

Consider the following unidirectional coupled chaotic systems

$$\dot{\mathbf{x}} = \mathbf{f}(t, \mathbf{x})$$
$$\dot{\mathbf{y}} = \mathbf{h}(t, \mathbf{y}) + \mathbf{u}$$
(5-1)

where $\mathbf{x} = [x_1, x_2, \cdots, x_n]^T \in R^n$, $\mathbf{y} = [y_1, y_2, \cdots, y_n]^T \in R^n$ denote two state vectors, $\mathbf{f}$ and $\mathbf{h}$ are nonlinear vector functions, and $\mathbf{u} = [u_1, u_2, \cdots, u_n]^T \in R^n$ is a control input vector.

The generalized synchronization can be accomplished when $t \to \infty$, the limit of the error vector $\mathbf{e} = [e_1, e_2, \cdots, e_n]^T$ approaches zero:

$$\lim_{t \to \infty} \mathbf{e} = 0$$
(5-2)

where

$$\mathbf{e} = \mathbf{G}(\mathbf{x}) - \mathbf{y}$$
(5-3)

By using the GYC partial region stability theory (Appendix-B), the Lyapunov function is a homogeneous linear function and the controllers can be designed in lower degree.

5.2 Hyperchaotic tachometer system and a new hyperchaotic Mathieu-Duffing system

The tachometer system of four-dimension shown in Fig. 1 is given by:

$$
\begin{cases}
\dfrac{d}{dt}x_1 = x_2 \\[2mm]
\dfrac{d}{dt}x_2 = \dfrac{1}{2m_1 + 4m_2 \sin^2 x_1}\left(\dfrac{-2m_2 g \sin x_1}{l} + \dfrac{2m_2 A \sin x_3 \sin x_1}{l}\right. \\[2mm]
\qquad\qquad \left. -4m_2 x_2^2 \sin x_1 \cos x_1 + 2m_1 \sin x_1 \cos x_1 \eta^2 - \dfrac{k_1 x_1}{l^2} - \dfrac{k_2 x_2}{l^2}\right) \\[2mm]
\dfrac{d}{dt}x_3 = x_4 \\[2mm]
\dfrac{d}{dt}x_4 = -A \sin x_3
\end{cases}
\tag{5-4}
$$

where x_1, x_2, x_3, x_4 are state variables and k_1, k_2, A, l, g, m_1, m_2 are constants, when $k_1 = 4$, $k_2 = 1$, $m_2 = 3$, $m_1 = 3$, A=5, $\eta = 4.55$, g=9.8, l=1.5. The system exhibits chaotic behavior with hyperchaotic Lyapunov exponents in Fig. 2. Its phase portrait as shown in Fig. 21.

The new hyperchaotic Mathieu-Duffing System is given by:

$$
\begin{cases}
\dfrac{d}{dt}z_1 = z_2 \\[2mm]
\dfrac{d}{dt}z_2 = -az_1 - bz_3 z_1 - az_1^3 - bz_3 z_1^3 - cz_2 + dz_3 \\[2mm]
\dfrac{d}{dt}z_3 = z_4 \\[2mm]
\dfrac{d}{dt}z_4 = -z_3 - z_3^3 - tz_4 + fz_1
\end{cases}
\tag{5-5}
$$

where its initial states is (5, 6, 4, 3), system parameters are a=5, b=0.597, c=0.005, d=-5, t=0.002, f=9, the system exhibits chaotic behavior with hyperchaotic Lyapunov exponents and its phase portrait as shown in Fig. 7 and Fig. 22.

5.3 Numerical simulations for hyperchaotic generalized synchronization of tachometer system by GYC partial region stability theory

The tachometer system is the master system:

$$
\begin{cases}
\dfrac{d}{dt}x_1 = x_2 \\[2mm]
\dfrac{d}{dt}x_2 = \dfrac{1}{2m_1 + 4m_2 \sin^2 x_1}\left(\dfrac{-2m_2 g \sin x_1}{l} + \dfrac{2m_2 A \sin x_3 \sin x_1}{l}\right. \\[2mm]
\qquad \left. -4m_2 x_2^2 \sin x_1 \cos x_1 + 2m_1 \sin x_1 \cos x_1 \eta^2 - \dfrac{k_1 x_1}{l^2} - \dfrac{k_2 x_2}{l^2}\right) \\[2mm]
\dfrac{d}{dt}x_3 = x_4 \\[2mm]
\dfrac{d}{dt}x_4 = -A \sin x_3
\end{cases}
\tag{5-6}
$$

The slave system is as follow:

$$
\begin{cases}
\dfrac{d}{dt}y_1 = y_2 + u_1 \\[2mm]
\dfrac{d}{dt}y_2 = \dfrac{1}{2m_1 + 4m_2 \sin^2 y_1}\left(\dfrac{-2m_2 g \sin y_1}{l} + \dfrac{2m_2 A \sin y_3 \sin y_1}{l}\right. \\[2mm]
\qquad \left. -4m_2 y_2^2 \sin y_1 \cos y_1 + 2m_1 \sin y_1 \cos y_1 \eta^2 - \dfrac{k_1 y_1}{l^2} - \dfrac{k_2 y_2}{l^2}\right) + u_2 \\[2mm]
\dfrac{d}{dt}y_3 = y_4 + u_3 \\[2mm]
\dfrac{d}{dt}y_4 = -A \sin y_3 + u_4
\end{cases}
\tag{5-7}
$$

CASE I. The generalized synchronization error function is $e = y - x + g$.

Our goal is $y = x - g$, i.e. $\lim\limits_{t\to\infty} e = \lim\limits_{t\to\infty}(y - x + g) = 0$ $\qquad$ (5-8)

where $g_1 = g_2 = g_3 = g_4 = 50$ are constants.

The error dynamics becomes:

$$\dot{e}_1 = \dot{y}_1 - \dot{x}_1 = y_2 - x_2 + 2e_2^2 - 2e_2^2 + u_1$$

$$\dot{e}_2 = \dot{y}_2 - \dot{x}_2$$

$$= \frac{1}{2m_1 + 4m_2 \sin^2 y_1}\left(\frac{-2m_2 g \sin y_1}{l} + \frac{2m_2 A \sin y_3 \sin y_1}{l}\right.$$

$$\left. -4m_2 y_2^2 \sin y_1 \cos y_1 + 2m_1 \sin y_1 \cos y_1 \eta^2 - \frac{k_1 y_1}{l^2} - \frac{k_2 y_2}{l^2}\right)$$

$$- \frac{1}{2m_1 + 4m_2 \sin^2 x_1}\left(\frac{-2m_2 g \sin x_1}{l} + \frac{2m_2 A \sin x_3 \sin x_1}{l}\right.$$

$$\left. -4m_2 x_2^2 \sin x_1 \cos x_1 + 2m_1 \sin x_1 \cos x_1 \eta^2 - \frac{k_1 x_1}{l^2} - \frac{k_2 x_2}{l^2}\right)$$ $\qquad$ (5-9)

$$+2e_2^2 - 2e_2^2 + u_2$$

$$\dot{e}_3 = \dot{y}_3 - \dot{x}_3 = y_4 - x_4 + 2e_3^2 - 2e_3^2 + u_3$$

$$\dot{e}_4 = \dot{y}_4 - \dot{x}_4 = -A \sin y_3 + A \sin x_3 + 2e_3^2 - 2e_3^2 + u_4$$

Let initial state be $(x_{10}, x_{20}, x_{30}, x_{40}) = (1.53, -0.47, 1.415, 0.5)$, $(y_{10}, y_{20}, y_{30}, y_{40}) = (1.7, 1, 1.6, 0.8)$, we find that the error dynamics always exists in first quadrant as shown in Fig. 23. By GYC partial region asymptotical stability theorem, one can choose a linear positive definite Lyapunov function in first quadrant:

$$V = e_1 + e_2 + e_3 + e_4 \qquad (5\text{-}10)$$

Its time derivative is

$$\dot{V} = \dot{e}_1 + \dot{e}_2 + \dot{e}_3 + \dot{e}_4$$

$$= \left(y_2 - x_2 + 2e_2^2 - 2e_2^2 + u_1 \right)$$

$$+ \left(\frac{1}{2m_1 + 4m_2 \sin^2 y_1} \left(\frac{-2m_2 g \sin y_1}{l} + \frac{2m_2 A \sin y_3 \sin y_1}{l} \right. \right.$$

$$\left. -4m_2 y_2^2 \sin y_1 \cos y_1 + 2m_1 \sin y_1 \cos y_1 \eta^2 - \frac{k_1 y_1}{l^2} - \frac{k_2 y_2}{l^2} \right)$$

$$- \frac{1}{2m_1 + 4m_2 \sin^2 x_1} \left(\frac{-2m_2 g \sin x_1}{l} + \frac{2m_2 A \sin x_3 \sin x_1}{l} \right.$$

$$\left. -4m_2 x_2^2 \sin x_1 \cos x_1 + 2m_1 \sin x_1 \cos x_1 \eta^2 - \frac{k_1 x_1}{l^2} - \frac{k_2 x_2}{l^2} \right)$$

$$+ 2e_2^2 - 2e_2^2 + u_2) + (y_4 - x_4 + 2e_3^2 - 2e_3^2 + u_3)$$

$$+ (-A \sin y_3 + A \sin x_3 + 2e_3^2 - 2e_3^2 + u_4)$$

(5-11)

Choose

$$u_1 = -y_2 + x_2 - e_1 + 2e_2^2$$

$$u_2 = -\frac{1}{2m_1 + 4m_2 \sin^2 y_1} \left(\frac{-2m_2 g \sin y_1}{l} + \frac{2m_2 A \sin y_3 \sin y_1}{l} \right.$$

$$\left. -4m_2 y_2^2 \sin y_1 \cos y_1 + 2m_1 \sin y_1 \cos y_1 \eta^2 - \frac{k_1 y_1}{l^2} - \frac{k_2 y_2}{l^2} \right)$$

$$+ \frac{1}{2m_1 + 4m_2 \sin^2 x_1} \left(\frac{-2m_2 g \sin x_1}{l} + \frac{2m_2 A \sin x_3 \sin x_1}{l} \right.$$

(5-12)

$$\left. -4m_2 x_2^2 \sin x_1 \cos x_1 + 2m_1 \sin x_1 \cos x_1 \eta^2 - \frac{k_1 x_1}{l^2} - \frac{k_2 x_2}{l^2} \right) - e_2 - 2e_2^2$$

$$u_3 = -y_4 + x_4 - e_3 + 2e_3^2$$

$$u_4 = +A \sin y_3 - A \sin x_3 - e_4 - 2e_3^2$$

We obtain

$$\dot{V} = -e_1 - e_2 - e_3 - e_4 < 0$$

(5-13)

which is negative definite function in first quadrant. Four state errors versus time and time histories of states are shown in Fig. 24 and Fig. 25.

CASE II. The generalized synchronization error function is $e_i = y_i - x_i + F_i \sin \omega t + g_i$ ($i = 1, 2, 3, 4$). Our goal is $\lim\limits_{t \to \infty} e_i = \lim\limits_{t \to \infty} (y_i - x_i + F_i \sin \omega t + g_i) = 0$.

where $g_1 = g_2 = g_3 = g_4 = 30$, $F_1 = F_2 = F_3 = F_4 = 20$, $\omega = 0.2$ are constants.

The error dynamics becomes:

$$\dot{e}_1 = y_2 - x_2 + u_1 + F\omega\cos\omega t + 2e_2^2 - 2e_2^2$$

$$\dot{e}_2 = \frac{1}{2m_1 + 4m_2\sin^2 y_1}(\frac{-2m_2 g\sin y_1}{l} + \frac{2m_2 A\sin y_3\sin y_1}{l}$$

$$-4m_2 y_2^2\sin y_1\cos y_1 + 2m_1\sin y_1\cos y_1\eta^2 - \frac{k_1 y_1}{l^2} - \frac{k_2 y_2}{l^2})$$

$$-\frac{1}{2m_1 + 4m_2\sin^2 x_1}(\frac{-2m_2 g\sin x_1}{l} + \frac{2m_2 A\sin x_3\sin x_1}{l} \qquad (5\text{-}14)$$

$$-4m_2 x_2^2\sin x_1\cos x_1 + 2m_1\sin x_1\cos x_1\eta^2 - \frac{k_1 x_1}{l^2} - \frac{k_2 x_2}{l^2})$$

$$+u_2 + F\omega\cos\omega t + 2e_2^2 - 2e_2^2$$

$$\dot{e}_3 = y_4 - x_4 + u_3 + F\omega\cos\omega t + 2e_3^2 - 2e_3^2$$

$$\dot{e}_4 = -A\sin y_3 + A\sin x_3 + u_4 + F\omega\cos\omega t + 2e_3^2 - 2e_3^2$$

Let initial states be $(x_{10}, x_{20}, x_{30}, x_{40}) = (1.53, -0.47, 1.415, 0.5)$, $(y_{10}, y_{20}, y_{30}, y_{40}) = (1.7, 1, 1.6, 0.8)$, we find the error dynamics always exists in first quadrant as shown in Fig. 26. By GYC partial region asymptotical stability theorem, one can choose a linear positive definite Lyapunov function function in first quadrant:

$$V = e_1 + e_2 + e_3 + e_4 \qquad (5\text{-}15)$$

Its time derivative is

$$\dot{V} = (y_2 - x_2 + u_1 + \omega\cos\omega t + 2e_2^2 - 2e_2^2)$$

$$+(\frac{1}{2m_1 + 4m_2\sin^2 y_1}(\frac{-2m_2 g\sin y_1}{l} + \frac{2m_2 A\sin y_3\sin y_1}{l}$$

$$-4m_2 y_2^2\sin y_1\cos y_1 + 2m_1\sin y_1\cos y_1\eta^2 - \frac{k_1 y_1}{l^2} - \frac{k_2 y_2}{l^2})$$

$$-\frac{1}{2m_1 + 4m_2\sin^2 x_1}(\frac{-2m_2 g\sin x_1}{l} + \frac{2m_2 A\sin x_3\sin x_1}{l} \qquad (5\text{-}16)$$

$$-4m_2 x_2^2\sin x_1\cos x_1 + 2m_1\sin x_1\cos x_1\eta^2 - \frac{k_1 x_1}{l^2} - \frac{k_2 x_2}{l^2})$$

$$+u_2 + \omega\cos\omega t + 2e_2^2 - 2e_2^2) + (y_4 - x_4 + u_3 + \omega\cos\omega t + 2e_3^2 - 2e_3^2)$$

$$+(-A\sin y_3 + A\sin x_3 + u_4 + \omega\cos\omega t + 2e_3^2 - 2e_3^2)$$

Choose

$$u_1 = -y_2 + x_2 - F\omega\cos\omega t - e_1 + 2e_2^2$$

$$u_2 = -\frac{1}{2m_1 + 4m_2\sin^2 y_1}(\frac{-2m_2 g\sin y_1}{l} + \frac{2m_2 A\sin y_3\sin y_1}{l}$$

$$-4m_2 y_2^2\sin y_1\cos y_1 + 2m_1\sin y_1\cos y_1\eta^2 - \frac{k_1 y_1}{l^2} - \frac{k_2 y_2}{l^2})$$

$$+\frac{1}{2m_1 + 4m_2\sin^2 x_1}(\frac{-2m_2 g\sin x_1}{l} + \frac{2m_2 A\sin x_3\sin x_1}{l}$$

$$-4m_2 x_2^2\sin x_1\cos x_1 + 2m_1\sin x_1\cos x_1\eta^2 - \frac{k_1 x_1}{l^2} - \frac{k_2 x_2}{l^2})$$

$$-F\omega\cos\omega t - e_2 - 2e_2^2$$

$$u_3 = -y_4 + x_4 - F\omega\cos\omega t - e_3 + 2e_3^2$$

$$u_4 = +A\sin y_3 - A\sin x_3 - F\omega\cos\omega t - e_4 - 2e_3^2$$

(5-17)

We obtain

$$\dot{V} = -e_1 - e_2 - e_3 - e_4 < 0$$

(5-18)

which is negative definite function in first quadrant. Four state errors versus time and time histories of $y_i - x_i + g_i$ and $-F_i\sin\omega t$ $(i = 1,2,3,4)$ are shown in Fig. 27. and Fig. 28.

CASE III. The generalized synchronization error function is $e_i = y_i - \frac{1}{2}x_i^2 + g_i$ $(i = 1,2,3,4)$. Our goal is

$$\lim_{t\to\infty} e_i = \lim_{t\to\infty}(y_i - \frac{1}{2}x_i^2 + g_i) = 0.$$

where $g_1 = g_2 = g_3 = g_4 = 30$ are constants.

The error dynamics becomes:

$$\dot{e}_1 = y_2 - x_1 x_2 + 2e_2^2 - 2e_2^2 + u_1$$

$$\dot{e}_2 = \frac{1}{2m_1 + 4m_2 \sin^2 y_1}(\frac{-2m_2 g \sin y_1}{l} + \frac{2m_2 A \sin y_3 \sin y_1}{l}$$

$$-4m_2 y_2^2 \sin y_1 \cos y_1 + 2m_1 \sin y_1 \cos y_1 \eta^2 - \frac{k_1 y_1}{l^2} - \frac{k_2 y_2}{l^2})$$

$$-\frac{x_2}{2m_1 + 4m_2 \sin^2 x_1}(\frac{-2m_2 g \sin x_1}{l} + \frac{2m_2 A \sin x_3 \sin x_1}{l}$$

$$-4m_2 x_2^2 \sin x_1 \cos x_1 + 2m_1 \sin x_1 \cos x_1 \eta^2 - \frac{k_1 x_1}{l^2} - \frac{k_2 x_2}{l^2})$$

$$+2e_2^2 - 2e_2^2 + u_2$$

$$\dot{e}_3 = y_4 - x_3 x_4 + 2e_3^2 - 2e_3^2 + u_3$$

$$\dot{e}_4 = -A \sin y_3 + A x_4 \sin x_3 + 2e_4^2 - 2e_4^2 + u_4$$

(5-19)

Let initial states be $(x_{10}, x_{20}, x_{30}, x_{40}) = (1.53, -0.47, 1.415, 0.5)$, $(y_{10}, y_{20}, y_{30}, y_{40}) = (1.7, 1, 1.6, 0.8)$, we find the error dynamics always exists in first quadrant as shown in Fig. 29. By GYC partial region asymptotical stability theorem, one can choose a linear positive definite Lyapunov function function in first quadrant:

$$V = e_1 + e_2 + e_3 + e_4 \qquad (5\text{-}20)$$

Its time derivative is

$$\dot{V} = \left(y_2 - x_1 x_2 + 2e_2^2 - 2e_2^2 + u_1\right)$$

$$+(\frac{1}{2m_1 + 4m_2 \sin^2 y_1}(\frac{-2m_2 g \sin y_1}{l} + \frac{2m_2 A \sin y_3 \sin y_1}{l}$$

$$-4m_2 y_2^2 \sin y_1 \cos y_1 + 2m_1 \sin y_1 \cos y_1 \eta^2 - \frac{k_1 y_1}{l^2} - \frac{k_2 y_2}{l^2})$$

$$-\frac{x_2}{2m_1 + 4m_2 \sin^2 x_1}(\frac{-2m_2 g \sin x_1}{l} + \frac{2m_2 A \sin x_3 \sin x_1}{l}$$

$$-4m_2 x_2^2 \sin x_1 \cos x_1 + 2m_1 \sin x_1 \cos x_1 \eta^2 - \frac{k_1 x_1}{l^2} - \frac{k_2 x_2}{l^2})$$

$$+2e_2^2 - 2e_2^2 + u_2) + \left(y_4 - x_3 x_4 + 2e_3^2 - 2e_3^2 + u_3\right)$$

$$+(-A \sin y_3 + A x_4 \sin x_3 + 2e_3^2 - 2e_3^2 + u_4)$$

(5-21)

Choose

$$u_1 = -y_2 + x_1 x_2 - e_1 + 2e_2^2$$

$$u_2 = -\frac{1}{2m_1 + 4m_2 \sin^2 y_1}(\frac{-2m_2 g \sin y_1}{l} + \frac{2m_2 A \sin y_3 \sin y_1}{l}$$

$$-4m_2 y_2^2 \sin y_1 \cos y_1 + 2m_1 \sin y_1 \cos y_1 \eta^2 - \frac{k_1 y_1}{l^2} - \frac{k_2 y_2}{l^2})$$

$$+\frac{x_2}{2m_1 + 4m_2 \sin^2 x_1}(\frac{-2m_2 g \sin x_1}{l} + \frac{2m_2 A \sin x_3 \sin x_1}{l}$$

$$-4m_2 x_2^2 \sin x_1 \cos x_1 + 2m_1 \sin x_1 \cos x_1 \eta^2 - \frac{k_1 x_1}{l^2} - \frac{k_2 x_2}{l^2})$$

$$-F\omega \cos \omega t - e_2 - 2e_2^2$$

$$u_3 = -y_4 + x_3 x_4 - e_3 + 2e_3^2$$

$$u_4 = +A \sin y_3 - A \sin x_3 - e_4 - 2e_3^2$$

(5-22)

We obtain

$$\dot{V} = -e_1 - e_2 - e_3 - e_4 < 0 \qquad (5\text{-}23)$$

which is negative definite function in first quadrant. Four state errors versus time are shown in Fig. 30.

CASE IV. The generalized synchronization error function is $\mathbf{e} = \mathbf{y} - \mathbf{x} + \mathbf{z} + \mathbf{g}$, $\mathbf{z}$ is the state vector of new Mathieu-Duffing system, where $g_1 = g_2 = g_3 = g_4 = 50$ are constants.

The goal system for synchronization is the new Mathieu-Duffing system

$$\begin{cases} \dfrac{d}{dt} z_1 = z_2 \\[2mm] \dfrac{d}{dt} z_2 = -az_1 - bz_3 z_1 - az_1^3 - bz_3 z_1^3 - cz_2 + dz_3 \\[2mm] \dfrac{d}{dt} z_3 = z_4 \\[2mm] \dfrac{d}{dt} z_4 = -z_3 - z_3^3 - tz_4 + fz_1 \end{cases} \qquad (5\text{-}24)$$

Our goal is

$$\lim_{t \to \infty} \mathbf{e} = \lim_{t \to \infty}(\mathbf{y} - \mathbf{x} + \mathbf{z} + \mathbf{g}) = 0$$

The error dynamics becomes:

$$\dot{e}_1 = y_2 - x_2 + z_2 + 2e_2^2 - 2e_2^2 + u_1$$

$$\dot{e}_2 = \frac{1}{2m_1 + 4m_2 \sin^2 y_1}(\frac{-2m_2 g \sin y_1}{l} + \frac{2m_2 A \sin y_3 \sin y_1}{l}$$

$$-4m_2 y_2^2 \sin y_1 \cos y_1 + 2m_1 \sin y_1 \cos y_1 \eta^2 - \frac{k_1 y_1}{l^2} - \frac{k_2 y_2}{l^2})$$

$$-\frac{1}{2m_1 + 4m_2 \sin^2 x_1}(\frac{-2m_2 g \sin x_1}{l} + \frac{2m_2 A \sin x_3 \sin x_1}{l} \qquad (5\text{-}25)$$

$$-4m_2 x_2^2 \sin x_1 \cos x_1 + 2m_1 \sin x_1 \cos x_1 \eta^2 - \frac{k_1 x_1}{2m_1 l^2} - \frac{k_2 x_2}{l^2})$$

$$+u_2 - az_1 - bz_3 z_1 - az_1^3 - bz_3 z_1^3 - cz_2 + dz_3 + 2e_2^2 - 2e_2^2$$

$$\dot{e}_3 = y_4 - x_3 x_4 + u_3 + z_4 + 2e_3^2 - 2e_3^2$$

$$\dot{e}_4 = -A \sin y_3 + Ax_4 \sin x_3 + u_4 - z_3 - z_3^3 - tz_4 + fz_1 + 2e_3^2 - 2e_3^2$$

Let initial states be $(x_{10}, x_{20}, x_{30}, x_{40}) = (1.53, -0.47, 1.415, 0.5)$, $(y_{10}, y_{20}, y_{30}, y_{40}) = (1.7, 1, 1.6, 0.8)$, we find that the error dynamics always exists in first quadrant as shown in Fig. 31. By GYC partial region asymptotical stability theorem, one can choose a linear positive definite Lyapunov function function in first quadrant:

$$V = e_1 + e_2 + e_3 + e_4 \qquad (5\text{-}26)$$

Its time derivative is

$$\dot{V} = \left(y_2 - x_2 + u_1 + z_2 + 2e_2^2 - 2e_2^2\right)$$

$$+(\frac{1}{2m_1 + 4m_2 \sin^2 y_1}(\frac{-2m_2 g \sin y_1}{l} + \frac{2m_2 A \sin y_3 \sin y_1}{l}$$

$$-4m_2 y_2^2 \sin y_1 \cos y_1 + 2m_1 \sin y_1 \cos y_1 \eta^2 - \frac{k_1 y_1}{l^2} - \frac{k_2 y_2}{l^2})$$

$$-\frac{1}{2m_1 + 4m_2 \sin^2 x_1}(\frac{-2m_2 g \sin x_1}{l} + \frac{2m_2 A \sin x_3 \sin x_1}{l} \qquad (5\text{-}27)$$

$$-4m_2 x_2^2 \sin x_1 \cos x_1 + 2m_1 \sin x_1 \cos x_1 \eta^2 - \frac{k_1 x_1}{l^2} - \frac{k_2 x_2}{l^2})$$

$$+u_2 - az_1 - bz_3 z_1 - az_1^3 - bz_3 z_1^3 - cz_2 + dz_3 + 2e_2^2 - 2e_2^2)$$

$$+\left(y_4 - x_3 x_4 + u_3 + z_4 + 2e_3^2 - 2e_3^2\right)$$

$$+(-A \sin y_3 + Ax_4 \sin x_3 + u_4 - z_3 - z_3^3 - tz_4 + fz_1 + 2e_3^2 - 2e_3^2)$$

Choose

$$u_1 = -y_2 + x_2 - z_2 - e_1 + 2e_2^2$$

$$u_2 = -\frac{1}{2m_1 + 4m_2 \sin^2 y_1}\left(\frac{-2m_2 g \sin y_1}{l} + \frac{2m_2 A \sin y_3 \sin y_1}{l}\right.$$

$$-4m_2 y_2^2 \sin y_1 \cos y_1 + 2m_1 \sin y_1 \cos y_1 \eta^2 - \frac{k_1 y_1}{l^2} - \frac{k_2 y_2}{l^2}\big)$$

$$+\frac{1}{2m_1 + 4m_2 \sin^2 x_1}\left(\frac{-2m_2 g \sin x_1}{l} + \frac{2m_2 A \sin x_3 \sin x_1}{l}\right.$$

$$-4m_2 x_2^2 \sin x_1 \cos x_1 + 2m_1 \sin x_1 \cos x_1 \eta^2 - \frac{k_1 x_1}{l^2} - \frac{k_2 x_2}{l^2}\big)$$

$$+az_1 + bz_3 z_1 + az_1^3 + bz_3 z_1^3 + cz_2 - dz_3 - e_2 - 2e_2^2$$

$$u_3 = -y_4 + x_4 - z_4 - e_3 + 2e_3^2$$

$$u_4 = +A\sin y_3 - A\sin x_3 + z_3 + z_3^3 + tz_4 - fz_1 + e_4 - 2e_3^2$$

(5-28)

We obtain

$$\dot{V} = -e_1 - e_2 - e_3 - e_4 < 0$$

(5-29)

which is negative definite function in first quadrant. Four state errors versus time and time histories of $y_i - x_i + g_i$ and $-z_i$ $(i = 1, 2, 3, 4)$ are shown in Fig. 32. and Fig. 33.
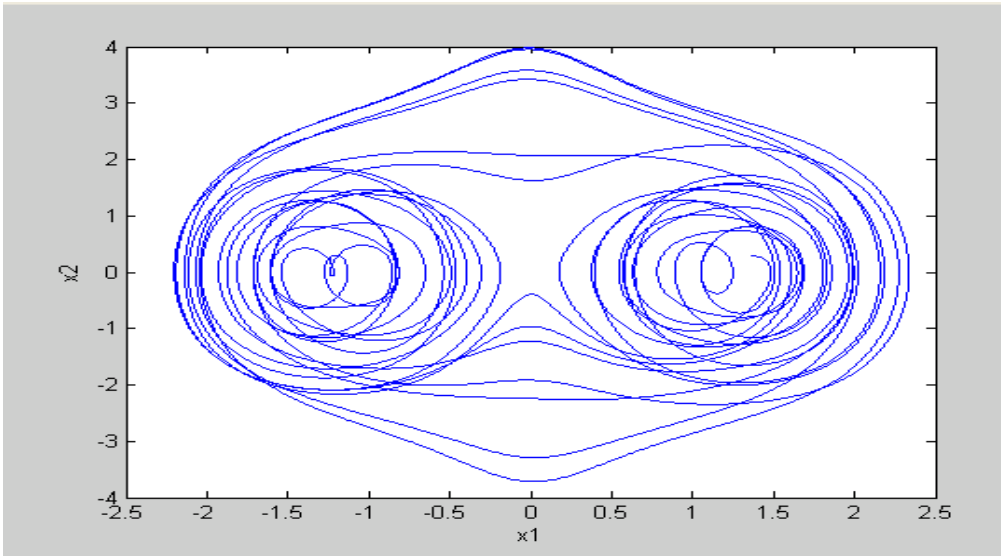
Fig. 21   Phase portrait for tachometer system.
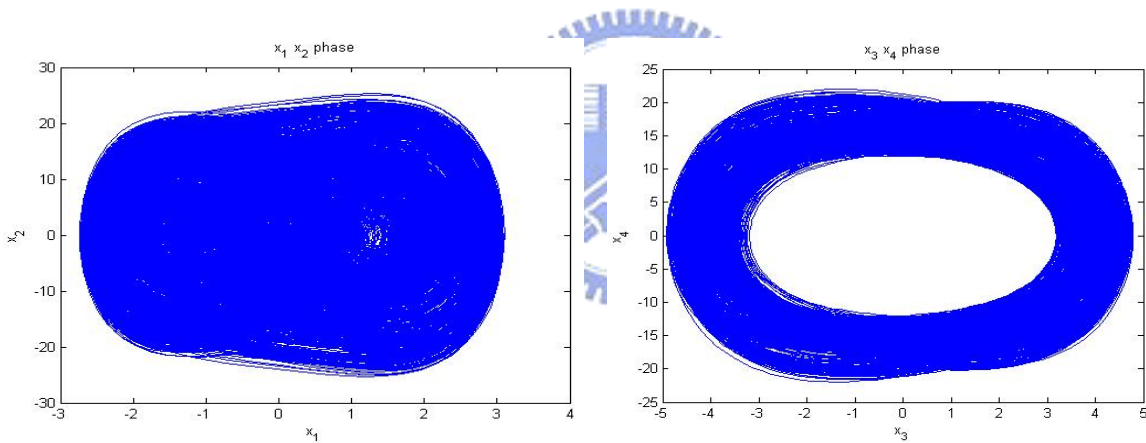
Fig. 22   Chaotic phase portraits for Mathieu-Duffing system in the first quadrant.
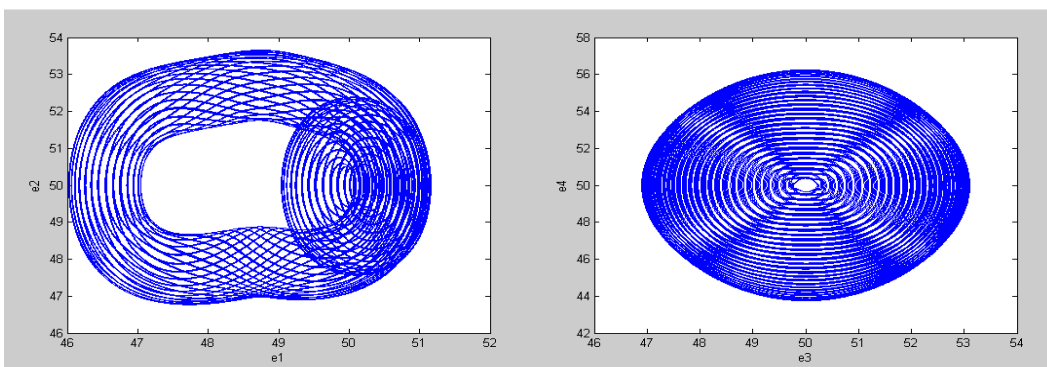
Fig. 23   Phase portrait of error dynamics for Case I.
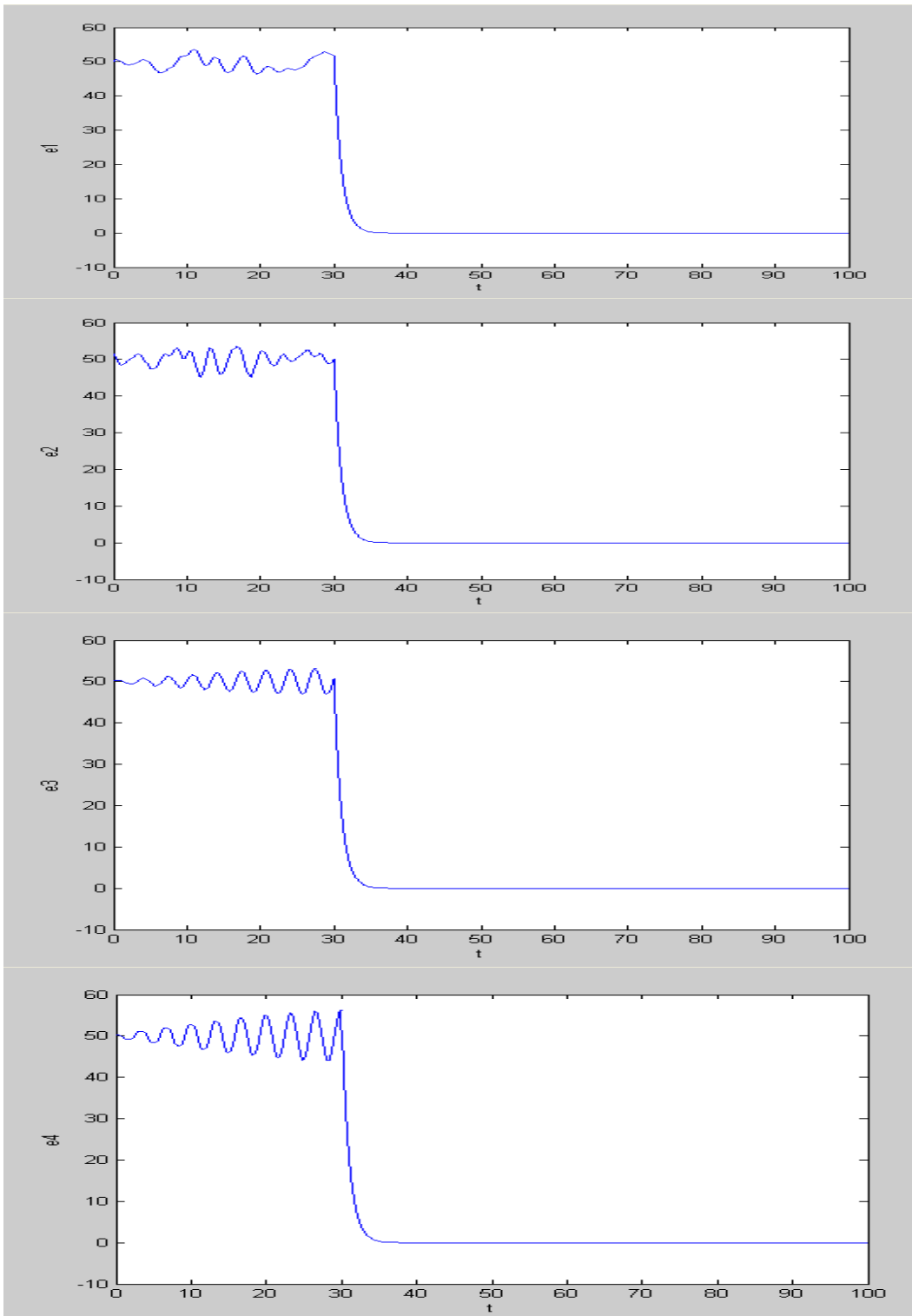
Fig. 24   Time histories of errors for Case I.
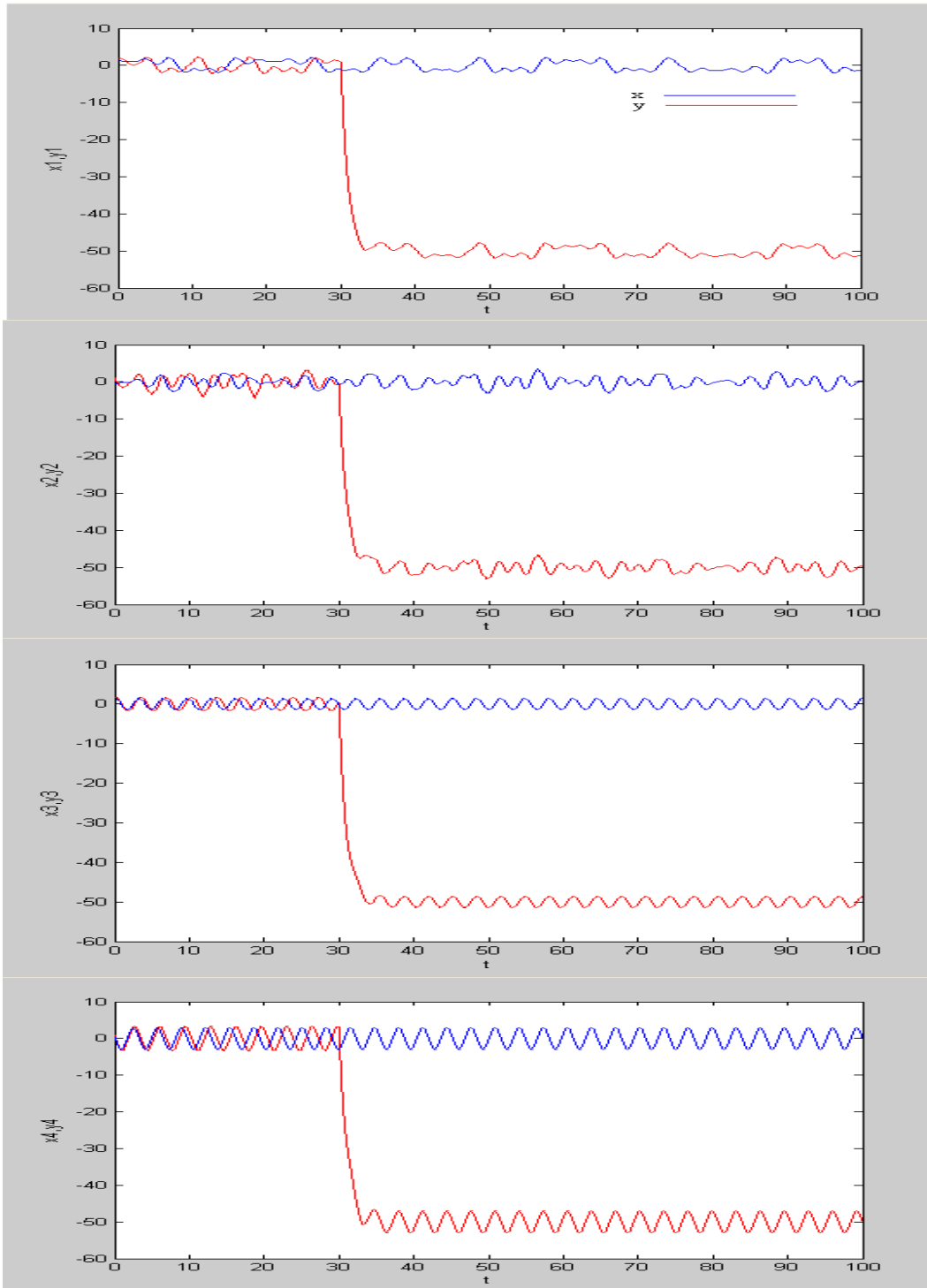
Fig. 25   Time histories of x_1, x_2, x_3, x_4, y_1, y_2, y_3, y_4 for Case I.
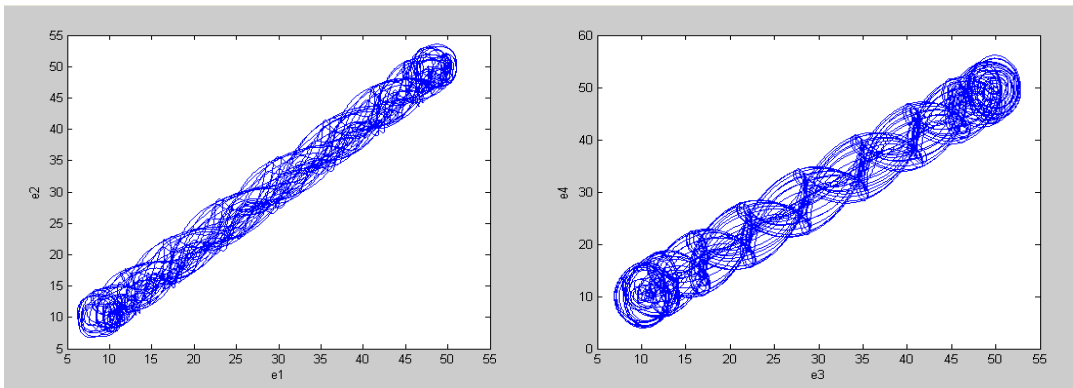
Fig. 26   Phase portrait of error dynamics for Case II.
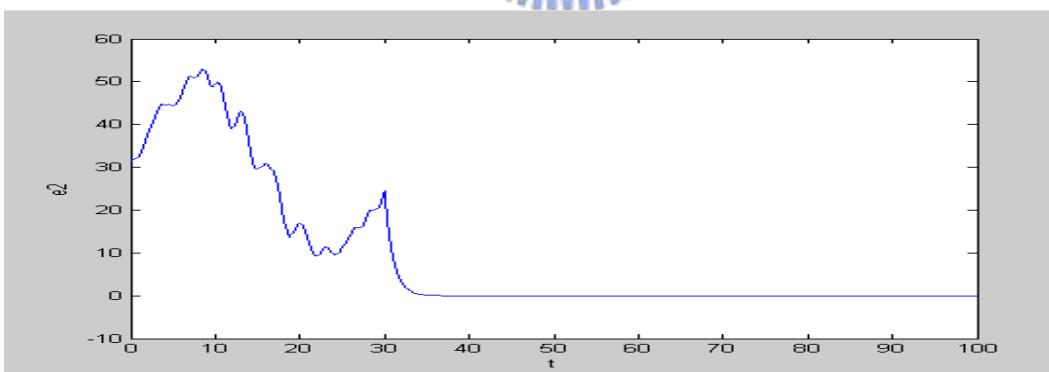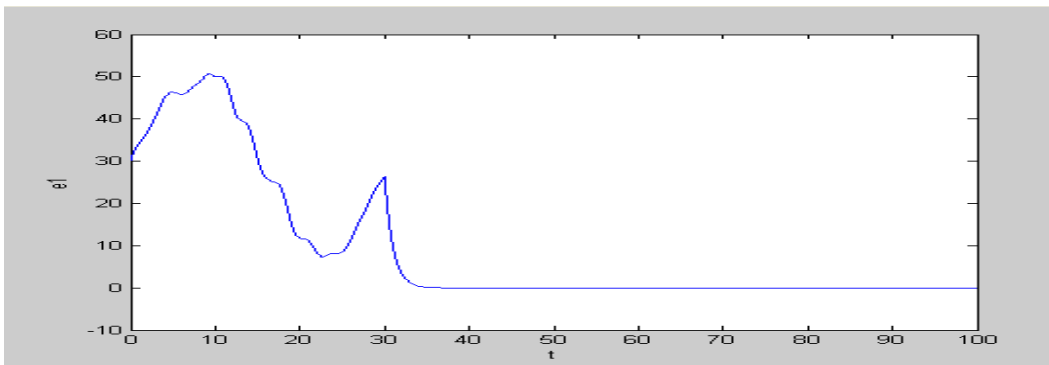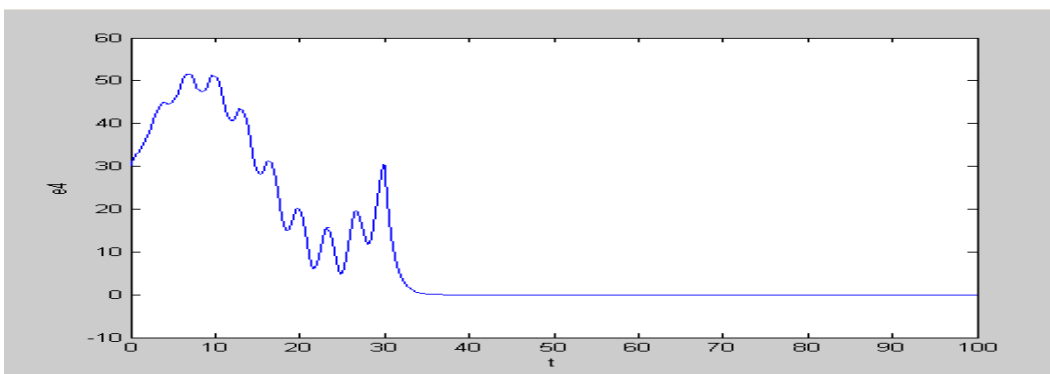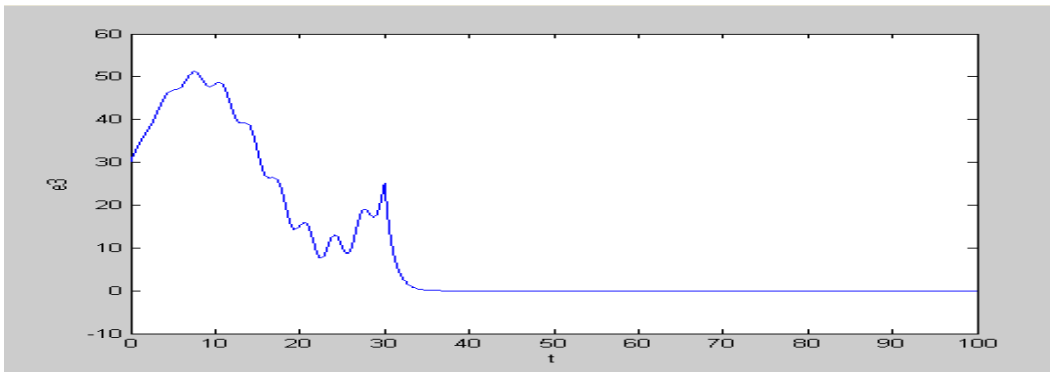
Fig. 27   Time histories errors for Case II.
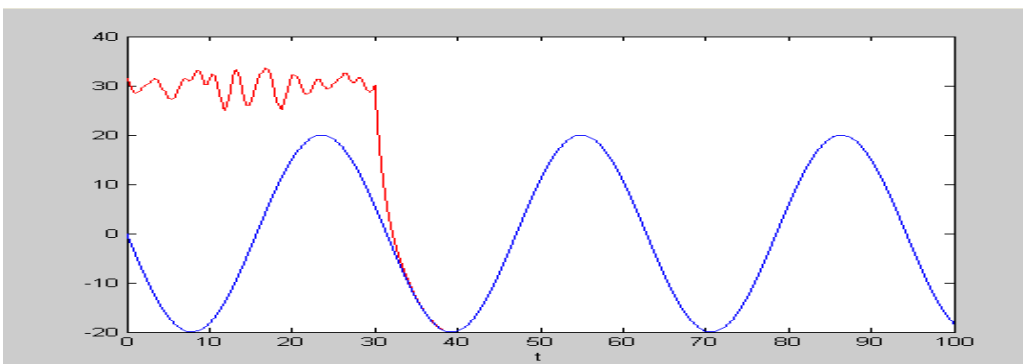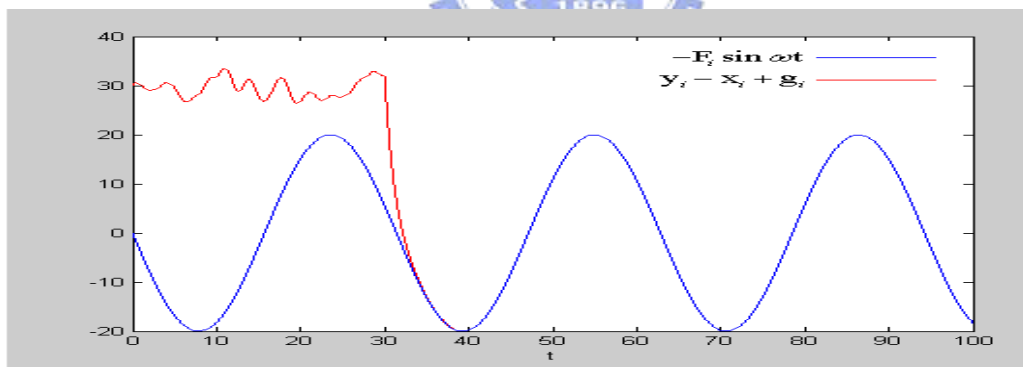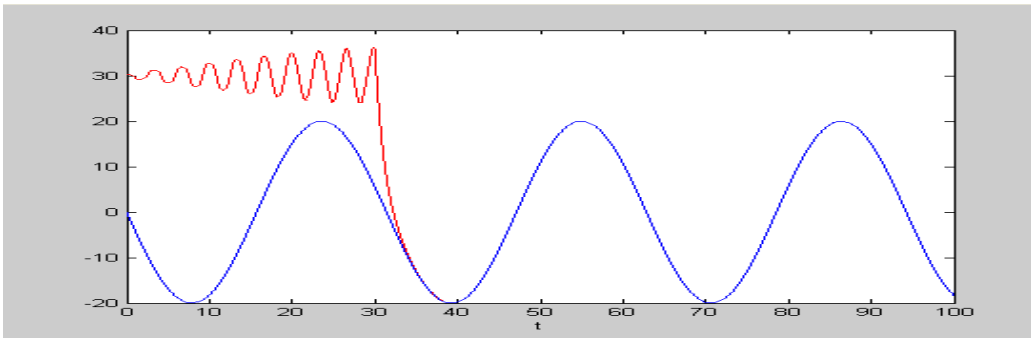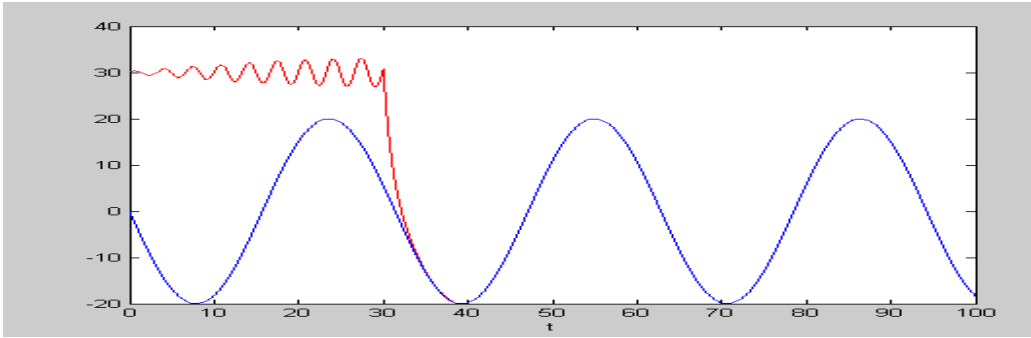
Fig. 28　Time histories of $y_i - x_i + g_i$ and $-F_i \sin \omega t$ $(i = 1, 2, 3, 4)$ for Case II.
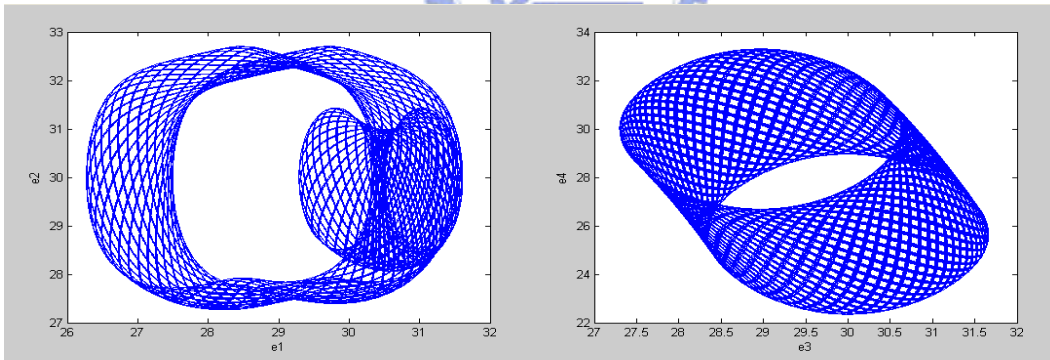
Fig. 29　Phase portrait of error dynamics for Case III.
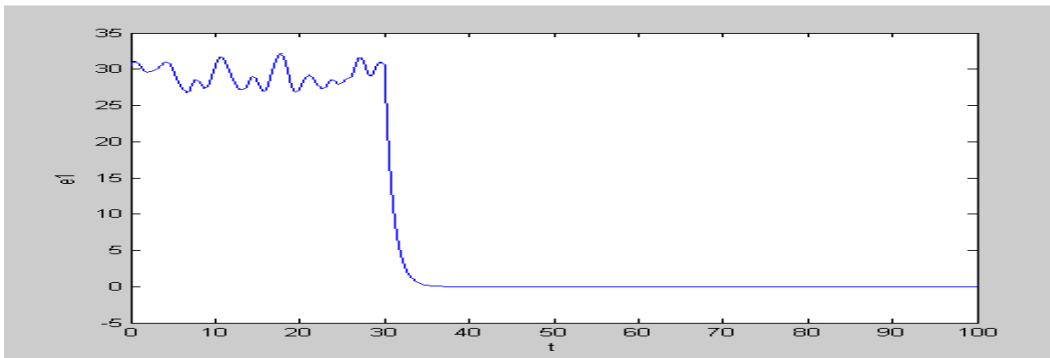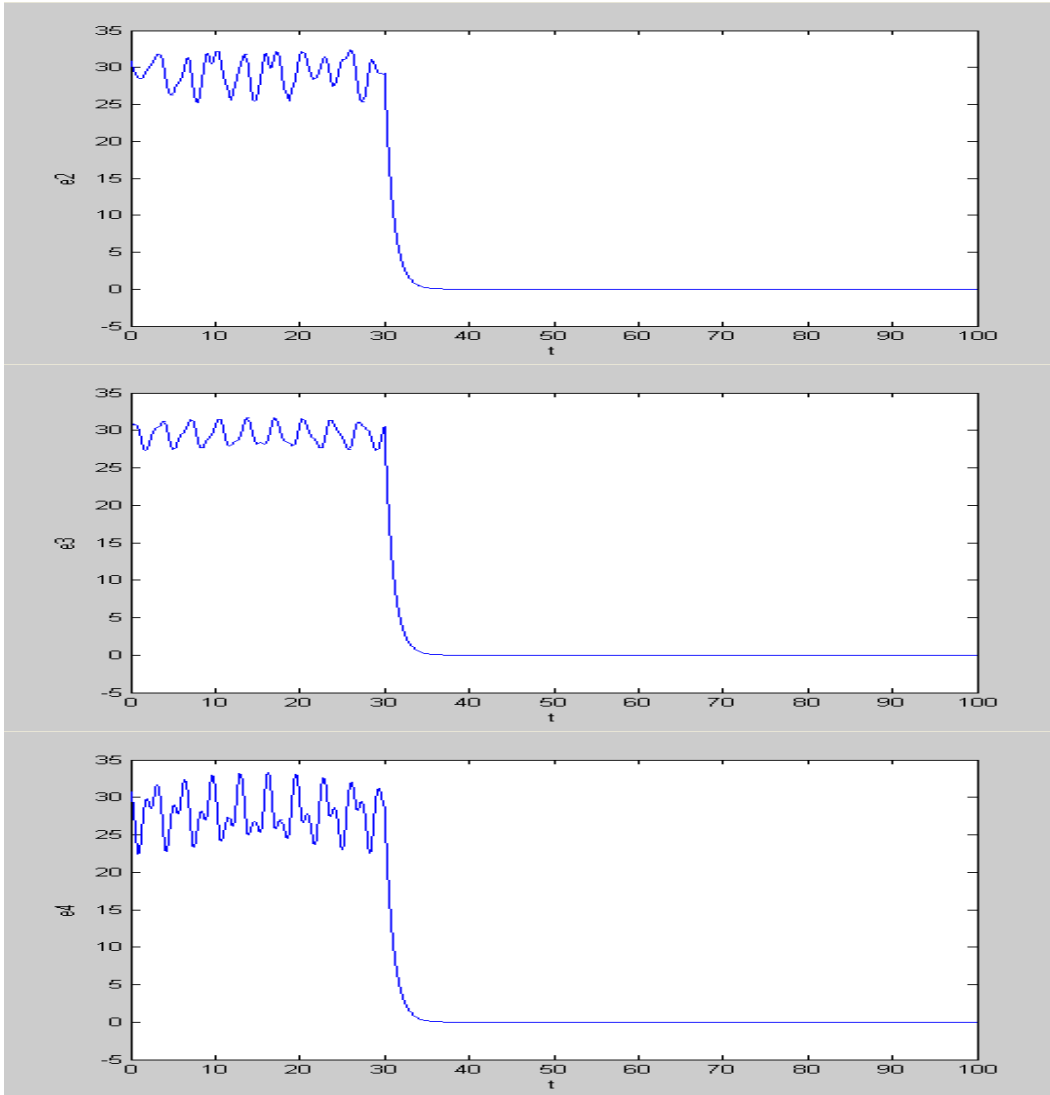
Fig. 30   Time histories errors for Case III.
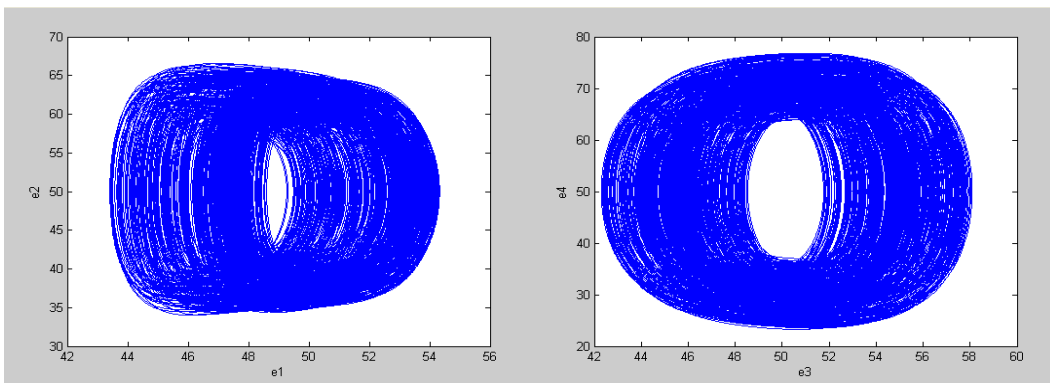
Fig. 31   Phase portraits of error dynamics for Case IV.
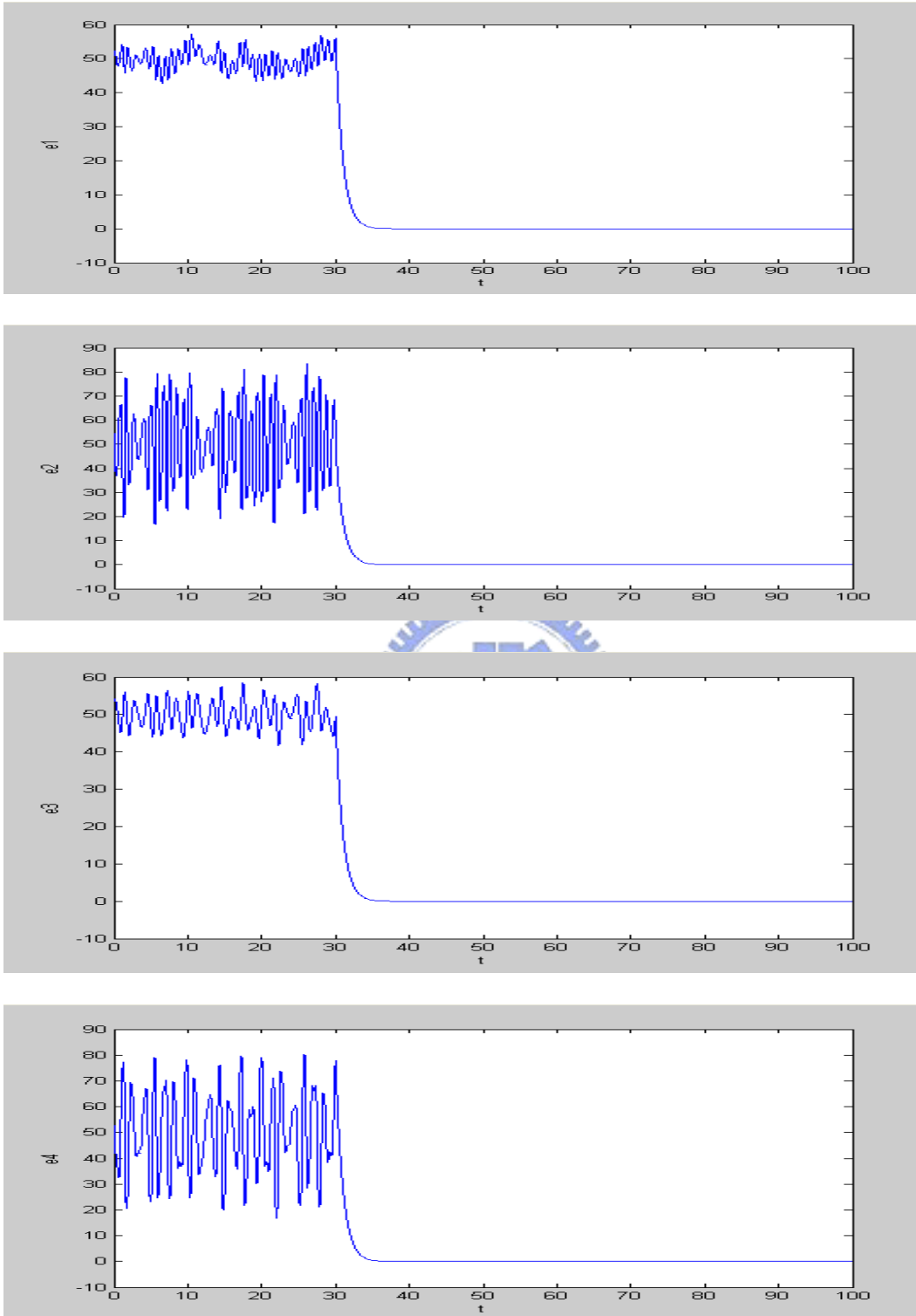
Fig. 32   Time histories errors for Case IV.
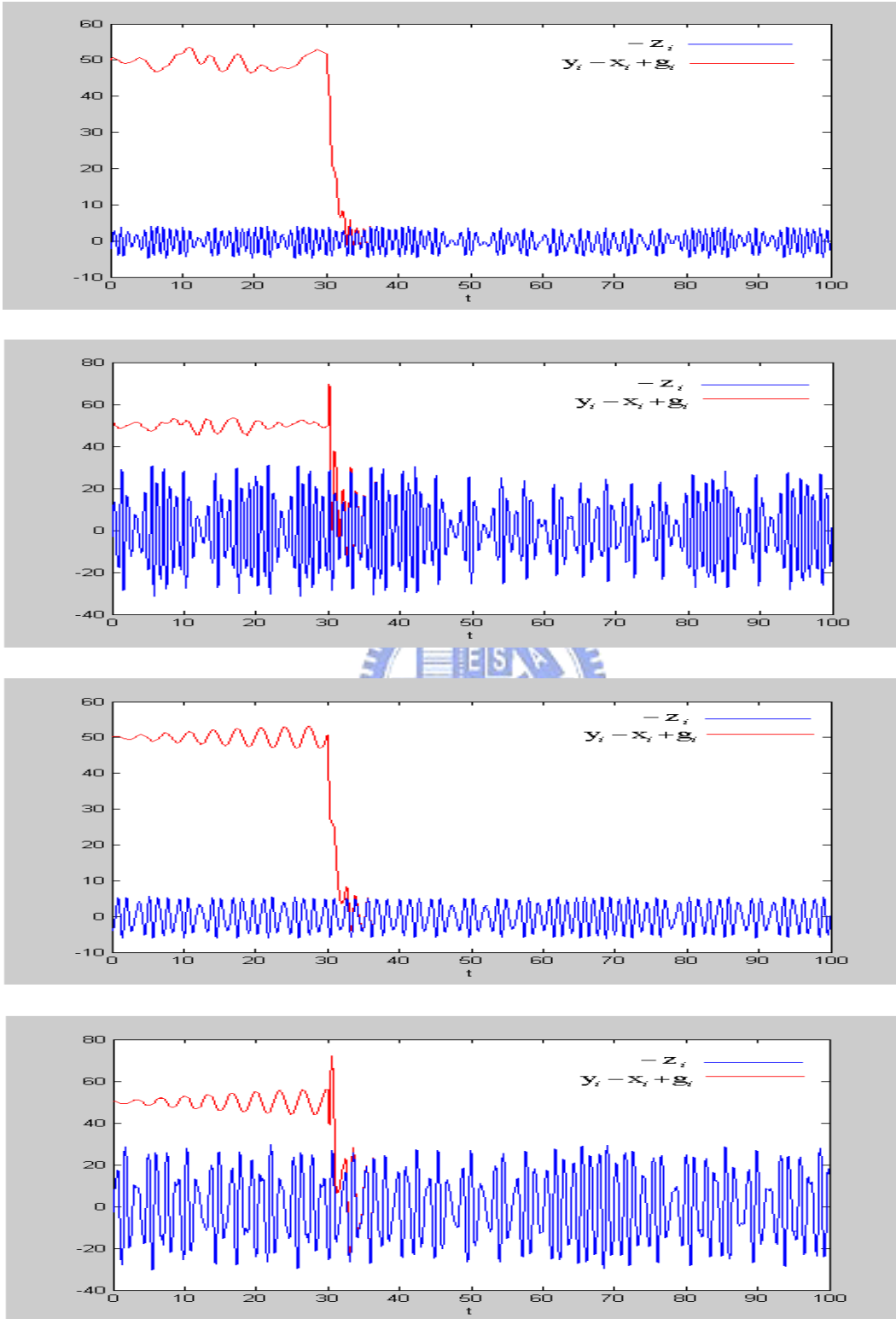
Fig. 33   Time histories of $y_i - x_i + g_i$ and $-z_i$ $(i = 1, 2, 3, 4)$ for Case IV.

Chapter 6

Chaos Control of Tachometer System by GYC Partial Region Stability Theory

In this chapter, chaos control of tachometer system by GYC partial region stability is proposed. The Lyapunov function is a simple linear function and the controllers are more simple by using the GYC partial region stability theory. The simulation results are more precise because the controllers are in lower order than that of traditional controllers. Chaos control of tachometer system by GYC partial region stability is obtained and verified by numerical simulation.

6.1 Chaos control scheme

Consider the following chaotic systems

$$\dot{\mathbf{x}} = \mathbf{f}(t, \mathbf{x}) \tag{6-1}$$

where $\mathbf{x} = [x_1, x_2, \cdots, x_n]^T \in R^n$ is a state vector, $\mathbf{f} : R_+ \times R^n \to R^n$ is a vector function.

The goal system which can be either chaotic or regular, is

$$\dot{\mathbf{y}} = \mathbf{g}(t, \mathbf{y}) \tag{6-2}$$

where $\mathbf{y} = [y_1, y_2, \cdots, y_n]^T \in R^n$ is a state vector, $\mathbf{g} : R_+ \times R^n \to R^n$ is a vector function. In order to make the chaotic state $\mathbf{x}$ approaching the goal state $\mathbf{y}$, define $\mathbf{e} = \mathbf{x} - \mathbf{y}$ as the state error. The chaos control is accomplished in the sense that [38, 43-49]:

$$\lim_{t \to \infty} \mathbf{e} = \lim_{t \to \infty} (\mathbf{x} - \mathbf{y}) = 0 \tag{6-3}$$

In this chapter, we will use examples in which the e state is placed in the first quadrant of coordinate system and use the GYC partial region stability theory, The Lyapunov function is a simple linear function and the controllers are more simple by using the GYC partial region stability theory (Appendix-B). The simulation results are more precise because the controllers are in lower order than that of traditional controllers.

6.2 Hyperchaotic tachometer system and new hyperchaotic Mathieu-Duffing system

The tachometer system of four-dimension shown in Fig. 1 is given by:

$$
\begin{cases}
\dfrac{d}{dt}x_1 = x_2 \\[2mm]
\dfrac{d}{dt}x_2 = \dfrac{1}{2m_1 + 4m_2 \sin^2 x_1}\left(\dfrac{-2m_2 g \sin x_1}{l} + \dfrac{2m_2 A \sin x_3 \sin x_1}{l} \right. \\[3mm]
\qquad \left. -4m_2 x_2^2 \sin x_1 \cos x_1 + 2m_1 \sin x_1 \cos x_1 \eta^2 - \dfrac{k_1 x_1}{l^2} - \dfrac{k_2 x_2}{l^2}\right) \\[3mm]
\dfrac{d}{dt}x_3 = x_4 \\[2mm]
\dfrac{d}{dt}x_4 = -A \sin x_3
\end{cases}
\qquad (6\text{-}4)
$$

where x_1, x_2, x_3, x_4 are state variables and k_1, k_2, A, l, g, m_1, m_2 are constants, when $k_1 = 4$, $k_2 = 1$, $m_2 = 3$, $m_1 = 3$, A=5, η =4.55, g=9.8, l=1.5. The system exhibits chaotic behavior with hyperchaotic Lyapunov exponents in Fig. 2. Its phase portrait as shown in Fig. 21.

The new hyperchaotic Mathieu-Duffing System is given by:

$$
\begin{cases}
\dfrac{d}{dt}z_1 = z_2 \\[2mm]
\dfrac{d}{dt}z_2 = -az_1 - bz_3 z_1 - az_1^3 - bz_3 z_1^3 - cz_2 + dz_3 \\[2mm]
\dfrac{d}{dt}z_3 = z_4 \\[2mm]
\dfrac{d}{dt}z_4 = -z_3 - z_3^3 - gz_4 + fz_1
\end{cases}
\qquad (6\text{-}5)
$$

where its initial states is (2, 3, 4, 2.5), system parameters are a=5, b==0.5970, c=0.005, d=-5, g=0.002, f=9, the system exhibits chaotic behavior with hyperchaotic Lyapunov exponents and its phase portraits as shown in Fig. 7 and Fig. 22.

6.3 Numerical simulations for hyperchaotic tachometer system and new hyperchaotic Mathieu-Duffing system

CASE I. Control the chaotic motion to zero.

The old origin of the tachometer system is translated to $(x_1, x_2, x_3, x_4) = (g_1, g_2, g_3, g_4)$

where $g_1 = 5, g_2 = 5, g_3 = 5, g_4 = 5$

$$\begin{cases} \dfrac{d}{dt}x_1 = x_2 - g_1 \\[2mm] \dfrac{d}{dt}x_2 = \dfrac{1}{2m_1 + 4m_2 \sin^2(x_1 - g_2)}\left(\dfrac{-2m_2 g \sin(x_1 - g_2)}{l}\right. \\[3mm] \qquad + \dfrac{2m_2 A \sin(x_3 - g_2)\sin(x_1 - g_2)}{l} \\[3mm] \qquad - 4m_2(x_2 - g_2)^2 \sin(x_1 - g_2)\cos(x_1 - g_2) \\[3mm] \qquad \left. + 2m_1 \sin(x_1 - g_2)\cos(x_1 - g_2)\eta^2 - \dfrac{k_1(x_1 - g_2)}{l^2} - \dfrac{k_2(x_2 - g_2)}{l^2}\right) \\[3mm] \dfrac{d}{dt}x_3 = x_4 - g_3 \\[2mm] \dfrac{d}{dt}x_4 = -A\sin(x_3 - g_4) \end{cases} \qquad (6\text{-}6)$$

and the chaotic motion always happens in the first quadrant of coordinate system (x_1, x_2, x_3, x_4). This tachometer system is presented as simulated examples where the initial conditions is $x_{10} = 6.53, x_{20} = 5.53, x_{30} = 6.415, x_{40} = 5.5$. The chaotic motion is shown in Fig. 34.

In order to lead (x_1, x_2, x_3, x_4) to the goal, we add controllers u_1, u_2, u_3, u_4 to each equation of Eq. (6-6), respectively:

$$\begin{cases}
\dfrac{d}{dt}x_1 = x_2 - g_1 + u_1 \\[2mm]
\dfrac{d}{dt}x_2 = \dfrac{1}{2m_1 + 4m_2\sin^2(x_1 - g_2)}\left(\dfrac{-2m_2 g\sin(x_1 - g_2)}{l} + \right. \\[3mm]
\qquad \dfrac{2m_2 A\sin(x_3 - g_2)\sin(x_1 - g_2)}{l} - 4m_2(x_2 - g_2)^2\sin(x_1 - g_2)\cos(x_1 - g_2) \\[3mm]
\qquad \left. +2m_1\sin(x_1 - g_2)\cos(x_1 - g_2)\eta^2 - \dfrac{k_1(x_1 - g_2)}{l^2} - \dfrac{k_2(x_2 - g_2)}{l^2}\right) + u_2 \\[3mm]
\dfrac{d}{dt}x_3 = x_4 - g_3 + u_3 \\[2mm]
\dfrac{d}{dt}x_4 = -A\sin(x_3 - g_4) + u_4
\end{cases} \qquad (6\text{-}7)$$

In this case, we will control the chaotic motion of the tachometer system (6-8) to zero. The goal is $y = 0$. The state error is $e_i = x_i - y_i = x_i$ where $i = (1,2,3,4)$ and error dynamics becomes:

$$\begin{cases}
\dot{e}_1 = \dot{x}_1 = x_2 - g_1 + 2e_2^2 - 2e_2^2 + u_1 \\[2mm]
\dot{e}_2 = \dot{x}_2 = \dfrac{1}{2m_1 + 4m_2\sin^2(x_1 - g_2)}\left(\dfrac{-2m_2 g\sin(x_1 - g_2)}{l} + \right. \\[3mm]
\qquad \dfrac{2m_2 A\sin(x_3 - g_2)\sin(x_1 - g_2)}{l} - 4m_2(x_2 - g_2)^2\sin(x_1 - g_2)\cos(x_1 - g_2) \\[3mm]
\qquad \left. +2m_1\sin(x_1 - g_2)\cos(x_1 - g_2)\eta^2 - \dfrac{k_1(x_1 - g_2)}{l^2} - \dfrac{k_2(x_2 - g_2)}{l^2}\right) + 2e_2^2 - 2e_2^2 + u_2 \\[3mm]
\dot{e}_3 = \dot{x}_3 = x_4 - g_3 + 2e_3^2 - 2e_3^2 + u_3 \\[2mm]
\dot{e}_4 = \dot{x}_4 = -A\sin(x_3 - g_4) + 2e_3^2 - 2e_3^2 + u_4
\end{cases} \qquad (6\text{-}8)$$

In Fig. 35, we see that the error dynamics always exists in first quadrant.

By GYC partial region stability, one can easily choose a linear Lyapunov function in the form of a positive definite function in first quadrant as:

$$V = e_1 + e_2 + e_3 + e_4 \qquad (6\text{-}9)$$

Its time derivative through error dynamics (6-8) is

$$
\begin{aligned}
\dot{V} &= \dot{e}_1 + \dot{e}_2 + \dot{e}_3 + \dot{e}_4 \\
&= \left(e_2 - g_1 + 2e_2^2 - 2e_2^2 + u_1 \right) \\
&\quad + (\frac{1}{2m_1 + 4m_2 \sin^2(e_1 - g_2)} (- \frac{2m_2 g \sin(e_1 - g_2)}{l} \\
&\quad + \frac{2m_2 A \sin(e_3 - g_2) \sin(e_1 - g_2)}{l} \\
&\quad - 4m_2 (e_2 - g_2)^2 \sin(e_1 - g_2) \cos(e_1 - g_2) \\
&\quad + 2m_1 \sin(e_1 - g_2) \cos(e_1 - g_2) \eta^2 \\
&\quad - \frac{k_1 (e_1 - g_2)}{l^2} - \frac{k_2 (e_2 - g_2)}{l^2}) + 2e_2^2 - 2e_2^2 + u_2) \\
&\quad + (e_4 - g_3 + 2e_3^2 - 2e_3^2 + u_3) + (-A \sin(e_3 - g_4) + 2e_3^2 - 2e_3^2 + u_4)
\end{aligned}
\tag{6-10}
$$

Choose

$$
\begin{aligned}
u_1 &= -e_2 + g_1 - e_1 + 2e_2^2 \\
u_2 &= - \frac{1}{2m_1 + 4m_2 \sin^2(e_1 - g_2)} (\frac{-2m_2 g \sin(e_1 - g_2)}{l} \\
&\quad + \frac{2m_2 A \sin(e_3 - g_2) \sin(e_1 - g_2)}{l} \\
&\quad - 4m_2 (e_2 - g_2)^2 \sin(e_1 - g_2) \cos(e_1 - g_2) \\
&\quad + 2m_1 \sin(e_1 - g_2) \cos(e_1 - g_2) \eta^2 \\
&\quad - \frac{k_1 (e_1 - g_2)}{l^2} - \frac{k_2 (e_2 - g_2)}{l^2}) \\
&\quad - e_2 - 2e_2^2 \\
u_3 &= -e_4 + g_3 - e_3 + 2e_3^2 \\
u_4 &= +A \sin(e_3 - g_4) - e_4 - 2e_3^2
\end{aligned}
\tag{6-11}
$$

We obtain

$$
\dot{V} = -e_1 - e_2 - e_3 - e_4 < 0
\tag{6-12}
$$

which is negative definite function in first quadrant. The numerical results are shown in

Fig. 36. After 30 sec, the motion trajectories approach the origin.

CASE II. Control the chaotic motion to a sine function.

The tacometer system of which the old origin is translated to $(x_1, x_2, x_3, x_4) = (g_1, g_2, g_3, g_4)$ where $g_1 = 30, g_2 = 30, g_3 = 30, g_4 = 30$ and the chaotic motion always happens in the first quadrant of coordinate system (x_1, x_2, x_3, x_4). This tachometer system is presented as simulated examples where the initial conditions is $x_{10} = 31.53, x_{20} = 29.53, x_{30} = 31.415, x_{40} = 30.5$.

In this case we will control the chaotic motion of the tachometer system (6-6) to sine function of time. The goal is $y = F \sin \omega t$. The error equation

$$e_i = x_i - y_i = x_i - F \sin \omega_i t \qquad (6\text{-}13)$$

$$\dot{e}_i = \dot{x}_i - \dot{y}_i = \dot{x}_i - \omega_i F \cos \omega_i t$$

where $F = 0.5$, $\omega_1 = 0.1$, $\omega_2 = 0.2$, $\omega_3 = 0.15$, $\omega_4 = 0.3$. Our goal is:
$$\lim_{t \to \infty} e_i = \lim_{t \to \infty} (x_i - F_i \sin \omega_i t) = 0, \qquad (i = 1, 2, 3, 4)$$

The error dynamics is

$$\dot{e}_1 = \dot{x}_1 - \omega_1 F \cos \omega_1 t = x_2 - g_1 - \omega_1 F \cos \omega_1 t + 2e_2^2 - 2e_2^2 + u_1$$

$$\dot{e}_2 = \dot{x}_2 - \omega_2 F \cos \omega_2 t$$

$$= \frac{1}{2m_1 + 4m_2 \sin^2(x_1 - g_2)} \left(\frac{-2m_2 g \sin(x_1 - g_2)}{l} \right.$$

$$+ \frac{2m_2 A \sin(x_3 - g_2) \sin(x_1 - g_2)}{l}$$

$$- 4m_2 (x_2 - g_2)^2 \sin(x_1 - g_2) \cos(x_1 - g_2) \qquad (6\text{-}14)$$

$$+ 2m_1 \sin(x_1 - g_2) \cos(x_1 - g_2) \eta^2$$

$$\left. - \frac{k_1 (x_1 - g_2)}{l^2} - \frac{k_2 (x_2 - g_2)}{l^2} \right) - \omega_2 F \cos \omega_2 t + 2e_2^2 - 2e_2^2 + u_2$$

$$\dot{e}_3 = \dot{x}_3 - \omega_3 F \cos \omega_3 t = x_4 - g_3 - \omega_3 F \cos \omega_3 t + 2e_3^2 - 2e_3^2 + u_3$$

$$\dot{e}_4 = \dot{x}_4 - \omega_4 F \cos \omega_4 t = -A \sin(x_3 - g_4) - \omega_4 F \cos \omega_4 t + 2e_3^2 - 2e_3^2 + u_4$$

In Fig. 37, the error dynamics always exists in first quadrant.

By GYC partial region stability, one can easily choose a linear Lyapunov function in the form of a positive definite function in first quadrant as:

$$V = e_1 + e_2 + e_3 + e_4 \tag{6-15}$$

Its time derivative is

$$
\begin{aligned}
\dot{V} &= \dot{e}_1 + \dot{e}_2 + \dot{e}_3 \\
&= (x_2 - g_1 - \omega_1 F \cos \omega_1 t + 2e_2^2 - 2e_2^2 + u_1) \\
&\quad + (\frac{1}{2m_1 + 4m_2 \sin^2(x_1 - g_2)}(\frac{-2m_2 g \sin(x_1 - g_2)}{l} + \\
&\quad \frac{2m_2 A \sin(x_3 - g_2)\sin(x_1 - g_2)}{l} \\
&\quad -4m_2(x_2 - g_2)^2 \sin(x_1 - g_2)\cos(x_1 - g_2) \\
&\quad +2m_1 \sin(x_1 - g_2)\cos(x_1 - g_2)\eta^2 \\
&\quad -\frac{k_1(x_1 - g_2)}{l^2} - \frac{k_2(x_2 - g_2)}{l^2}) - \omega_2 F \cos \omega_2 t + 2e_2^2 - 2e_2^2 + u_2) \\
&\quad +(x_4 - g_3 - \omega_3 F \cos \omega_3 t + 2e_3^2 - 2e_3^2 + u_3) \\
&\quad +(-A \sin(x_3 - g_4) - \omega_4 F \cos \omega_4 t + 2e_3^2 - 2e_3^2 + u_4)
\end{aligned}
\tag{6-16}
$$

Choose

$$
\begin{aligned}
u_1 &= -x_2 + g_1 + \omega_1 F \cos \omega_1 t - e_1 + 2e_2^2 \\
u_2 &= -\frac{1}{2m_1 + 4m_2 \sin^2(x_1 - g_2)}(\frac{-2m_2 g \sin(x_1 - g_2)}{l} + \\
&\quad \frac{2m_2 A \sin(x_3 - g_2)\sin(x_1 - g_2)}{l} \\
&\quad -4m_2(x_2 - g_2)^2 \sin(x_1 - g_2)\cos(x_1 - g_2) \\
&\quad +2m_1 \sin(x_1 - g_2)\cos(x_1 - g_2)\eta^2 - \frac{k_1(x_1 - g_2)}{l^2} - \frac{k_2(x_2 - g_2)}{l^2}) \\
&\quad +\omega_2 F \cos \omega_2 t - e_2 - 2e_2^2 \\
u_3 &= -x_4 + g_3 + \omega_3 F \cos \omega_3 t - e_3 + 2e_3^2 \\
u_4 &= A \sin(x_3 - g_4) + \omega_4 F \cos \omega_4 t - e_4 - 2e_3^2
\end{aligned}
\tag{6-17}
$$

We obtain

$$\dot{V} = -e_1 - e_2 - e_3 - e_4 < 0 \tag{6-18}$$

which is negative definite function in first quadrant. The numerical results are shown in Fig.38 and Fig. 49. After 30 sec., the errors approach zero and the motion trajectories approach to sine functions.

CASE III. Control the chaotic motion of tachometer system to chaotic motion of a new hyperchaotic Mathieu-Duffing System.

The tachometer system of which the old origin is translated to $(x_1, x_2, x_3, x_4) = (g_1, g_2, g_3, g_4)$ where $g_1 = 30, g_2 = 30, g_3 = 30, g_4 = 30$

and the chaotic motion always happens in the first quadrant of coordinate system (x_1, x_2, x_3, x_4). This tachometer system is presented as simulated examples where the initial conditions is $x_{10} = 51.53, x_{20} = 49.53, x_{30} = 51.415, x_{40} = 50.5$.

In this case we will control chaotic motion of to that of a new hyperchaotic Mathieu-Duffing System. The goal system is a new hyperchaotic Mathieu-Duffing System:
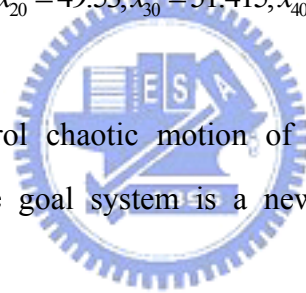
$$
\begin{cases}
\dfrac{d}{dt} z_1 = z_2 \\
\dfrac{d}{dt} z_2 = -az_1 - bz_3 z_1 - az_1^3 - bz_3 z_1^3 - cz_2 + dz_3 \\
\dfrac{d}{dt} z_3 = z_4 \\
\dfrac{d}{dt} z_4 = -z_3 - z_3^3 - tz_4 + fz_1
\end{cases}
\tag{6-19}
$$

The error equation is $e_i = x_i - z_i$, $(i = 1, 2, 3, 4)$ Our goal is $\lim\limits_{t \to \infty} e = 0$.

The error dynamics becomes:

$$\dot{e}_1 = \dot{x}_1 - \dot{z}_1 = x_2 - g_1 - z_2 + 2e_2^2 - 2e_2^2 + u_1$$

$$\dot{e}_2 = \dot{x}_2 - \dot{z}_2$$

$$= \frac{1}{2m_1 + 4m_2 \sin^2(x_1 - g_2)} \left(\frac{-2m_2 g \sin(x_1 - g_2)}{l} + \right.$$

$$\frac{2m_2 A \sin(x_3 - g_2) \sin(x_1 - g_2)}{l}$$

$$-4m_2(x_2 - g_2)^2 \sin(x_1 - g_2) \cos(x_1 - g_2)$$

$$+2m_1 \sin(x_1 - g_2) \cos(x_1 - g_2)\eta^2 \qquad (6\text{-}20)$$

$$\left. -\frac{k_1(x_1 - g_2)}{l^2} - \frac{k_2(x_2 - g_2)}{l^2} \right)$$

$$+az_1 + bz_3z_1 + az_1^3 + bz_3z_1^3 + cz_2 - dz_3 + 2e_2^2 - 2e_2^2 + u_2$$

$$\dot{e}_3 = \dot{x}_3 - \dot{z}_3 = x_4 - g_3 - z_4 + 2e_3^2 - 2e_3^2 + u_3$$

$$\dot{e}_4 = \dot{x}_4 - \dot{z}_4 = -A \sin(x_3 - g_4) + z_3 + z_3^3 + tz_4 - fz_1 + 2e_3^2 - 2e_3^2 + u_4$$

By Fig. 40, we know the error dynamics always exists in first quadrant.

By GYC partial region stability, one can easily choose a Lyapunov function in the form of a positive definite function in first quadrant as:

$$V = e_1 + e_2 + e_3 + e_4 \qquad (6\text{-}21)$$

Its time derivative is

$$\dot{V} = \dot{e}_1 + \dot{e}_2 + \dot{e}_3 + \dot{e}_4$$

$$= \left(x_2 - g_1 - z_2 + 2e_2^2 - 2e_2^2 + u_1 \right)$$

$$+ \left(\frac{1}{2m_1 + 4m_2 \sin^2(x_1 - g_2)} \left(\frac{-2m_2 g \sin(x_1 - g_2)}{l} + \right. \right.$$

$$\frac{2m_2 A \sin(x_3 - g_2) \sin(x_1 - g_2)}{l}$$

$$-4m_2(x_2 - g_2)^2 \sin(x_1 - g_2) \cos(x_1 - g_2)$$

$$+2m_1 \sin(x_1 - g_2) \cos(x_1 - g_2)\eta^2 \qquad (6\text{-}22)$$

$$\left. -\frac{k_1(x_1 - g_2)}{l^2} - \frac{k_2(x_2 - g_2)}{l^2} \right)$$

$$+az_1 + bz_3z_1 + az_1^3 + bz_3z_1^3 + cz_2 - dz_3 + 2e_2^2 - 2e_2^2 + u_2 \Big)$$

$$+ \left(x_4 - g_3 - z_4 + 2e_3^2 - 2e_3^2 + u_3 \right)$$

$$+ \left(-A \sin(x_3 - g_4) + z_3 + z_3^3 + tz_4 - fz_1 + 2e_3^2 - 2e_3^2 + u_4 \right)$$

Choose

$$u_1 = -x_2 + g_1 + z_2 - e_1 + 2e_2^2$$

$$u_2 = -\frac{1}{2m_1 + 4m_2\sin^2(x_1 - g_2)}\left(\frac{-2m_2 g\sin(x_1 - g_2)}{l} + \right.$$

$$\frac{2m_2 A\sin(x_3 - g_2)\sin(x_1 - g_2)}{l}$$

$$-4m_2(x_2 - g_2)^2\sin(x_1 - g_2)\cos(x_1 - g_2)$$

$$+2m_1\sin(x_1 - g_2)\cos(x_1 - g_2)\eta^2$$

$$\left.-\frac{k_1(x_1 - g_2)}{l^2} - \frac{k_2(x_2 - g_2)}{l^2}\right)$$

$$-az_1 - bz_3z_1 - az_1^3 - bz_3z_1^3 - cz_2 + dz_3 - e_2 - 2e_2^2$$

$$u_3 = -x_4 + g_3 + z_4 - e_3 + 2e_3^2$$

$$u_4 = +A\sin(x_3 - g_4) - z_3 - z_3^3 - tz_4 + fz_1 - e_4 - 2e_3^2$$

(6-23)

We obtain

$$\dot{V} = -e_1 - e_2 - e_3 - e_4 < 0$$

(6-24)

which is negative definite function in first quadrant. The numerical results are shown in Fig.41 and Fig. 42. After 30 sec., the errors approach zero and the chaotic trajectories of tachometer system approach to that of the new Mathieu-Duffing system.
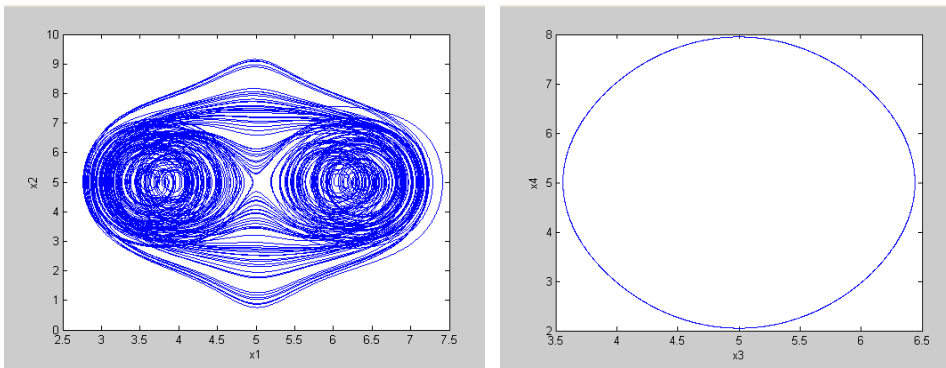
Fig. 34   Chaotic phase portraits for tachometer system in the first quadrant.
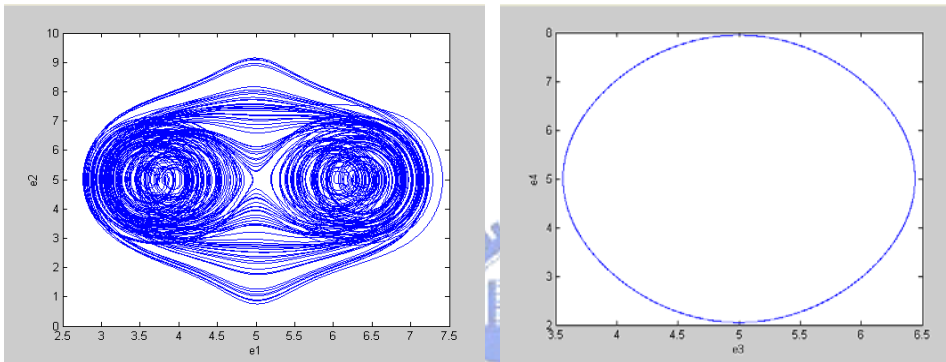
Fig. 35   Phase portraits of error dynamics for Case I.
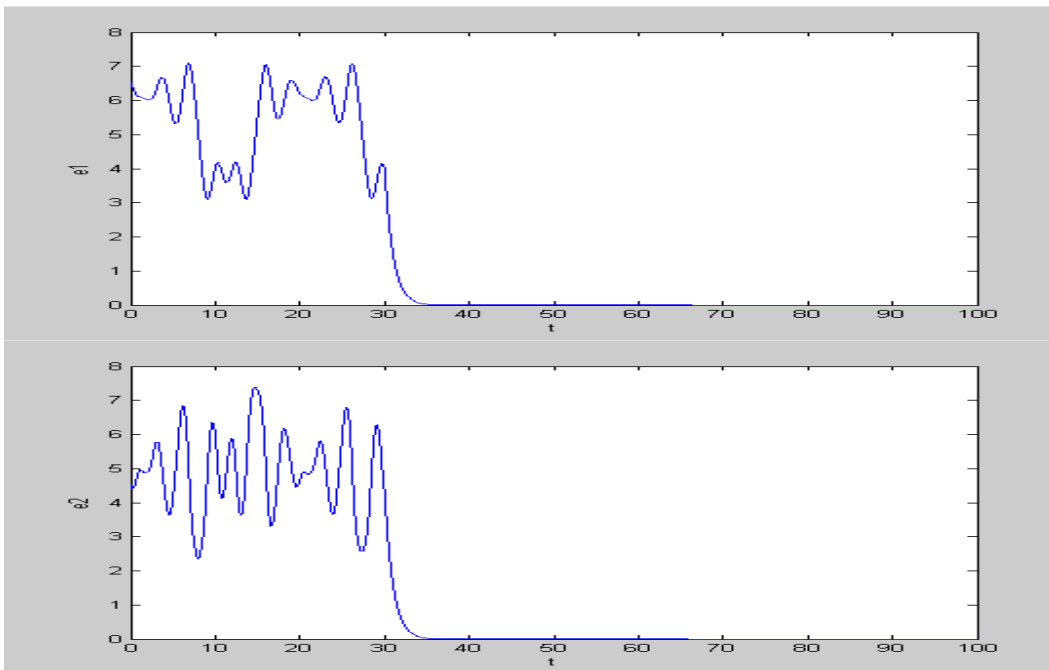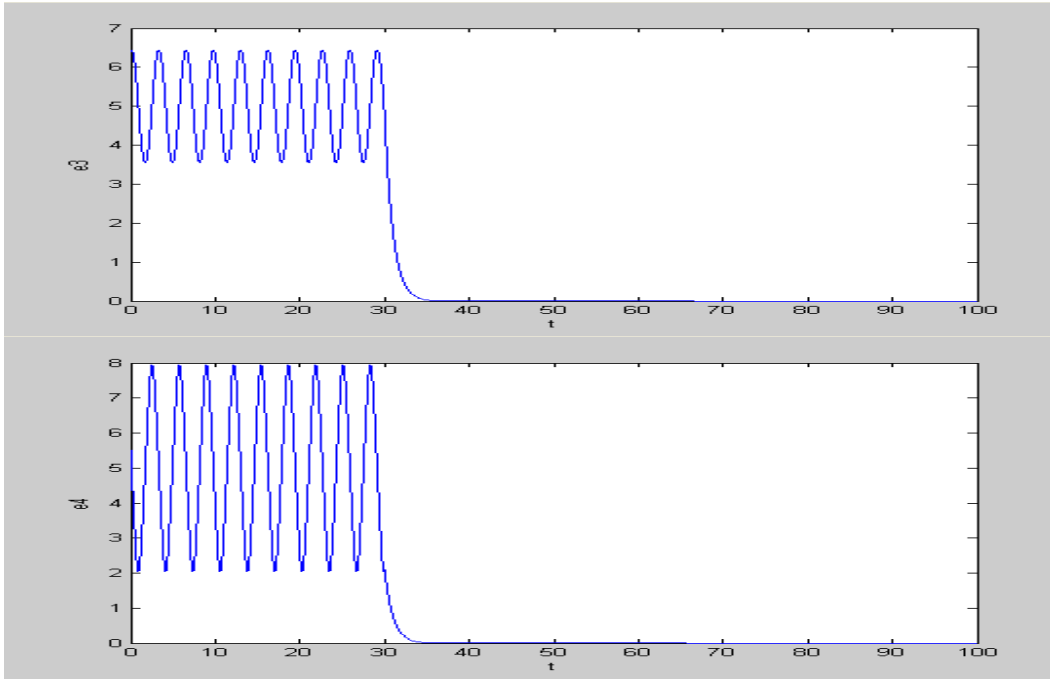
Fig. 36   Time histories of errors for Case I.
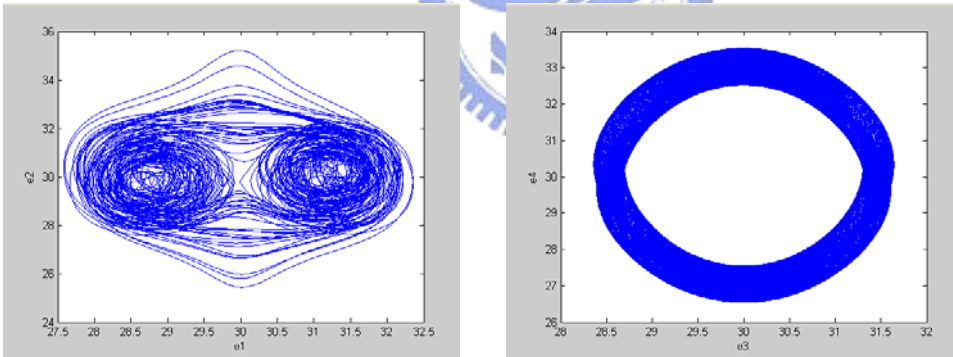
Fig. 37   Phase portraits of error dynamics for Case II.
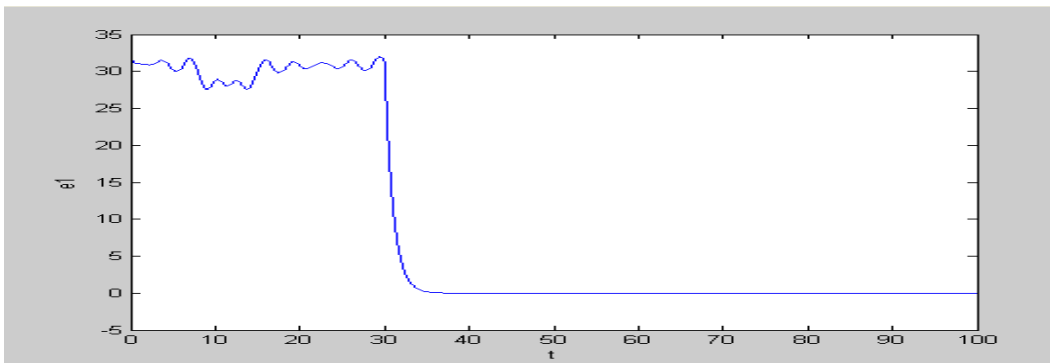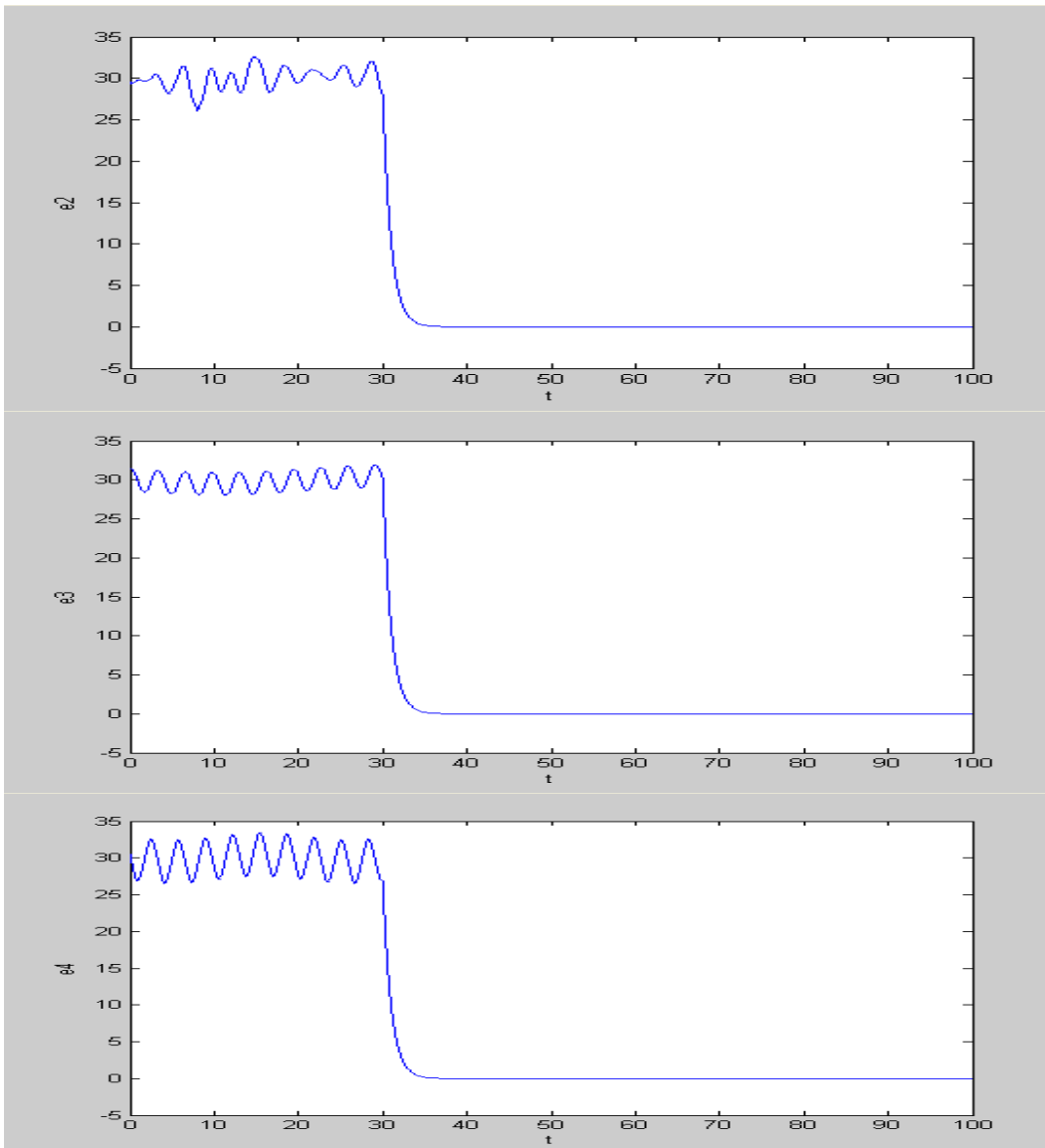
Fig. 38   Time histories of errors for Case II.
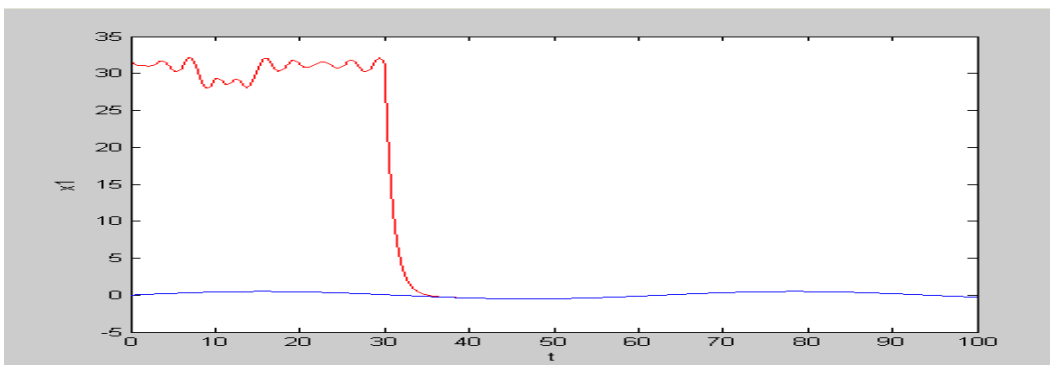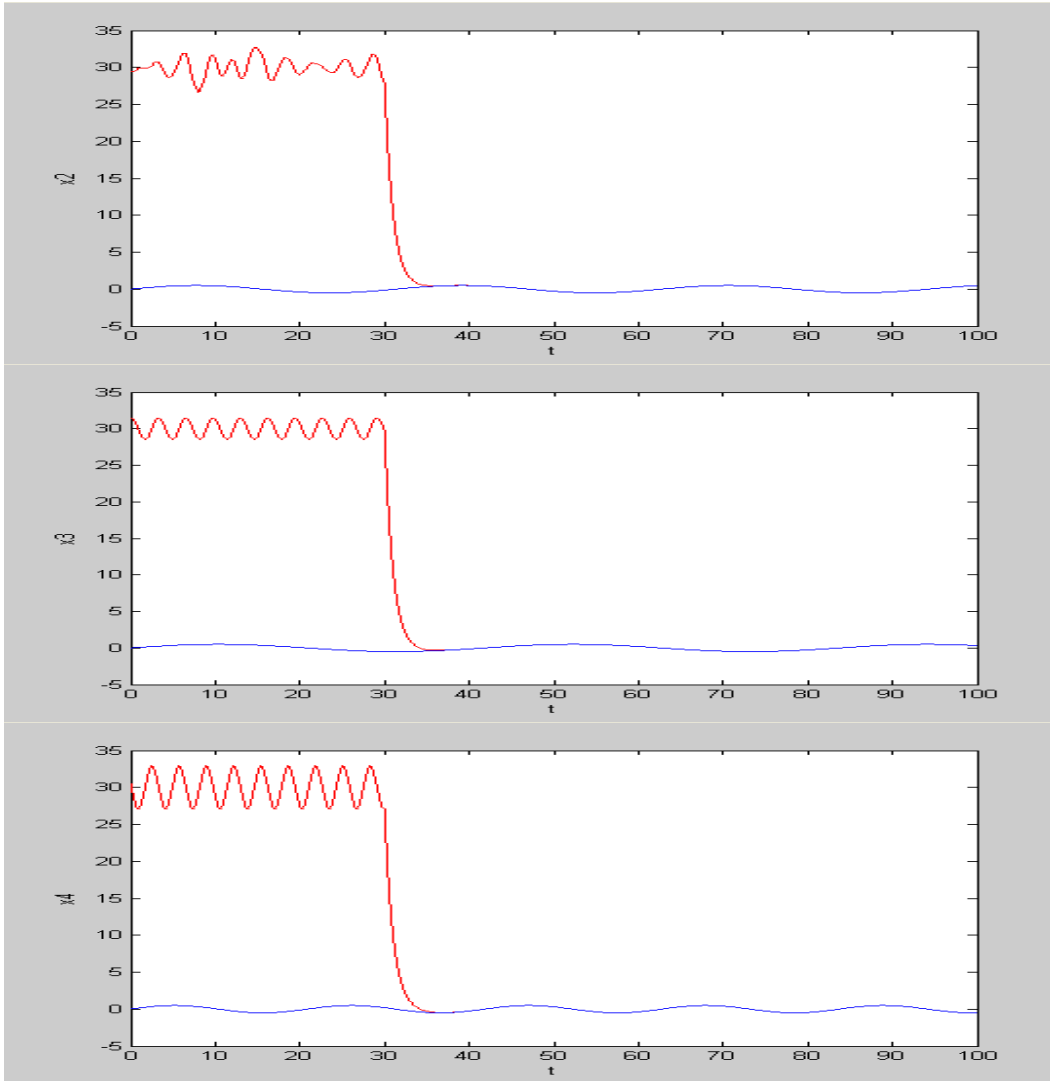
Fig. 39   Time histories of x_1, x_2, x_3, x_4 for Case II.
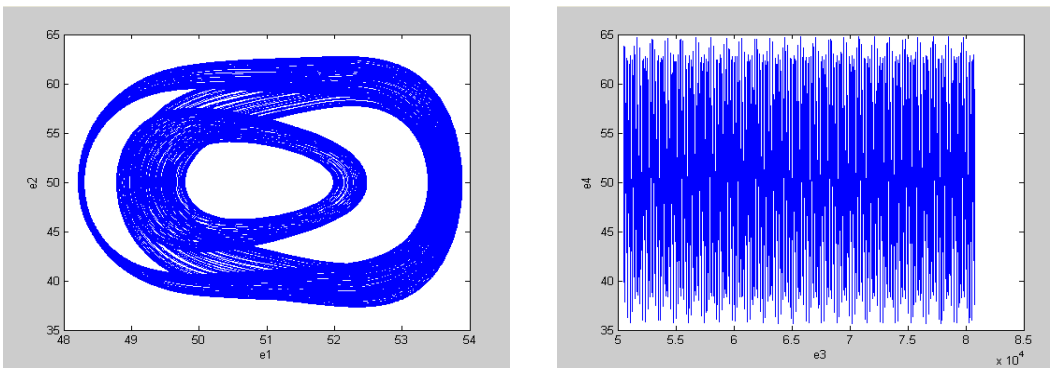
Fig. 40   Phase portraits of error dynamics for Case III.
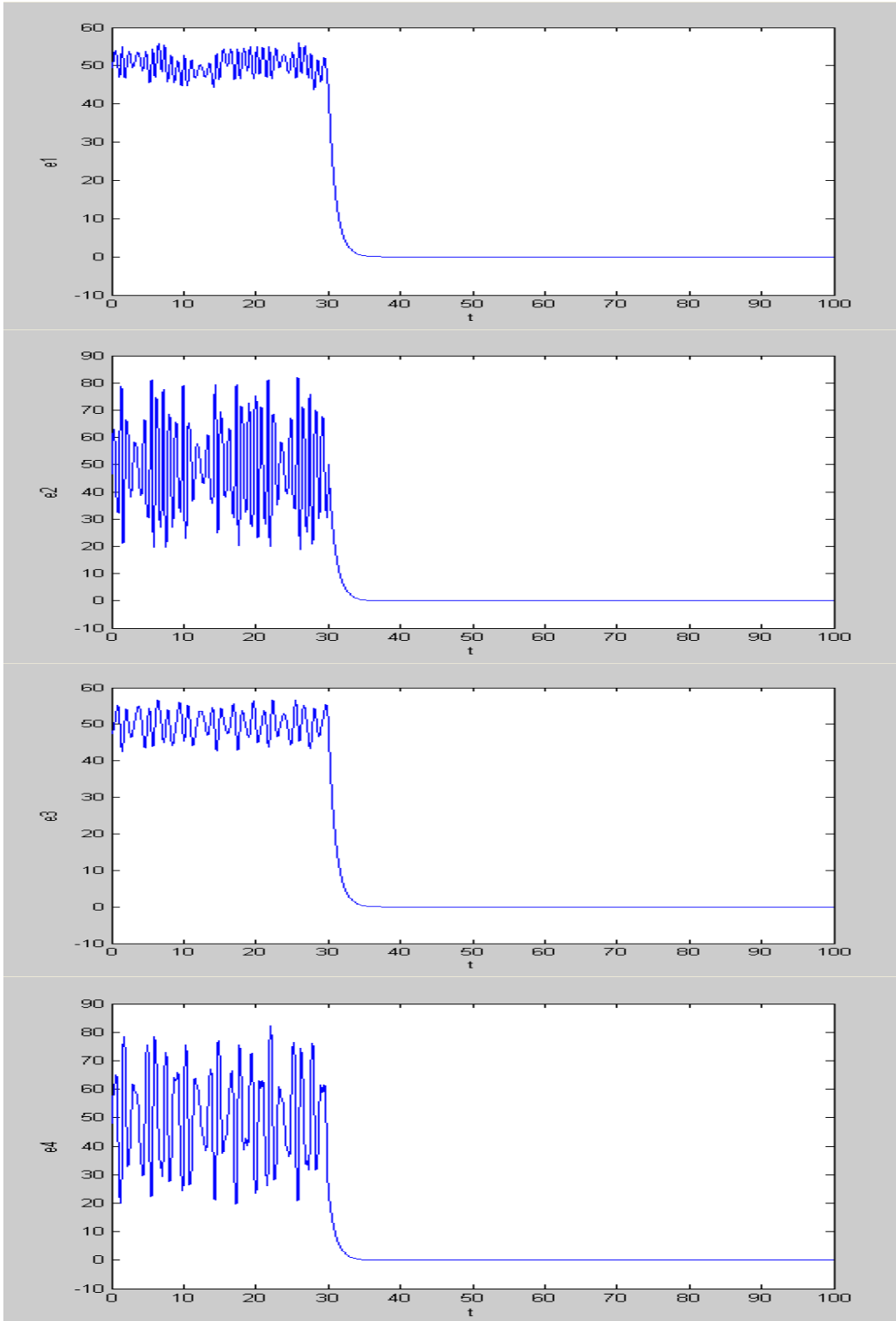
Fig. 41   Time histories of errors for Case III.
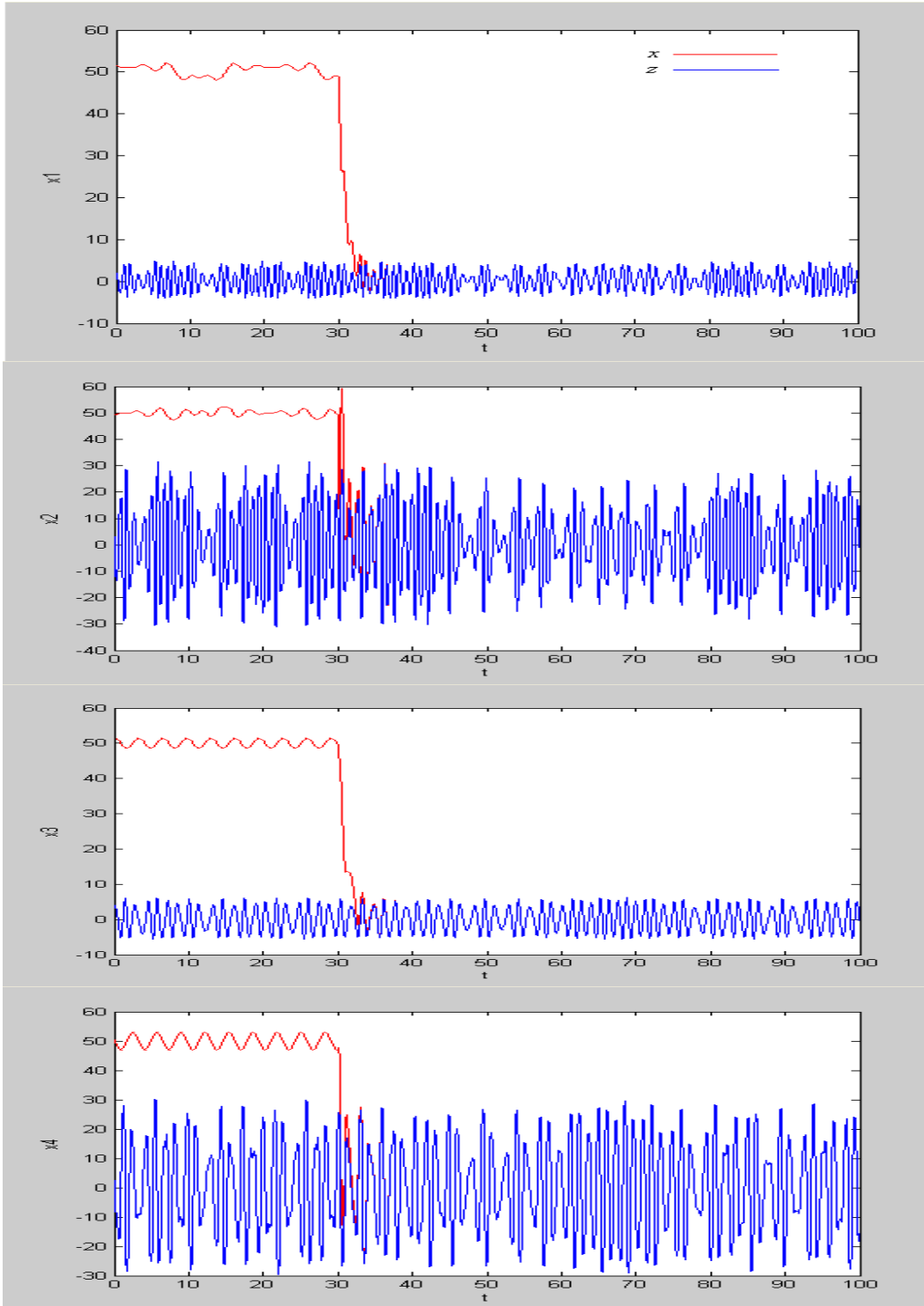
Fig. 42　Time histories of x_1, x_2, x_3, x_4, z_1, z_2, z_3, z_4 for Case III.

Chapter 7

BOIDS CONTROL OF CHAOS FOR TACHOMETER SYSTEM

The aggregate motion of a flock of birds or a herd of land animals is a beautiful and familiar part of the natural world. They exhibit complex and emergent behaviors such as flocking behavior, separation behavior, and obstacle avoiding behavior. This paper explores an approach based on simulation as an alternative to scripting the paths of each bird individually. Flock centering and separation, obstacle avoidance are studied. A nonautonomous tachometer system is used for simulation example.

7.1 Boids nonlinear control scheme

Many nonlinear systems which are known to present chaotic behavior are modeled by a set of nonlinear nonautonomous differential equations:

$$\frac{dx_i}{dt} = f_i(x_1, x_2, \cdots, x_n, t) \quad (i = 1, 2, \cdots, n) \tag{7-1}$$

where $x = (x_1(t), x_2(t), \cdots, x_n(t))$ are state variables, and

$f(x,t) = (f_1(x,t), f_2(x,t), \cdots, f_n(x,t))$ is a nonlinear vector function of x and t. Given initial state $x_i^\alpha(0)$ at t=0, the state x_i^α of each isolated boid B_α is assumed to evolve for all $t \geq 0$ via state equations:

$$\frac{dx_i^\alpha}{dt} = f_i(x_1^\alpha, x_2^\alpha, \cdots, x_n^\alpha, t) \quad (i = 1, 2, \cdots, n) \tag{7-2}$$

We will assume for simplicity that all boids are identical and each boid is coupled locally only to those neighbor boids whose trajectories lie inside a prescribed sphere S_α of radius ε:

$$S_\alpha(\varepsilon, t) = \left\{ B_\beta : \gamma_{\alpha,\beta} \triangleq \sqrt{\sum_{i=1}^{n}(x_i^\alpha(t) - x_i^\beta(t))^2} \leq \varepsilon \right\}, \tag{7-3}$$

at time t, where $\gamma_{\alpha,\beta}$ indicates the distance between the boids B_α and B_β. We will usually delete ε and t from $S_\alpha(\varepsilon,t)$ and simply write S_α to avoid clutter. Then, the dynamics of the locally coupled chaotic nonlinear networks, namely, the dynamics of boids nonlinear networks is defined by

$$\frac{dx_i^\alpha}{dt} = f_i(x_1^\alpha, x_2^\alpha, \cdots, x_n^\alpha, t) + \sum_{B_\beta \in S_\alpha} D_i^\beta g_i(x_1^\beta, x_2^\beta, \cdots, x_n^\beta, t)$$

$$(i=1,2,\cdots,n, \quad \alpha=1,2,\cdots,M) \tag{7-4}$$

where D_i^β $(i=1,2,\cdots,n)$ are coupling coefficients, and $g(x) = (g_1(x), g_2(x), \cdots, g_n(x))$ is a nonlinear vector function of x.

Case I   Flock Centering: Boids attempt to move toward the average position of nearby flockmates.

The center of nearby flockmates is defined by

$$\overline{x_i^\alpha}(t) = \frac{\sum_{\beta \in S\alpha} x_i^\beta(t)}{N_\alpha}, \tag{7-5}$$

where N_α indicates the number of nearby flockmates. The boids can move toward the center $\overline{x_i^\alpha}$ by using chaotic synchronization [50]. Therefore, flock centering is implemented here by imposing the control dynamics

$$\frac{dx_i^\alpha}{dt} = f_i(x_1^\alpha, x_2^\alpha, \cdots, x_n^\alpha, t) + d_i^\alpha(\overline{x_i^\alpha} - x_i^\alpha) \tag{7-6}$$

where $d_i^\alpha > 0$.

Case II   Separation of Flocks: Boids keep a distance from different kinds of flocks.

A flock may attempt to go away from other kinds of flocks. If a flock gets close enough to a different groups of flocks, that is, if the distance between the centers of two flocks becomes less than $\varepsilon_g > 0$, boids attempt to scatter. Separation of flocks is implemented by the dynamics of chaotic desynchronization

$$\frac{dx_i^{\alpha}}{dt} = f_i(x_1^{\alpha}, x_2^{\alpha}, \cdots, x_n^{\alpha}, t) + s_i^{\alpha}(\overline{x_i^{\alpha}} - x_i^{\alpha}) \tag{7-7}$$

where $s_i^{\alpha} > 0$ and $\overline{x_i^{\alpha}}$ indicates a center of nearby flockmates. Although $s_i > 0$, the purpose of separation of flocks can be obtained.

Case III Obstacle Avoidance: Boids attempt to dodge static obstacles.

Assume that a static obstacle is defined by the equation

$$h(x_1, x_2, \cdots, x_n) = b \quad (i = 1, 2, \cdots, n) \tag{7-8}$$

where h is a scalar function of $x = (x_1, x_2, \cdots, x_n)$ and b is a constant. The normal vector at $x = (x_1, x_2, \cdots, x_n)$ on a surface $h(x_1, x_2, \cdots, x_n) = b$ is given by

$$\nabla h(x_1, x_2, \cdots, x_n) \triangleq \left(\frac{\partial h(x_1, x_2, \cdots, x_n)}{\partial x_1}, \frac{\partial h(x_1, x_2, \cdots, x_n)}{\partial x_2}, \right.$$
$$\left. \cdots, \frac{\partial h(x_1, x_2, \cdots, x_n)}{\partial x_n} \right). \tag{7-9}$$

If a boid gets close enough to a static obstacle, that is, if the distance between a boid and a static obstacle is less than ε_0, the boids must attempt to dodge the static obstacle.

Obstacle avoidance can be implemented by switching over to a new vector field:

$$\frac{dx_i^{\alpha}}{dt} = (1 - u_i) f_i(x_1^{\alpha}, x_2^{\alpha}, \cdots, x_n^{\alpha}, t) + u_i \gamma \frac{\partial h(x_1, x_2, \cdots, x_n)}{\partial x_i} \tag{7-10}$$

where $0 \le u_i \le 1$ and $\gamma > 0$.

7.2 Hyperchaotic tachometer system

The dynamic equation of a tachometer system with vibrating base shown in Fig. 43. is given by:

$$\begin{cases} \dfrac{d}{dt} x_1 = x_2 \\[2mm] \dfrac{d}{dt} x_2 = \dfrac{1}{2m_1 + 4m_2 \sin^2 x_1} \left(\dfrac{-2m_2 g \sin x_1}{\omega^2 l} - \dfrac{2m_2 A \omega^2 \sin \omega t \sin x_1}{\omega^2 l} \right. \\[4mm] \qquad \left. -4m_2 x_2^2 \sin x_1 \cos x_1 + 2m_1 \sin x_1 \cos x_1 x_3^2 - \dfrac{k_1 x_1}{\omega^2 l^2} - \dfrac{k_2 x_2}{\omega l^2} \right) \\[4mm] \dfrac{d}{dt} x_3 = \dfrac{-2x_2 x_3 \cos x_1}{\sin x_1} \end{cases} \tag{7-11}$$

where x_1, x_2, x_3, are state variables and k_1, k_2, A, l, g, m_1, m_2, ω are constants,

when $k_1 = 3$, $k_2 = 2$, $m_2 = 2$, $m_1 = 3$, A=25, g=9.8, l=1.5, $\omega = \sqrt{\dfrac{g}{l}}$. The system exhibits hyperchaotic behavior. Its Lyapunov exponents and phase portraits are shown in Figs. 44~46.

7.3 Numerical simulations for boids control of chaos for tachometer system

The tachometer system is the master system:

$$
\begin{cases}
\dfrac{d}{dt}x_1 = x_2 \\[2mm]
\dfrac{d}{dt}x_2 = \dfrac{1}{2m_1 + 4m_2 \sin^2 x_1}\left(\dfrac{-2m_2 g \sin x_1}{\omega^2 l} - \dfrac{2m_2 A\omega^2 \sin \omega t \sin x_1}{\omega^2 l}\right. \\[3mm]
\qquad\qquad \left. -4m_2 x_2^2 \sin x_1 \cos x_1 + 2m_1 \sin x_1 \cos x_1 x_3^2 - \dfrac{k_1 x_1}{\omega^2 l^2} - \dfrac{k_2 x_2}{\omega l^2}\right) \\[3mm]
\dfrac{d}{dt}x_3 = \dfrac{-2x_2 x_3 \cos x_1}{\sin x_1}
\end{cases}
\tag{7-12}
$$

The slave system is

$$
\begin{cases}
\dfrac{d}{dt}y_1 = y_2 \\[2mm]
\dfrac{d}{dt}y_2 = \dfrac{1}{2m_1 + 4m_2 \sin^2 y_1}\left(\dfrac{-2m_2 g \sin y_1}{\omega^2 l} - \dfrac{2m_2 A\omega^2 \sin \omega t \sin y_1}{\omega^2 l}\right. \\[3mm]
\qquad\qquad \left. -4m_2 y_2^2 \sin y_1 \cos y_1 + 2m_1 \sin y_1 \cos y_1 y_3^2 - \dfrac{k_1 y_1}{\omega^2 l^2} - \dfrac{k_2 y_2}{\omega l^2}\right) \\[3mm]
\dfrac{d}{dt}y_3 = \dfrac{-2y_2 y_3 \cos y_1}{\sin y_1}
\end{cases}
\tag{7-13}
$$

Case I.   Flock Centering: Boids attempt to move toward the average position of nearby flockmates.

Flock centering is implemented here by imposing the control dynamics:

$$
\frac{dx_i^\alpha}{dt} = f_i(x_1^\alpha, x_2^\alpha, \cdots, x_n^\alpha, t) + d_i^\alpha(\overline{x_i^\alpha} - x_i^\alpha)
\tag{7-14}
$$

72

The slave system is rewritten as follows:

$$
\begin{cases}
\dfrac{d}{dt}y_1 = y_2 + d((x_1+x_2+x_3)/3-y_1)\\[2mm]
\dfrac{d}{dt}y_2 = \dfrac{1}{2m_1+4m_2\sin^2 y_1}\left(\dfrac{-2m_2 g\sin y_1}{\omega^2 l} - \dfrac{2m_2 A\omega^2 \sin\omega t \sin y_1}{\omega^2 l}\right.\\[3mm]
\qquad\qquad \left. -4m_2 y_2^2 \sin y_1 \cos y_1 + 2m_1 \sin y_1 \cos y_1 y_3{}^2 - \dfrac{k_1 y_1}{\omega^2 l^2} - \dfrac{k_2 y_2}{\omega l^2}\right)\\[3mm]
\qquad\qquad + d((x_1+x_2+x_3)/3-y_2)\\[3mm]
\dfrac{d}{dt}y_3 = \dfrac{-2y_2 y_3 \cos y_1}{\sin y_1} + d((x_1+x_2+x_3)/3-y_3)
\end{cases}
\qquad (7\text{-}15)
$$

where d=0.0001.

The simulations of flocking behavior of tachometer systems are shown in Figs. 47-49. The trajectories between two tachometer systems are illustrated in Fig. 47. The distance between two systems is given in Fig. 48. The synchronization behavior of two tachometer systems is given in Fig. 49.
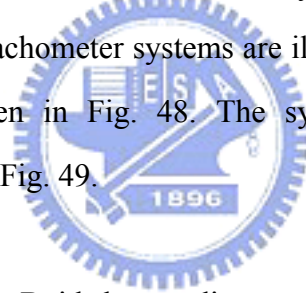
Case II   Separation of Flocks: Boids keep a distance from different kinds of flocks.

Separation of flocks is implemented by the dynamics of chaotic desynchronization:

$$
\frac{dx_i^\alpha}{dt} = f_i(x_1^\alpha, x_2^\alpha, \cdots, x_n^\alpha, t) + s_i^\alpha(\overline{x_i^\alpha} - x_i^\alpha)
\qquad (7\text{-}16)
$$

The slave system is rewritten as follows:

$$
\begin{cases}
\dfrac{d}{dt}y_1 = y_2 + s_i((x_1+x_2+x_3)/3-y_1)\\[2mm]
\dfrac{d}{dt}y_2 = \dfrac{1}{2m_1+4m_2\sin^2 y_1}\left(\dfrac{-2m_2 g\sin y_1}{\omega^2 l} - \dfrac{2m_2 A\omega^2 \sin\omega t \sin y_1}{\omega^2 l}\right.\\[3mm]
\qquad\qquad \left. -4m_2 y_2^2 \sin y_1 \cos y_1 + 2m_1 \sin y_1 \cos y_1 y_3{}^2 - \dfrac{k_1 y_1}{\omega^2 l^2} - \dfrac{k_2 y_2}{\omega l^2}\right)\\[3mm]
\qquad\qquad + s_i((x_1+x_2+x_3)/3-y_2)\\[3mm]
\dfrac{d}{dt}y_3 = \dfrac{-2y_2 y_3 \cos y_1}{\sin y_1} + s_i((x_1+x_2+x_3)/3-y_3)
\end{cases}
\qquad (7\text{-}17)
$$

where $s_i = 1$.

The simulations of flocking behavior of tachometer systems are shown in Figs. 50-52. The trajectories between two tachometer systems are illustrated in Fig. 50. The distance between two systems is given in Fig. 51. The synchronization behavior of two tachometer systems is given in Fig. 52.

Case III. Obstacle Avoidance: Boids attempt to dodge static obstacles.

Obstacle avoidance can be implemented by switching over to a new vector field:

$$\frac{dx_i^{\alpha}}{dt} = (1 - u_i) f_i (x_1^{\alpha}, x_2^{\alpha}, \cdots, x_n^{\alpha}, t) + u_i \gamma \frac{\partial h(x_1, x_2, \cdots, x_n)}{\partial x_i} \tag{7-18}$$

Define a sphere of radius r_1 centered at (x_1, y_1, z_1) by

$$(x - x_1)^2 + (y - y_1)^2 + (z - z_1)^2 = r_1^2 \tag{7-19}$$

and its normal vector $n = (n_x, n_y, n_z)$ at the point (x, y, z) by

$$(n_x, n_y, n_z) = (2(x - x_1), 2(y - y_1), 2(z - z_1)) \tag{7-20}$$

Define a cylinder of radius r_2 centered at (x_2, y_2) by

$$(x - x_1)^2 + (y - y_1)^2 = r_2^2 \tag{7-21}$$

and its normal vector $n = (n_x, n_y, n_z)$ at the point (x, y, z) by

$$(n_x, n_y, n_z) = (2(x - x_1), 2(y - y_1), 0) \tag{7-22}$$

Therefore, the "sphere" and the "cylinder" obstacles are specified by the parameters: (x_1, y_1, z_1, r_1) and (x_2, y_2, r_2) respectively.

III-1: Sphere Avoidance

The tachometer system is rewritten as follows:

$$
\begin{cases}
\dfrac{d}{dt}x_1 = (1-u_1)x_2 + 2\gamma u_1(x_1 - X) \\[2mm]
\dfrac{d}{dt}x_2 = (1-u_2)(\dfrac{1}{2m_1 + 4m_2 \sin^2 x_1}(\dfrac{-2m_2 g \sin x_1}{\omega^2 l} - \dfrac{2m_2 A\omega^2 \sin wt \sin x_1}{\omega^2 l} \\[4mm]
\qquad -4m_2 x_2^2 \sin x_1 \cos x_1 + 2m_1 \sin x_1 \cos x_1 x_3^2 - \dfrac{k_1 x_1}{\omega^2 l^2} - \dfrac{k_2 x_2}{\omega l^2})) \\[4mm]
\qquad +2\gamma u_2(x_2 - Y) \\[4mm]
\dfrac{d}{dt}x_3 = (1-u_3)(\dfrac{-2x_2 x_3 \cos x_1}{\sin x_1}) + 2\gamma u_3(x_3 - Z)
\end{cases}
\tag{7-23}
$$

where u_1=0.025, u_2 =0.025, u_3=0.025, a sphere centered at $X = 2.1, Y = 0, Z = 2.9$, γ=0.001. The simulations of the obstacle avoidance behavior for sphere are illustrated in Figs.53-54.

III-2: Cylinder Avoidance

The tachometer system is rewritten as follows:

$$
\begin{cases}
\dfrac{d}{dt}x_1 = (1-u_1)x_2 + 2\gamma u_1(x_1 - X) \\[2mm]
\dfrac{d}{dt}x_2 = (1-u_2)(\dfrac{1}{2m_1 + 4m_2 \sin^2 x_1}(\dfrac{-2m_2 g \sin x_1}{\omega^2 l} - \dfrac{2m_2 A\omega^2 \sin \omega t \sin x_1}{\omega^2 l} \\[4mm]
\qquad -4m_2 x_2^2 \sin x_1 \cos x_1 + 2m_1 \sin x_1 \cos x_1 x_3^2 - \dfrac{k_1 x_1}{\omega^2 l^2} - \dfrac{k_2 x_2}{\omega l^2})) \\[4mm]
\qquad +2\gamma u_2(x_2 - Y) \\[4mm]
\dfrac{d}{dt}x_3 = \dfrac{-2x_2 x_3 \cos x_1}{\sin x_1}
\end{cases}
\tag{7-24}
$$

where u_1=0.025, u_2=0.025, a cylinder centered at $X = 2.1, Y = 0, Z = 6.5$, γ=0.001.

The simulations of the obstacle avoidance behavior for cylinder are illustrated in Figs. 55-56.
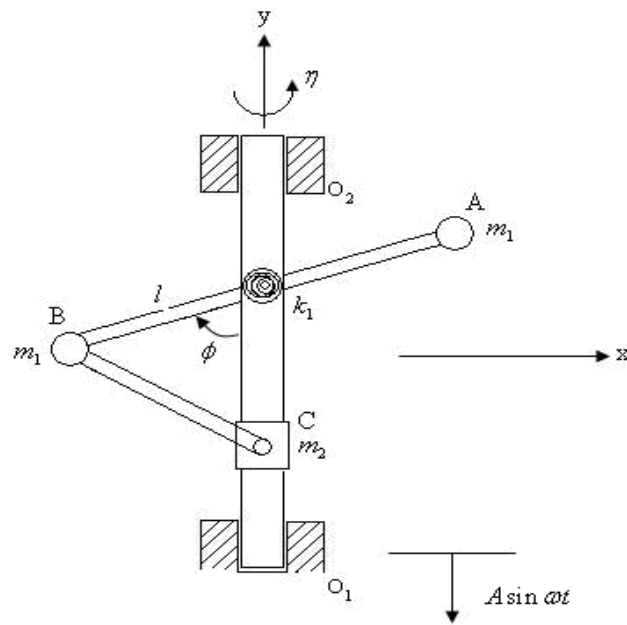
Fig. 43   Sketch of a tachometer with vibrating base.
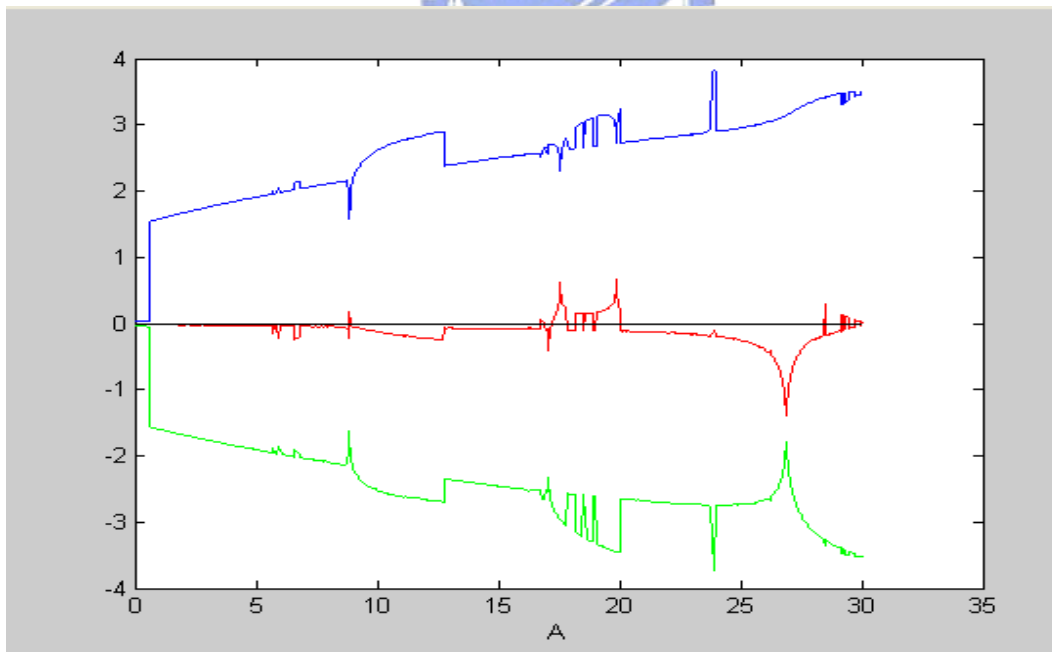
Fig. 44   Lyapunov exponents for tachometer system.
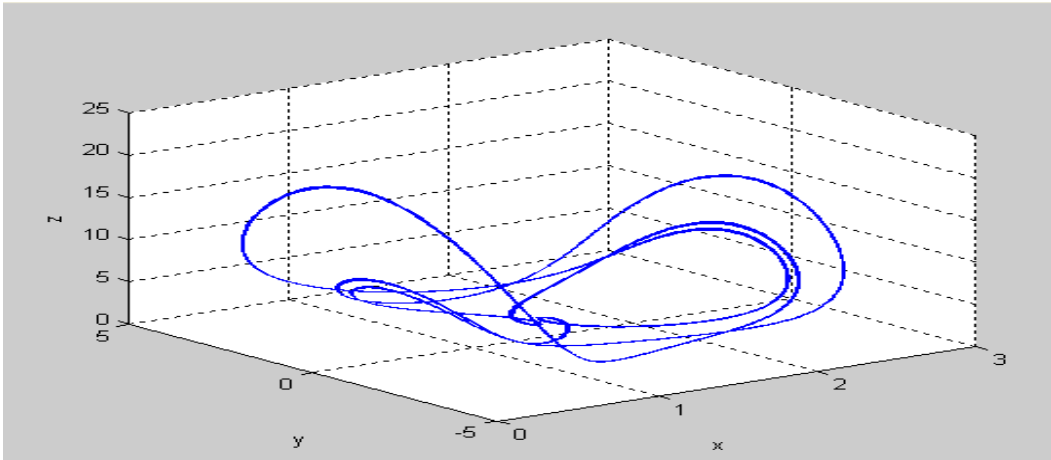
Fig. 45   Chaotic phase portrait of chaotic for tachometer system.
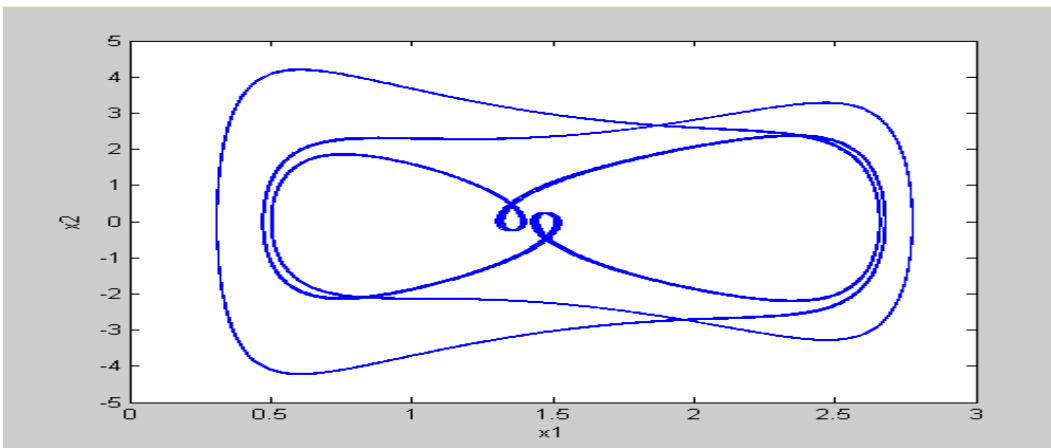
Fig. 46   Phase portrait of chaotic for tachometer system.
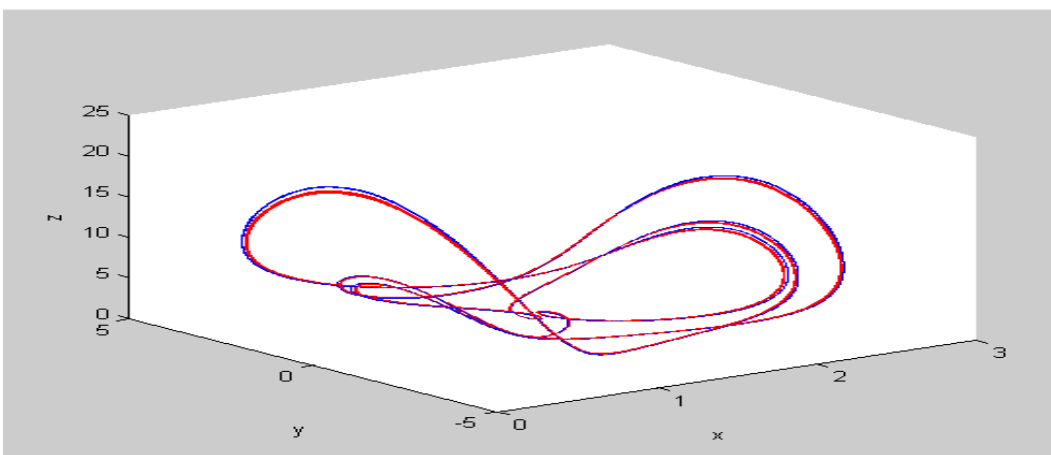
Fig. 47   Flocking of two tachometer systems.
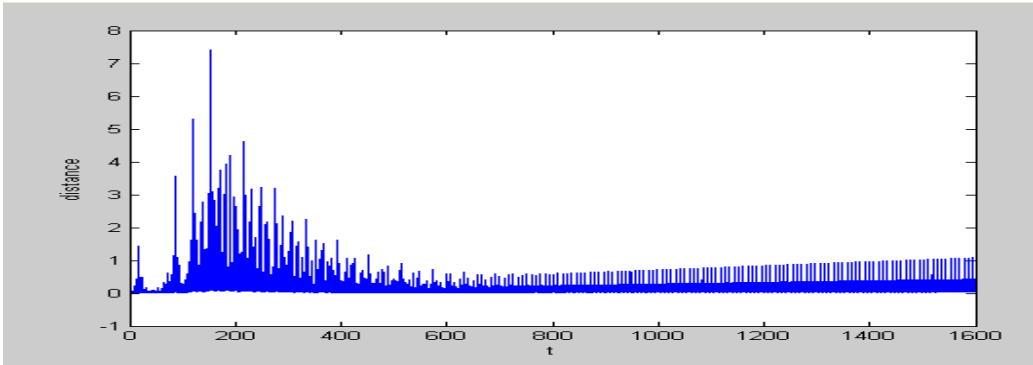
Fig. 48   Distance between two tachometer systems.
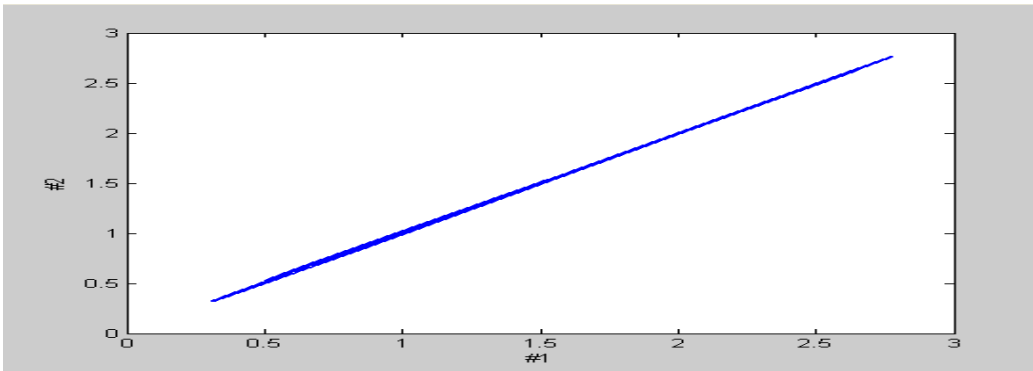
Fig. 49   Synchronization of two tachometer systems.
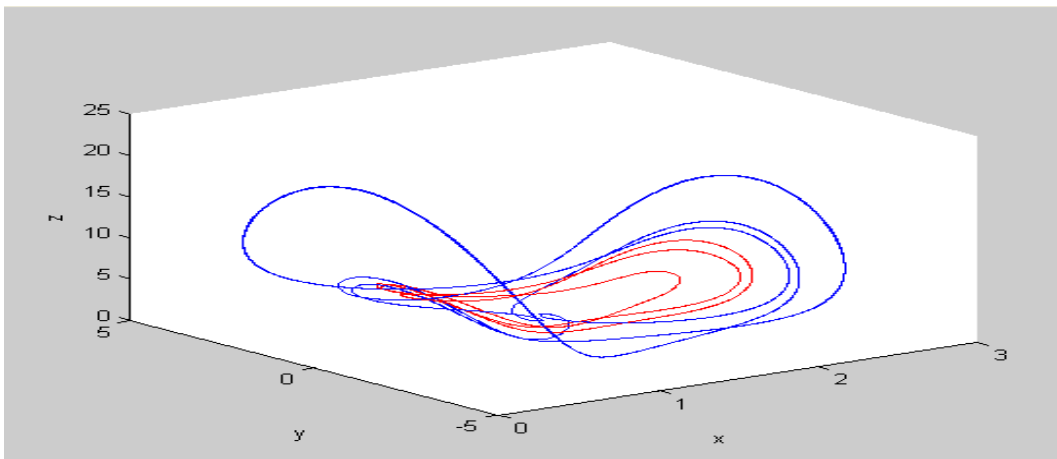
Fig. 50   Separation of two tachometer systems.
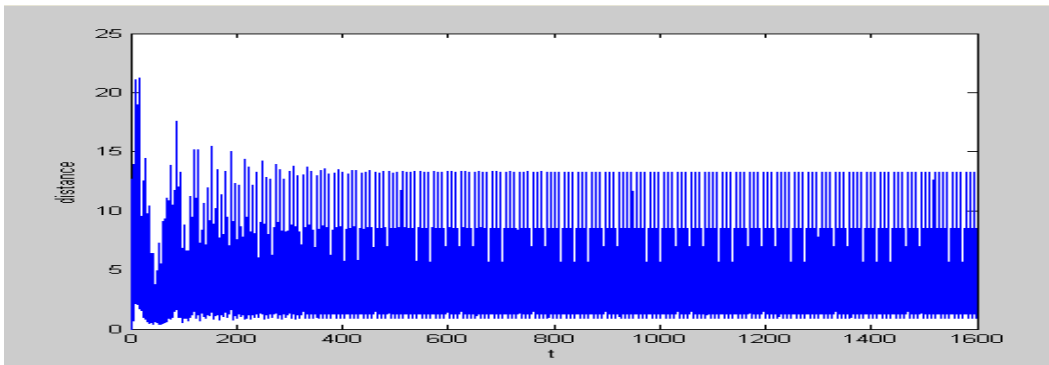
Fig. 51   Distance between two tachometer systems.
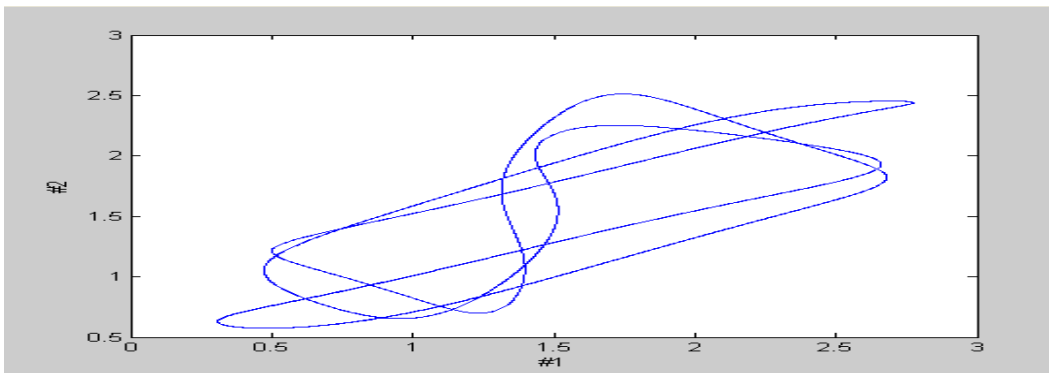
Fig. 52   Desynchronization of two tachometer systems.
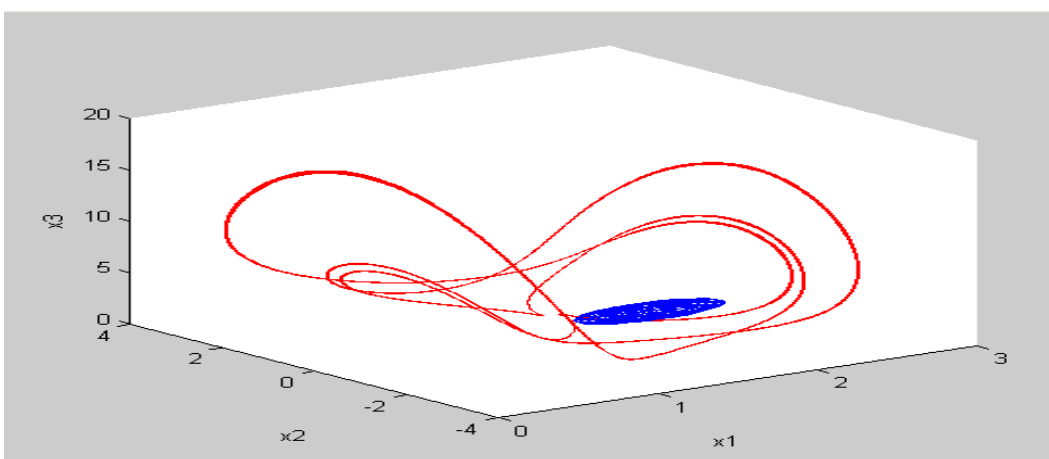
Fig. 53   Sphere avoidance for tachometer system.

79
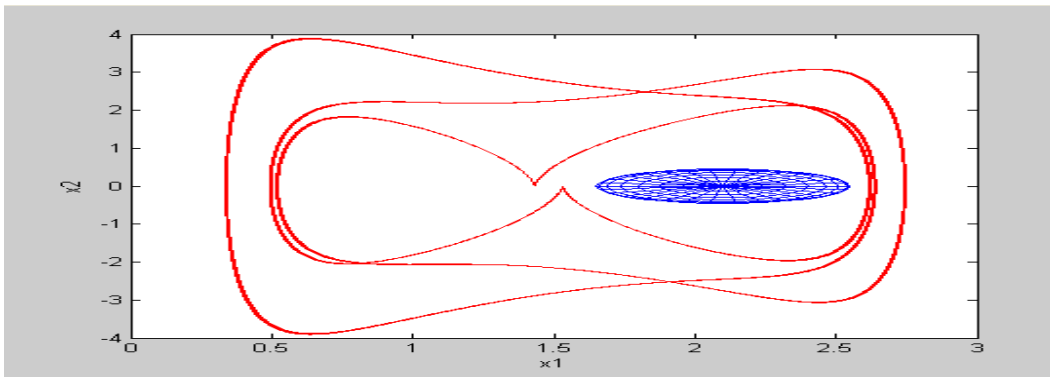
Fig. 54   Sphere avoidance for tachometer system.
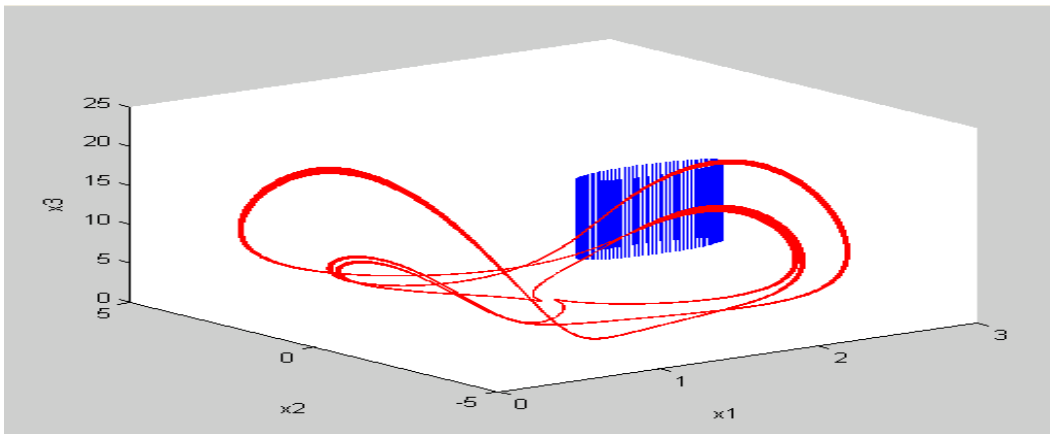
Fig. 55   Cylinder avoidance for tachometer system.
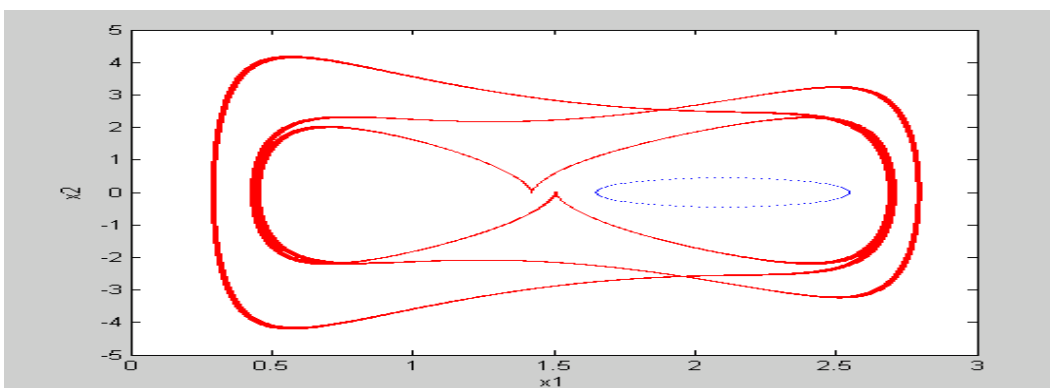
Fig. 56   Cylinder avoidance for tachometer system.

Chapter 8

Lag Synchronization for Tachometer System

In this Chapter, lag synchronization for two tachometer systems is studied by backstepping control.

8.1 Lag synchronization of two hyperchaotic tachometer systems by backstepping control

The tachometer system is the master system:

$$
\begin{cases}
\dfrac{d}{dt}x_1 = x_2 \\[2mm]
\dfrac{d}{dt}x_2 = \dfrac{-k_1 x_1}{2m_1 l^2} + \cdots + \dfrac{1}{2m_1 + 4m_2 \sin^2 x_1}\left(\dfrac{-2m_2 g \sin x_1}{l} + \dfrac{2m_2 A \sin x_3 \sin x_1}{l}\right. \\[3mm]
\qquad\quad \left. - 4m_2 x_2^2 \sin x_1 \cos x_1 + 2m_1 \sin x_1 \cos x_1 \eta^2 - \dfrac{k_2 x_2}{l^2}\right) \\[3mm]
\dfrac{d}{dt}x_3 = x_4 \\[2mm]
\dfrac{d}{dt}x_4 = -A \sin x_3
\end{cases}
\tag{8-1}
$$

where x_1, x_2, x_3, x_4 are state variables and k_1, k_2, A, l, g, m_1, m_2 are constants, when $k_1 = 4$, $k_2 = 1$, $m_2 = 3$, m_1=3, A=5, η=4.5, g=9.8, l=1.5, the system exhibits chaotic behavior as shown in Fig 2.

The slave system is

$$\begin{cases} \dfrac{d}{dt}y_1 = y_2 \\[2mm] \dfrac{d}{dt}y_2 = \dfrac{-k_1 y_1}{2m_1 l^2} + \cdots + \dfrac{1}{2m_1 + 4m_2 \sin^2 y_1}\left(\dfrac{-2m_2 g \sin y_1}{l} + \dfrac{2m_2 A \sin y_3 \sin y_1}{l}\right. \\[2mm] \qquad\qquad \left. -4m_2 y_2^2 \sin y_1 \cos y_1 + 2m_1 \sin y_1 \cos y_1 \eta^2 - \dfrac{k_2 y_2}{l^2}\right) \\[2mm] \dfrac{d}{dt}y_3 = y_4 \\[2mm] \dfrac{d}{dt}y_4 = -A \sin y_3 \end{cases} \qquad (8\text{-}2)$$

where y_1, y_2, y_3, y_4 are state variables.

In order to lead (y_1, y_2, y_3, y_4) to ($x_1(t-\tau)$, $x_2(t-\tau)$, $x_3(t-\tau)$, $x_4(t-\tau)$), add u_1, u_2, u_3, u_4 as controllers in Eq (8-2):

$$\begin{cases} \dfrac{d}{dt}y_1 = y_2 + u_1 \\[2mm] \dfrac{d}{dt}y_2 = \dfrac{-k_1 y_1}{2m_1 l^2} + \cdots + \dfrac{1}{2m_1 + 4m_2 \sin^2 y_1}\left(\dfrac{-2m_2 g \sin y_1}{l} + \dfrac{2m_2 A \sin y_3 \sin y_1}{l}\right. \\[2mm] \qquad\qquad \left. -4m_2 y_2^2 \sin y_1 \cos y_1 + 2m_1 \sin y_1 \cos y_1 \eta^2 - \dfrac{k_2 y_2}{l^2}\right) + u_2 \\[2mm] \dfrac{d}{dt}y_3 = y_4 + u_3 \\[2mm] \dfrac{d}{dt}y_4 = -A \sin y_3 + u_4 \end{cases} \qquad (8\text{-}3)$$

Define error state vectors as follows:

$$\begin{cases} e_1 = y_1 - x_1(t-\tau) \\ e_2 = y_2 - x_2(t-\tau) \\ e_3 = y_3 - x_3(t-\tau) \\ e_4 = y_4 - x_4(t-\tau) \end{cases} \qquad (8\text{-}4)$$

where τ is time delay constant, and we choose $\tau = 5$ in order to get lag synchronization.

Differentiate Eg (8-4) with respect to time, error dynamics is

$$\dot{e}_1 = e_2 + x_2(t-\tau) - \dot{x}_1(t-\tau) + u_1$$

$$\dot{e}_2 = -\frac{k_1 e_1}{2m_1 l^2} - \frac{k_1 x_1(t-\tau)}{2m_1 l^2} + \cdots$$

$$+ \frac{1}{2m_1 + 4m_2 \sin^2 y_1}\left(-\frac{2m_2 g \sin y_1}{l} + \frac{2m_2 A \sin y_3 \sin y_1}{l} - 4m_2 y_2^2 \sin y_1 \cos y_1 \right. \qquad (8\text{-}5)$$

$$\left. +2m_1 \sin y_1 \cos y_1 \eta^2 - \frac{k_2 y_2}{l^2}\right) - \dot{x}_2(t-\tau) + u_2$$

$$\dot{e}_3 = e_4 + x_4(t-\tau) - \dot{x}_3(t-\tau) + u_3$$

$$\dot{e}_4 = -A\sin y_3 - \dot{x}_4(t-\tau) + u_4$$

Choose a positive definite Lyapunov function

$$V_1 = \frac{1}{2}e_1^2 \qquad (8\text{-}6)$$

Differentiate Eq (8-6) with respect to time, we have:

$$\dot{V}_1 = e_1(e_2 + x_2(t-\tau) - \dot{x}_1(t-\tau) + u_1) \qquad (8\text{-}7)$$

Choose $u_1 = -x_2(t-\tau) + \dot{x}_1(t-\tau)$, and $e_2 = \alpha_1(e_1) = -e_1$, Eq (8-7) becomes:

$$\dot{V}_1 = -e_1^2 < 0 \qquad (8\text{-}8)$$

$e_1=0$ is asymptotically stable. When e_2 is considered as a controller, $\alpha_1(e_1)$ is an estimative function, define $W_2 = e_2 - \alpha_1(e_1) = e_2 + e_1$ and its derivative is

$$\dot{W}_2 = \dot{e}_2 + \dot{e}_1 . \qquad (8\text{-}9)$$

Choose a positive definite Lyapunov function

$$V_2 = V_1 + \frac{1}{2}W_2^2 \qquad (8\text{-}10)$$

Then:

$$\dot{V}_2 = \dot{V}_1 + W_2\dot{W}_2 \qquad (8\text{-}11)$$

$$\dot{V}_2 = -e_1^2 + W_2(W_2 - e_1 - \frac{k_1 e_1}{2m_1 l^2} - \frac{k_1 x_1(t-\tau)}{2m_1 l^2} + \cdots$$

$$+ \frac{1}{2m_1 + 4m_2 \sin^2 y_1}\left(-\frac{2m_2 g \sin y_1}{l} + \frac{2m_2 A \sin y_3 \sin y_1}{l} - 4m_2 y_2^2 \sin y_1 \cos y_1 \right. \quad (8\text{-}12)$$

$$\left. +2m_1 \sin y_1 \cos y_1 \eta^2 - \frac{k_2 y_2}{l^2}\right) - \dot{x}_2(t-\tau) + u_2)$$

Choose:

$$u_2 = -2W_2 + e_1 + \frac{k_1 e_1}{2m_1 l^2} + \frac{k_1 x_1(t-\tau)}{2m_1 l^2} + \cdots$$

$$- \frac{1}{2m_1 + 4m_2 \sin^2 y_1}(-\frac{2m_2 g \sin y_1}{l} + \frac{2m_2 A \sin y_3 \sin y_1}{l} - 4m_2 y_2^2 \sin y_1 \cos y_1$$

$$+ 2m_1 \sin y_1 \cos y_1 \eta^2 - \frac{k_2 y_2}{l^2}) + \dot{x}_2(t-\tau)$$

Eq (8-12) becomes:

$$\dot{V}_2 = -e_1^2 - W_2^2 < 0 \tag{8-13}$$

$e_2 = 0$ is asymptotically stable.

Choose a positive definite Lyapunov function

$$V_3 = V_1 + V_2 + \frac{1}{2}e_3^2 \tag{8-14}$$

Then by the third equation of Eq (8-14), we have

$$\dot{V}_3 = \dot{V}_1 + \dot{V}_2 + e_3\dot{e}_3$$
$$= -e_1^2 - W_2^2 + e_3(e_4 + x_4(t-\tau) - \dot{x}_3(t-\tau) + u_3) \tag{8-15}$$

Choose $u_3 = -x_4(t-\tau) + \dot{x}_3(t-\tau)$, and put $e_4 = \alpha_1(e_3) = -e_3$, Eq (8-15) becomes

$$\dot{V}_3 = -e_1^2 - W_2^2 - e_3^2 < 0 \tag{8-16}$$

$e_3 = 0$ is asymptotically stable. When e_4 is considered as a controller, $\alpha_1(e_3)$ is an estimative function, define

$$W_4 = e_4 - \alpha_1(e_3) = e_4 + e_3 \quad \text{and}$$

$$\dot{W}_4 = \dot{e}_4 + \dot{e}_3 \tag{8-17}$$

Choose a positive definite Lyapunov function

$$V_4 = V_1 + V_2 + V_3 + \frac{1}{2}W_4^2 \tag{8-18}$$

Then by the fourth equation of Eq (8-18), we have

$$\dot{V}_4 = \dot{V}_1 + \dot{V}_2 + \dot{V}_3 + W_4\dot{W}_4$$
$$= -e_1^2 - W_2^2 - e_3^2 + W_4(W_4 - e_3 - A\sin y_3 - \dot{x}_4(t-\tau) + u_4) \tag{8-19}$$

Choose $u_4 = -2W_4 + e_3 + A\sin y_3 + \dot{x}_4(t-\tau)$, Eq (8-19) becomes :

$$\dot{V}_4 = -e_1^2 - W_2^2 - e_3^2 - W_4^2 < 0 \tag{8-20}$$

$e_4 = 0$ is asymptotically stable.

Numerical simulations show that the result is satisfactory as shown in Figs. 57.
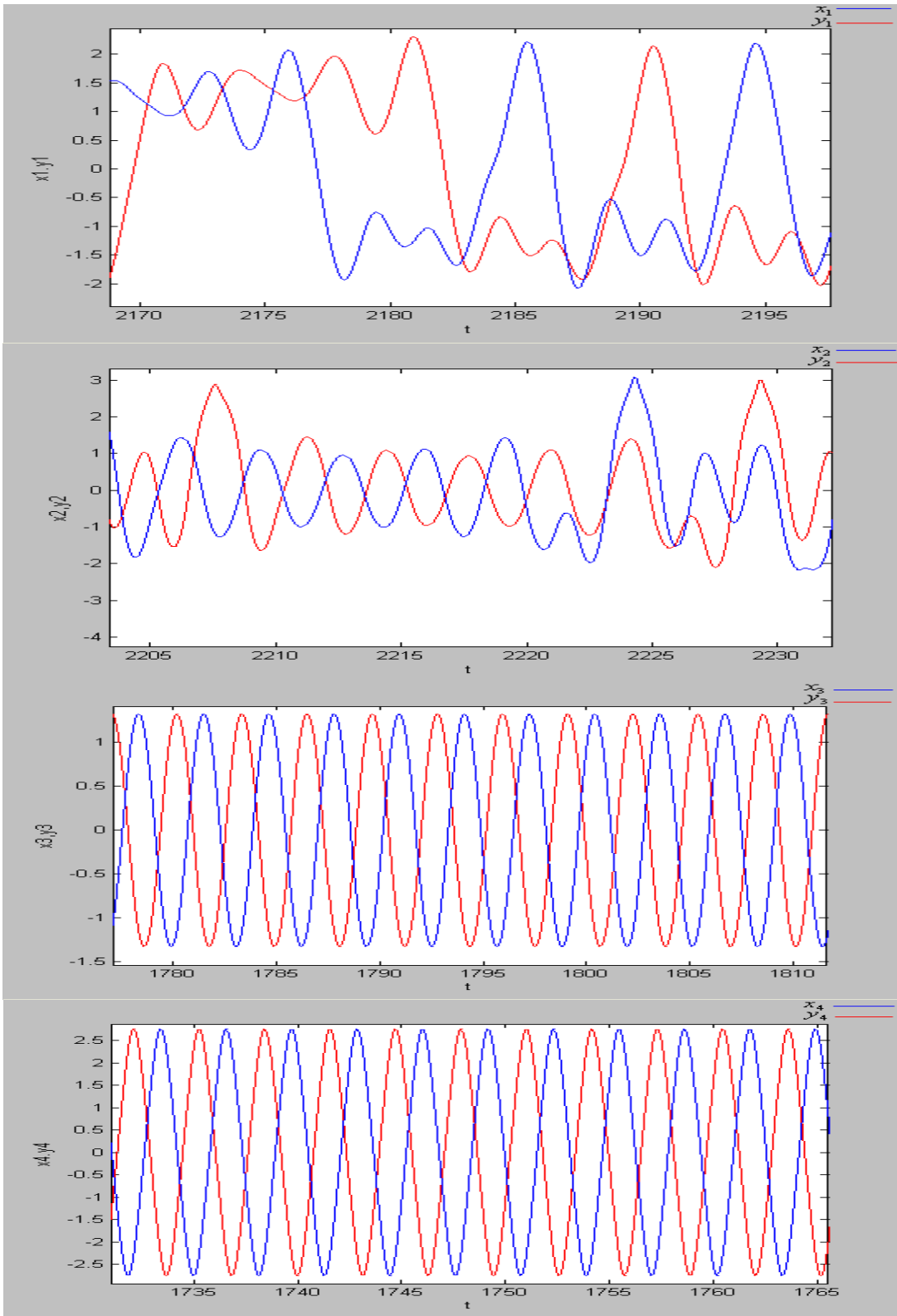
Fig. 57   Time history of x and y.

Chapter 9

Conclusions

In this thesis, chaos, pragmatical hybrid projective generalized and symplectic synchronization of a tachometer system by adaptive backstepping control are studied. Furthermore, a generalized synchronization and control by GYC partial region stability theory, boids control of chaos and lag synchronization of the same system are studied.

In Chapter 2, the chaotic behaviors of a hyperchaotic tachometer system is studied by phase portraits, Poincare maps, bifurcation diagram, power spectra and Lyapunov exponents. Two positive Lyapunov exponents shows the hyperchaos of the system.

In Chapter 3, pragmatical hybrid projective hyperchaotic generalized synchronization (PHPHGS) of two first given hyperchaotic tachometer systems with hyperchaotic Lyapunov exponents by adaptive backstepping control is studied. Another hyperchaotic Mathieu-Duffing system with two positive Lyapunov exponents is used as functional system which is first given by [51]. PHPHGS is more complicated than usual generalized synchronization. For secret communication, the security is greatly increased.

In Chapter 4, pragmatical hybrid projective hyperchaotic symplectic synchronization (PHPHSS) of two first given hyperchaotic tachometer systems as partner A and partner B by adaptive backstepping control is studied. Another chaotic Lorenz system is used as functional system with different order system. PHPHSS is more complicated than usual generalized synchronization.

In Chapter 5, hyperchaotic generalized synchronization of tachometer system by GYC partial region stability is studied. The Lyapunov function is a simple linear function and the controllers are more simple by using the GYC partial region stability theory. The simulation results are more precise because the controllers are in lower degree than that of traditional controllers.

In Chapter 6, chaos control of tachometer system by GYC partial region stability is studied. The Lyapunov function is a simple linear function and the controllers are more simple by using the GYC partial region stability theory. The simulation results are more precise because the controllers are in lower degree than that of traditional controllers.

In Chapter 7, boids control of chaos for tachometer system is studied. In this chapter, the chaotic tachometer systems are controlled by using three state variables, and systems are assumed to be identical for simplicity. The method of chaotic synchronization is well used to complete boids control scheme.

In Chapter 8, lag synchronization for tachometer system is studied. In this chapter, backstepping control is used to achieve the lag synchronization of two tachometer system. Controllers are obtained by backstepping design method that recursively interlace the choice of a Lyapunov function with the design of feedback control. This method allows us to arbitrarily amplify or reduce the scale of the dynamics of the response system through a control. The simulations for the tachometer system show that the control technique is successful.

Appendix-A   GYC   Pragmatical   Stability Theory

The stability for many problems in real dynamical systems is actual asymptotical stability, although it may not be mathematical asymptotical stability. The mathematical asymptotical stability demands that trajectories from all initial states in the neighborhood of zero solution must approach the origin as $t \to \infty$. If there are only a small part or one of the initial states from which the trajectories or trajectory do not approach the origin as $t \to \infty$, the zero solution is not mathematically asymptotically stable. However, when the probability of occurrence of an event is zero, it means the event does not occur actually. If the probability of occurrence of the event that the trajectries from the initial states are that they do not approach zero when $t \to \infty$, is zero, the stability of zero solution is actual asymptotical stability though it is not mathematical asymptotical stability. In order to analyze the asymptotical stability of the equilibrium point of such systems, the pragmatical asymptotical stability theorem is used.

Let X and Y be two manifolds of dimensions m and n $(m < n)$, respectively, and φ be a differentiable map from X to Y; then $\varphi(X)$ is a subset of Lebesque measure 0 of Y [52].

For an autonomous system

$$\frac{dx}{dt} = f(x_1, x_2, \cdots x_n) \tag{A-1}$$

where $x = [x_1, x_2, \cdots x_n]^T$, the function $f = [f_1, f_2, \cdots f_n]^T$ is defined on $D \subset R^n$. Let $x = 0$ be an equilibrium point for the system (A-1), then

$$f(0) = 0 \tag{A-2}$$

For nonautonomous system:

$$\frac{dx}{dt} = f(x_1, x_2, \cdots, x_{n+1}) \tag{A-3}$$

where $t = x_{n+1} \subset R_+$. The equilibrium point is

$$f(0, x_{n+1}) = 0 \hspace{6cm} \text{(A-4)}$$

Definition:

The equilibrium point for the dynamic system is pragmatically asymptotically stable provided that with initial points on C which is a subset of Lebesque measure 0 of D, the behaviors of the corresponding trajectories cannot be determined, while with initial points on $D - C$, the corresponding trajectories behave as that agree with traditional asymptotical stability [53,54].

Theorem:

Let $V = [x_1, x_2, \cdots x_n]^T : D \to R_+$ be positive definite, analytic on D, where $x_1, \cdots, x_n$ are all space coordinates such that the derivative of V differential equation, $\dot{V}$, is negative semi-definite of $[x_1, x_2, \cdots, x_n]^T$.

For autonomous system, let X be the m-manifold consisting of point set for which $\forall x \neq 0$, $\dot{V}(x) = 0$ and D is an n-manifold. If $m+1 < n$, i.e. m+1 $<$n then the equilibrium point of the system is pragmatically asymptotically stable.

For nonautonomous system, let X be the m+1-manifold consisting of point set for which $\forall x \neq 0$, $\dot{V}(x_1, x_2, \cdots, x_n) = 0$ and D is an n+1-manifold. If m+1+1$<$n+1, i.e. m+1$<$n then the equilibrium point of the system is pragmatically asymptotically stable. There, for both autonomous and nonautonomous system the formula m+1$<$n is universal. So the following proof is only for autonomous system. The proof for nonautonomous system is similar.

Proof:

Since every point of X can be passed by a trajectory of Eq (A-1), which is one dimensional, the collection of these trajectories, C, is a $(m+1)$-manifold [53,54]. If $(m+1) < n$, then the collection C is a subset of Lebesque measure 0 of D. By the above definition, the equilibrium point of the system is pragmatically asymptotically stable.

If an initial point is ergodicly chosen in D, the probability of that the initial point falls on the collection C is zero. Here, equal probability is assumed for every point chosen as an initial point in the neighborhood of the equilibrium point. Hence, the event that the initial point is chosen from collection C does not occur actually. Therefore, under the equal probability assumption, pragmatical asymptotical stability becomes actual asymptotical stability. When the initial point falls on $D - C$, $\dot{V}(x) < 0$, the corresponding trajectories behave as if they agree with traditional asymptotical stability because by the existence and uniqueness of the solution of initial-value problem, these trajectories never meet C.

For Eq (33), the Lyapunov function is a positive definite function of n variables, i.e. p error state variables and $n - p = m$ differences between unknown and estimated parameters, while $\dot{V} = e^T C e$ is a negative semi-definite function of n variables. Since the number of error state variables is always more than one, $p > 1$, $(m + 1) < n$ is always satisfied; by pragmatical asymptotical stability theorem we have

$$\lim_{t \to \infty} e = 0 \tag{A-5}$$

and the estimated parameters approach the uncertain parameters. The pargmatical generalized synchronizations is obtained. Therefore, the equilibrium point of the system is pragmatically asymptotically stable. Under the equal probability assumption, it is actually asymptotically stable for both error state variables and parameter variables.

Appendix-B   GYC   Partial Region Stability Theory

Consider the differential equations of disturbed motion of a nonautonomous system in the normal form

$$\frac{dx_s}{dt} = X_s(t, x_1, \cdots, x_n), \qquad (s = 1, \cdots, n) \tag{B-1}$$

where the function X_s is defined on the intersection of the partial region Ω (shown in Fig. 58) and

$$\sum_s x_s^2 \leq H \tag{B-2}$$

and $t > t_0$, where t_0 and H are certain positive constants. X_s which vanishes when the variables x_s are all zero, is a real valued function of t, $x_1, \cdots, x_n$. It is assumed that X_s is smooth enough to ensure the existence, uniqueness of the solution of the initial value problem. When X_s does not contain t explicitly, the system is autonomous.

Obviously, $x_s = 0$ $(s = 1, \cdots n)$ is a solution of Eq. (B-1). We are interested to the asymptotical stability of this zero solution on partial region Ω (including the boundary) of the neighborhood of the origin which in general may consist of several subregions (Fig. 58).

Definition 1:

For any given number $\varepsilon > 0$, if there exists a $\delta > 0$, such that on the closed given partial region Ω when

$$\sum_s x_{s0}^2 \leq \delta, \quad (s = 1, \cdots, n) \tag{B-3}$$

for all $t \geq t_0$, the inequality

$$\sum_s x_s^2 < \varepsilon, \quad (s = 1, \cdots, n) \tag{B-4}$$

is satisfied for the solutions of Eq.(B-27) on Ω, then the disturbed motion $x_s = 0$ $(s = 1, \cdots n)$ is stable on the partial region Ω.

Definition 2:

If the undisturbed motion is stable on the partial region Ω, and there exists a $\delta' > 0$, so that on the given partial region Ω when

$$\sum_s x_{s0}^2 \leq \delta', \quad (s = 1, \cdots, n) \tag{B-5}$$

The equality

$$\lim_{t\to\infty}\left(\sum_s x_s^2\right) = 0 \tag{B-6}$$

is satisfied for the solutions of Eq.(B-1) on Ω, then the undisturbed motion $x_s = 0 \quad (s=1,\cdots,n)$ is asymptotically stable on the partial region Ω.

The intersection of Ω and region defined by Eq. (B-2) is called the region of attraction.

Definition of Functions $V(t,x_1,\cdots,x_n)$:

Let us consider the functions $V(t,x_1,\cdots,x_n)$ given on the intersection Ω_1 of the partial region Ω and the region

$$\sum_s x_s^2 \le h, \quad (s=1,\cdots,n) \tag{B-7}$$

for $t \ge t_0 > 0$, where t_0 and h are positive constants. We suppose that the functions are single-valued and have continuous partial derivatives and become zero when $x_1 = \cdots = x_n = 0$.

Definition 3:

If there exists $t_0 > 0$ and a sufficiently small $h > 0$, so that on partial region Ω_1 and $t \ge t_0$, $V \ge 0$ (or ≤ 0), then V is a positive (or negative) semidefinite, in general semidefinite, function on the Ω_1 and $t \ge t_0$.

Definition 4:

If there exists a positive (negative) definitive function $W(x_1\ldots x_n)$ on Ω_1, so that on the partial region Ω_1 and $t \ge t_0$

$$V - W \ge 0 \, (or -V - W \ge 0), \tag{B-8}$$

then $V(t,x_1,\ldots,x_n)$ is a positive definite function on the partial region Ω_1 and $t \ge t_0$.

Definition 5:

If $V(t,x_1,\ldots,x_n)$ is neither definite nor semidefinite on Ω_1 and $t \ge t_0$, then $V(t,x_1,\ldots,x_n)$ is an indefinite function on partial region Ω_1 and $t \ge t_0$. That is, for any small $h > 0$ and any large $t_0 > 0$, $V(t,x_1,\ldots,x_n)$ can take either positive or negative value on the partial region Ω_1 and $t \ge t_0$.

Definition 6: Bounded function V

If there exists $t_0 > 0$, $h > 0$, so that on the partial region Ω_1, we have

$$|V(t,x_1,\ldots,x_n)| < L \tag{B-9}$$

where L is a positive constant, then V is said to be bounded on Ω_1.

Definition 7: Function with infinitesimal upper bound

If V is bounded, and for any $\lambda > 0$, there exists $\mu > 0$, so that on Ω_1 when
$$\sum_s x_s^2 \le \mu, \text{ and } t \ge t_0, \text{ we have}$$

$$|V(t, x_1, \dots, x_n)| \le \lambda \tag{B-10}$$

then V admits an infinitesimal upper bound on Ω_1.

Theorem 1 [55, 56]

If there can be found for the differential equations of the disturbed motion (Eq. (B-27)) a definite function $V(t, x_1, \dots, x_n)$ on the partial region, and for which the derivative with respect to time based on these equations as given by the following :

$$\frac{dV}{dt} = \frac{\partial V}{\partial t} + \sum_{s=1}^{n} \frac{\partial V}{\partial x_s} X_s \tag{B-11}$$

is a semidefinite function on the parital region whose sense is opposite to that of V, or if it becomes zero identically, then the undisturbed motion is stable on the partial region.

Proof:

Let us assume for the sake of definiteness that V is a positive definite function. Consequently, there exists a sufficiently large number t_0 and a sufficiently small number h < H, such that on the intersection Ω_1 of partial region Ω and

$$\sum_s x_s^2 \le h, \quad (s = 1, \dots, n) \tag{B-12}$$

and $t \ge t_0$, the following inequality is satisfied

$$V(t, x_1, \dots, x_n) \ge W(x_1, \dots, x_n) \tag{B-13}$$

where W is a certain positive definite function which does not depend on t. Besides that, Eq. (B-7) may assume only negative or zero value in this region.

Let ε be an arbitrarily small positive number. We shall suppose that in any case $\varepsilon < h$. Let us consider the aggregation of all possible values of the quantities $x_1, \dots, x_n$, which are on the intersection ω_2 of Ω_1 and

$$\sum_s x_s^2 = \varepsilon, \tag{B-14}$$

and let us designate by $l > 0$ the precise lower limit of the function W under this

condition. by virtue of Eq. (B-5), we shall have

$$V(t, x_1, \ldots, x_n) \geq l \quad \text{for} \quad (x_1, \ldots, x_n) \quad \text{on} \quad \omega_2. \tag{B-15}$$

We shall now consider the quantities x_s as functions of time which satisfy the differential equations of disturbed motion. We shall assume that the initial values x_{s0} of these functions for $t = t_0$ lie on the intersection Ω_2 of Ω_1 and the region

$$\sum_s x_s^2 \leq \delta, \tag{B-16}$$

where δ is so small that

$$V(t_0, x_{10}, \ldots, x_{n0}) < l$$

(B-17)

By virtue of the fact that $V(t_0, 0, \ldots, 0) = 0$, such a selection of the number δ is obviously possible. We shall suppose that in any case the number δ is smaller than ε. Then the inequality

$$\sum_s x_s^2 < \varepsilon, \tag{B-18}$$

being satisfied at the initial instant will be satisfied, in the very least, for a sufficiently small $t - t_0$, since the functions $x_s(t)$ very continuously with time. We shall show that these inequalities will be satisfied for all values $t > t_0$. Indeed, if these inequalities were not satisfied at some time, there would have to exist such an instant t=T for which this inequality would become an equality. In other words, we would have

$$\sum_s x_s^2(T) = \varepsilon, \tag{B-19}$$

and consequently, on the basis of Eq. (B-9)

$$V(T, x_1(T), \ldots, x_n(T)) \geq l \tag{B-20}$$

On the other hand, since $\varepsilon < h$, the inequality (Eq.(B-4)) is satisfied in the entire interval of time [t_0, T], and consequently, in this entire time interval $\dfrac{dV}{dt} \leq 0$. This yields

$$V(T, x_1(T), \ldots, x_n(T)) \leq V(t_0, x_{10}, \ldots, x_{n0}), \tag{B-21}$$

which contradicts Eq. (B-12) on the basis of Eq. (B-11). Thus, the inequality (Eq. (B-1))

must be satisfied for all values of $t > t_0$, hence follows that the motion is stable.

Finally, we must point out that from the view-point of mathenatics, the stability on partial region in general does not be related logically to the stability on whole region. If an undisturbed solution is stable on a partial region, it may be either stable or unstable on the whole region and vice versa. From the viewpoint of dynamics, we wre not interesting to the solution starting from Ω_2 and going out of Ω.

Theorem 2 [55, 56]

If in satisfying the conditions of theorem 1, the derivative $\dfrac{dV}{dt}$ is a definite function on the partial region with opposite sign to that of V and the function V itself permits an infinitesimal upper limit, then the undisturbed motion is asymptotically stable on the partial region.

Proof:

Let us suppose that V is a positive definite function on the partial region and that consequently, $\dfrac{dV}{dt}$ is negative definite. Thus on the intersection Ω_1 of Ω and the region defined by Eq. (B-4) and $t \geq t_0$ there will be satisfied not only the inequality (Eq. (B-5)), but the following inequality as will:

$$\frac{dV}{dt} \leq -W_1(x_1, \ldots x_n),$$

(B-22)

where W_1 is a positive definite function on the partial region independent of t.

Let us consider the quantities x_s as functions of time which satisfy the differential equations of disturbed motion assuming that the initial values $x_{s0} = x_s(t_0)$ of these quantities satisfy the inequalities (Eq. (B-10)). Since the undisturbed motion is stable in any case, the magnitude δ may be selected so small that for all values of $t \geq t_0$ the quantities x_s remain within Ω_1. Then, on the basis of Eq. (B-13) the derivative of function $V(t, x_1(t), \ldots, x_n(t))$ will be negative at all times and, consequently, this function will approach a certain limit, as t increases without limit, remaining larger than this limit at all times. We shall show that this limit is equal to some positive quantity

different from zero. Then for all values of $t \geq t_0$ the following inequality will be satisfied:

$$V(t, x_1(t), \ldots, x_n(t)) > \alpha \tag{B-23}$$

where $\alpha > 0$.

Since V permits an infinitesimal upper limit, it follows from this inequality that

$$\sum_s x_s^2(t) \geq \lambda, \quad (s = 1, \ldots, n), \tag{B-24}$$

where λ is a certain sufficiently small positive number. Indeed, if such a number λ did not exist, that is, if the quantity $\sum_s x_s(t)$ were smaller than any preassigned number no matter how small, then the magnitude $V(t, x_1(t), \ldots, x_n(t))$, as follows from the definition of an infinitesimal upper limit, would also be arbitrarily small, which contradicts.

If for all values of $t \geq t_0$ the inequality (Eq. (B-15)) is satisfied, then Eq. (B-13) shows that the following inequality will be satisfied at all times:

$$\frac{dV}{dt} \leq -l_1, \tag{B-25}$$

where l_1 is positive number different from zero which constitutes the precise lower limit of the function $W_1(t, x_1(t), \ldots, x_n(t))$ under condition (Eq. (B-15)). Consequently, for all values of $t \geq t_0$ we shall have:

$$V(t, x_1(t), \ldots, x_n(t)) = V(t_0, x_{10}, \ldots, x_{n0}) + \int_{t_0}^t \frac{dV}{dt} dt \leq V(t_0, x_{10}, \ldots, x_{n0}) - l_1(t - t_0),$$

which is, obviously, in contradiction with Eq.(B-14). The contradiction thus obtained shows that the function $V(t, x_1(t), \ldots, x_n(t))$ approached zero as t increase without limit. Consequently, the same will be true for the function $W(x_1(t), \ldots, x_n(t))$ as well, from which it follows directly that

$$\lim_{t \to \infty} x_s(t) = 0, \quad (s = 1, \ldots, n), \tag{B-26}$$

which proves the theorem.

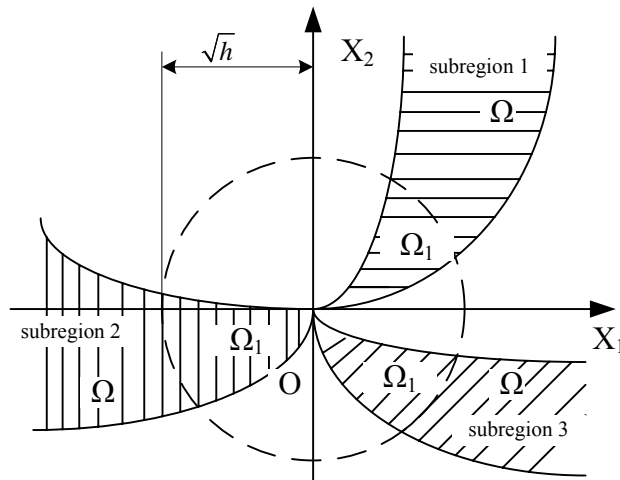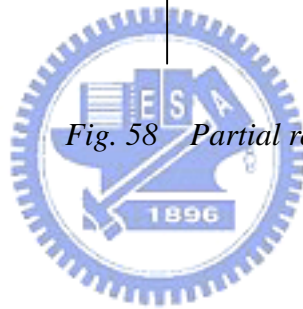*Fig. 58　Partial regions* Ω *and* Ω_1.

References

[1] Lakshmanan M., Rajasekar R., *Nonlinear Dynamics*, Springer, New York,p.101, 2003.

[2] Pecora LM, Carroll TL., "Synchronization in chaotic systems". Phys Rev Lett 1; 64:821-4, 1990.

[3] Pecora LM, Carroll TL., "Synchronization of chaotic systems". Phys Rev Lett ; 64(8):821-30, 1990.

[4] Carroll TL, Pecora LM., "Synchronizing a chaotic systems". IEEE Trans Circ Syst; 38:453-6, 1991.

[5] Chen G, Xie Q., "Synchronization stability analysis of the chaotic Rossler system". Int J Bifurcat Chaos; 6(11):2153-61, 1996.

[6] Bai EW. Bai, Lonngren KE., "Synchronization and control of chaotic systems". Chaos, Solitons and Fractals; 10:1571-6, 1997.

[7] Cuomo KM., Oppenheim AV., "Circuit implementation of synchronized chaos with applications to communications". Phys Rev Lett; 71:65, 1993.

[8] Wu C, Yang T, Chua LO.,"On adaptive synchronization and control of nonlinear dynamical systems". Int J Bifurcat Chaos; 6(3):455-72, 1996.

[9] Zeng Y, Singh SN.,"Adaptive control of chaos in Lorenz systems". Dyn Control; 7:143-54,1996.

[10] Elabbasy E. M. , Agiza H.N., E1-Dessoky M. M., "Adaptive synchronization of *Lü* system with uncertain parameters". Chaos, Solitons and Fractals; 21:657-67, 2004.

[11] Bai EW., Lonngren KE., "Sequential synchronization of two Lorenz system using active control". Chaos, Solitons & Fractals; 11:1041-4, 2000.

[12] Agiza HN., Yassen MT., "Synchronization of Rossler and Chen chaotic dynamical systems using active control". Phys Lett A; 278:191-7, 2001.

[13] Li Z, Han C, Shi S., "Modification for synchronization of Rossler and Chen chaotic Systems". Phys Lett A; 301:224-30, 2002.

dynamical systems using active control". Phys Lett A; 278:191-7, 2001.

[13] Li Z, Han C, Shi S., "Modification for synchronization of Rossler and Chen chaotic Systems". Phys Lett A; 301:224-30, 2002.

[14] Chen G, Dong X., *Form chaos to order : methodologies, perspectives and applications*. Singapore: World Scientific; 1998.

[15] Mainieri R., Rehacek J., "Projective synchronization in three-dimensional chaotic systems". Phys Rev Lett; 82:3042-5, 1992.

[16] Tan XH, Zhang JY, Yang YR., "Synchronization chaotic systems using backstepping design". Chaos, Solitons & Fractals; 16:37-45, 2003.

[17] Ge SS, Wang C.,"Adaptive control of uncertain Chua'Circuits". IEEE Trans Circ Syst I; 47(9):1397-402, 2000.

[18] Wang C, Ge SS.,"Adaptive backstepping control of uncertain Lorenz system". Int J Bifurcation Chaos; 11(4):1115-9, 2001.

[19] Yu YG, Zhang SC.,"Adaptive backstepping control of the uncertain *Lü* system". Chin Phys; 11(12):1249-53, 2002.

[20] Chen S., Zhang Q., Xie J., Wang C., "A stable-manifold-based method for chaos control and synchronization", Chaos, Solitons and Fractals, 20(5), pp. 947-954, 2004.

[21] Chen S., Lu J., "Synchronization of uncertain unified chaotic system via adaptive control", Chaos, Solitons and Fractals, 14(4), pp. 643-647, 2002.

[22] Park Ju H., ''Adaptive Synchronization of Hyperchaotic Chen System with Uncertain Parameters'', Chaos, Solitons and Fractals, 26, pp. 959-964, 2005.

[23] Park Ju H., ''Adaptive Synchronization of Rossler System with Uncertain Parameters'', Chaos, Solitons and Fractals, 25, pp. 333-338, 2005.

[24] Elabbasy E. M., Agiza H. N., El-Desoky M. M., ''Adaptive synchronization of a hrperchaotic system with uncertain parameter'', Chaos, Solitons and Fractals, 30,

pp. 1133-1142, 2006.

[25]   Park J.H. "Adaptive synchronization of hyperchaotic chen system with uncertain parameters", Chaos Solitons Fractals 26 (2005) 959.

[26]   Park J.H. "Adaptive synchronization of rossler system with uncertain parameters", Chaos Solitons Fractals 25 (2005) 333.

[27]   Elabbasy E.M., Agiza H.N., El-Desoky M.M., "Adaptive synchronization of a hyperchaotic system with uncertain parameter", Chaos Solitons Fractals 30 (2006) 1133.

[28]   Wu X., Guan Z.-H, Wu Z., Li T., "Chaos synchronization between Chen system and Genesio system", Phys. Lett. A 364 (2007) 315.

[29]   Hu M., Xu Z., Zhang R., Hu A., "Adaptive full state hybrid projective synchronization of chaotic systems with the same and different order", Phys. Lett. A 365 (2007) 315.

[30]   Yang X.-S., Chen G., "Some observer-based criteria for discrete-time generalized chaos synchronization", Chaos, Solitons and Fractals, 13, pp. 1303-1308, 2002.

[31]   Terry J. R., Van Wiggeren G. D., ''Chaotic communication using generalized synchronization", Chaos, Solitons and Fractals, 12, pp. 145-152, 2001.

[32]   Ge Z.-M., Yang, C.-H., "Synchronization of Complex Chaotic Systems in Series Expansion Form," accepted by Chaos, Solitons, and Fractals, 2006.

[33]   Ge Z.-M., Yang C.-H., Chen H.-H., and Lee S.-C., "Non-linear dynamics and chaos control of a physical pendulum with vibrating and rotation support" , Journal of Sound and Vibration, 242 (2), pp.247-264, 2001.

[34]   Lü J., Zhou T., Zhang S., "Chaos synchronization between linearly coupled chaotic systems", Chaos, Solitons and Fractals, 14(4), pp. 529-541, 2002.

[35]   Lu J., Xi Y., "Linear generalized synchronization of continuous-time chaotic systems", Chaos, Solitons and Fractals, 17, pp. 825-831, 2003.

[36]   Ge Z.-M., Yang C.-H., "Symplectic synchronization of different chaotic systems", accepted by Chaos, Solitons and Fractals, 2007.

[37]   Ge, Z.-M., Yao, C.-W. and Chen, H.-K. "Stability on Partial Region in Dynamics",   Journal of Chinese Society of Mechanical Engineer, Vol.15, No.2, pp.140-151, 1994.

[38]   Ge, Z.-M. and Chen, H.-K. "Three Asymptotical Stability Theorems on Partial Region with Applications", Japanse Journal of Applied Physics, Vol. 37, pp.2762-2773, 1998.

[39]   Itoh, M. and Chua, L. O., "Boids Control of Chaos" International Journal of Bifurcation and Chaos N0.2 427-444, 2007.

[40]   Reynolds, C.W. "Flocks, herds, and schools: A distributed behavior model" Comput. Graph. 21, 25-34, 1987.

[41]   Ge, Z.-M. and Shiue, J.-S., *"Nonlinear Dynamics and Control of Chaos for Tachometer"*, Journal of Sound and Vibration, Vol, 253, No.4, pp773-793, 2002..

[42]   Rossler O.E., An equation for hyperchaos, Physics Letters A 71, 155

[43]   Ge, Z.-M., Yang, C.-H., Chen, H.-H., and Lee, S.-C., "Non-linear dynamics and chaos control of a physical pendulum with vibrating and rotation support" , Journal of Sound and Vibration, 242 (2), pp.247-264, 2001.

[44]   Ge, Z.-M. and Yu, J.-K. "Pragmatical Asymptotical Stability Theoremon Partial Region and for Partial Variable with Applications to Gyroscopic Systems", The Chinses Journal of Mechanics, 16(4), pp. 179-187, 2000.

[45]   Ge, Z.-M. and Chang, C.-M. "Chaos Synchronization and Parameters Identification of Single Time Scale Brushless DC Motors", Chaos, Solitons and Fractals 20, pp. 883-903, 2004.

[46] Liu F., Ren Y., Shan X., Qiu Z., "A linear feedback synchronization theorem for a class of chaotic systems", Chaos, Solitons and Fractals, 13(4), pp. 723-730, 2002.

[47] Ge, Z.-M. and Yang, C.-H., "Generalized Synchronization of Quantum-CNN Chaotic Oscillator with Different Order Systems," accepted by Chaos, Solitons, and Fractals, 2006.

[48] Krawiecki A and Sukiennicki A., "Generalizations of the concept of marginal synchronization of chaos", Chaos, Solitons and Fractals, 11(9), pp. 1445–1458, 2000.

[49] Ge, Z.-M. and Yang, C.-H., "Synchronization of Complex Chaotic Systems in Series Expansion Form," accepted by Chaos, Solitons, and Fractals, 2006.

[50] Itoh., M. and Chua, L. O. "Star cellular neural networks for associative and dynamic memories" International Journal of Bifurcation and Chaos 14, 1725-1772, 2004.

[51] Ge, Z.-M. and Hsu, K.-M.," Pragmatical hybrid projective hyperchaotic generalized synchronization of hyperchaotic systems with uncertain parameters by adaptive control "Submitted to Chaos, Solitons and Fractals

[52] Matsushima Y., *Differentiable manifolds*, Marcel Dekker, City, pp.56-57, 1972.

[53] Ge Z.-M. and Yu J.-K., and Chen Y.-T., ''Pragmatical asymptotical stability theorem with application to satellite system'', Jpn. J. Appl. Phys., 38, pp. 6178-6179, 1999.

[54] Ge Z.-M. and Yu J.-K., ''Pragmatical asymptotical stability theoremon partial region and for partial variable with applications to gyroscopic systems'', The Chinses Journal of Mechanics, 16(4), pp. 179-187, 2000.

[55] Ge, Z.-M., Yao, C.-W. and Chen, H.-K. "Stability on Partial Region in Dynamics", Journal of Chinese Society of Mechanical Engineer, Vol.15, No.2, pp.140-151, 1994.

[56] Ge, Z.-M. and Chen, H.-K. "Three Asymptotical Stability Theorems on Partial Region with Applications", Japanse Journal of Applied Physics, Vol. 37, pp.2762-2773, 1998.